Relative-Story Displacement Sensing for Seismic Health Monitoring of Building Structures

地震動に対する建築物のヘルスモニタリングのための層間変位計測に関する研究

February 2011

Waseda University
Graduate School of Science and Engineering
Major in Nanoscience and Nanoengineering

Iwao MATSUYA

Committee:

Associate Professor
Dr. Takashi Tanii, Supervisor
Graduate School of Advanced Science and Engineering
Waseda University

Professor
Dr. Akira Nishitani
Graduate School of Creative Science and Engineering
Waseda University

Professor
Dr. Shuichi Shoji
Graduate School of Advanced Science and Engineering
Waseda University

Professor Emeritus
Dr. Iwao Ohdomari
Waseda University

Acknowledgements

The research work for this doctoral thesis was carried out during the years from 2006 to 2010 at the Nano-electronics, Information and Communication Technology, Sensor Network Consortium (NICS) of Waseda University, which was an academic-industrial collaborative project between the Nano-Electronics Laboratories, the Structural System Control and Modeling Laboratory, and several private companies.

First I wish to express my deepest gratitude to my supervisors, Prof. Iwao Ohdomari and Prof. Takashi Tanii, for their unlimited patience and skillful scientific guidance. I am also grateful to Prof. Akira Nishitani, Prof. Yoshihiro Nitta, Prof. Shuichi Shoji, Prof. Jun Mizuno, and Prof. Tetsushi Sekiguchi for their continuous support and sincere interest towards my work.

I would also like to express my sincere appreciation to the members of Kajima Corporation, Dr. Motoichi Takahashi, Dr. Satoru Miura, Dr. Yasutsugu Suzuki, Dr. Tomohiko Hatada, Mr. Ryuta Katamura, Mr. Makoto Oshio, and Mr. Naohito Adachi, for giving me a precious opportunities and a lot of financial support via the Waseda-Kajima research collaboration in NICS.

I wish to thank my co-workers of the Sensor Group in NICS framework, Mr. Ryota Tomishi, Ms. Maya Sato, Mr. Miroku Iba, Mr. Hideaki Kondo, Mr. Kiyoshi Kanekawa, Mr. Meiki Nakamoto, Mr. Mitsuaki Sakairi, Dr. Ferrer Domingo, Mr. Osamu Osaki, Mr. Yuki Nagao, Mr. Hiroshi Osaki, Mr. Yoshinori Yamada, Mr. Tomoki Yaguchi, Mr. Yudai Sugiura, Mr. Akio Murakami, Mr. Yoshiyasu Akaza, and

Prof. Susumu Ito for their sincere help and support.

I also wish to thank all my colleagues in the Prof. Ohdomari's laboratory and Prof. Tanii's laboratory for their kind support and pleasant working environment, in particular: Prof. Takanobu Watanabe, Prof. Takahiro Shinada, Dr. Aya Seike, Dr. Takefumi Kamioka, Dr. Takeo Miyake, Dr. Hideaki Yamamoto, Mr. Kou Sato, Ms. Mutsuko Aoki, Mr. Yanwai Zyu, Mr. Yutaka Kazama, Mr. Kousuke Sasaki, Mr. Tomoya Onda, Mr. Ryo Tosaka, Mr. Masahiro Hori, Mr. Tomofumi Zushi, Mr. Takahiro Yoshida, Mr. Jun-ichi Wada, and Mrs. Atsuko Kobayashi.

This research was also supported by "Ambient SoC Global COE Program of Waseda University", Grants-in-Aid for Young Scientists (B), and Scientific Research (B) of KAKENHI, of the Ministry of Education, Culture, Sports, Science and Technology, Japan.

Finally I express my deepest gratitude to my parents, Azuma and Takako Matsuya, for their patience and support during long years.

Tokyo

January 2011 Iwao MATSUYA

Table of contents

Chapter 1
Introduction

1.1 Background and motivation of this study

The safety of our residence space is the base of our life. However, buildings collapse due to damage from a severe earthquake. The Hyogo Prefecture Medical Association reported that, by the Hanshin-Awaji earthquake, not only senior people who have failed to escape but also considerable amount of young people were killed to be buried in the crushed buildings because the early twenties lived in cheap rented apartments due to their economic reasons [1]. It was reported in government survey that 7,309 elementary-school buildings which were equivalent to 33% of elementary schools in Japan were assumed to collapse if an earthquake above level 6.0 on the Japanese scale occurred [2]. Furthermore, it takes almost half a year for victims to return back to their own house and resume their life as before [3]. This is because the visual assessment of buildings is the only way to judge the safety of the buildings, and it takes excessive amount of time for even professional architects to evaluate the residual seismic capacity of all the damaged buildings one by one. These reports indicate that our society requires a novel system that is capable of

automatically evaluating the seismic capacity of buildings.

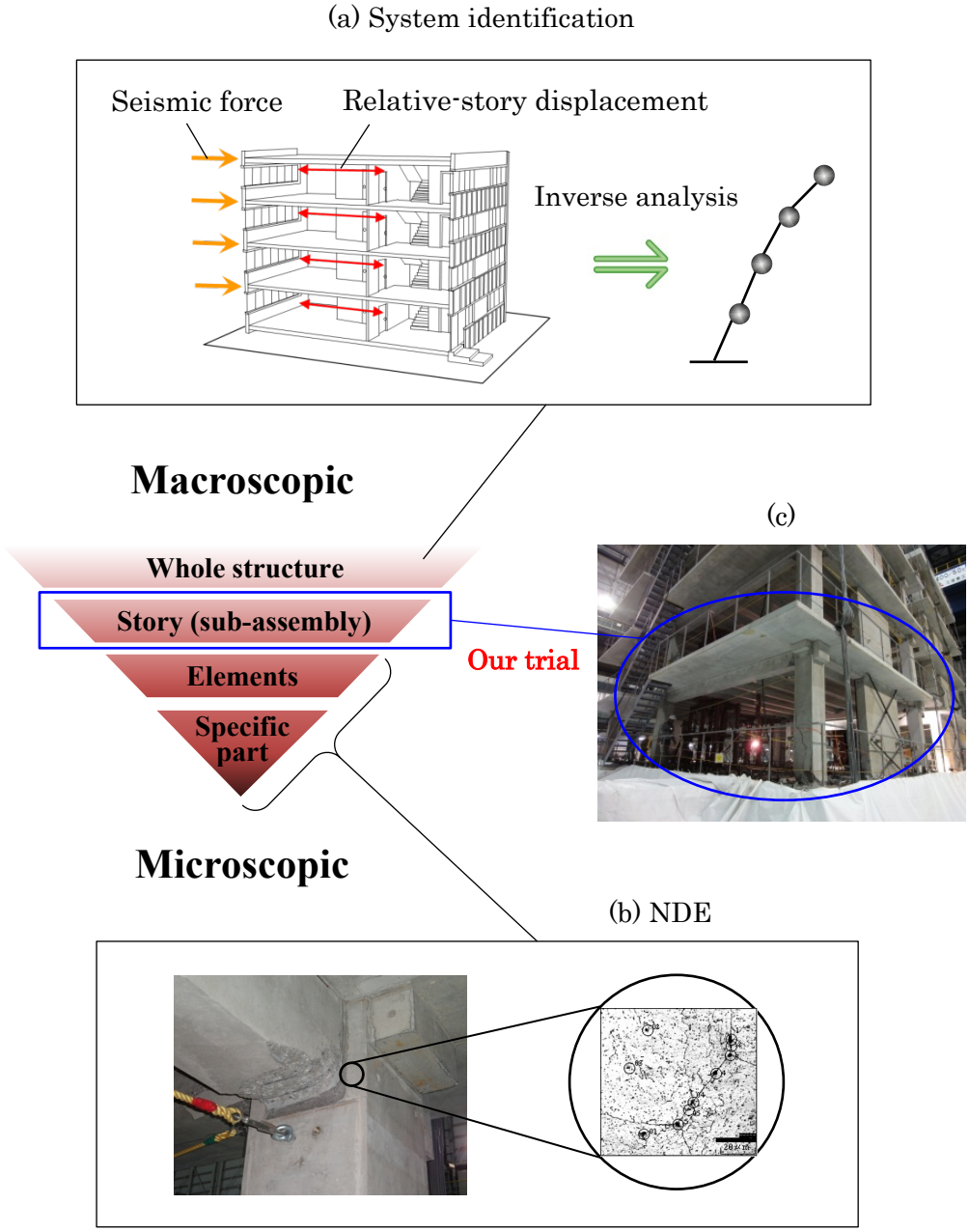

Fig. 1.1 Classification of the damage evaluation technology from the view point of the object scale. (a) The system identification for the entire structure. (b) Non-destructive evaluation (NDE) for the element and the specific part of the structures. (c) The inter-story of a building on which we focus strategically.

Recently, various kinds of electronic sensors are commercially available, and they are sufficiently small and low-cost. Since these sensors have the lifetime as long as that of a building, the history of building movement can be recorded for long period without the maintenance of sensors. Applying such electronic sensors for structural health monitoring is expected to tap a new market of electronics devices. In particular, developing a novel ambient sensor network system is in a technology field where Japan can play an active role by taking advantage of the electronics industry in Japan. Furthermore, based on the structural health monitoring system, we can provide a total solution business which links infrastructure and insurance. Thus, developing a novel system for structural health monitoring is a next-generation challenge.

Structural health monitoring is a technology that enables us to monitor structural responses of a building to external excitations, such as strong winds and earthquakes. Using an array of sensors, we can measure the structural responses and evaluate the "health" condition of the building. The concept of structural health monitoring goes back to the accidents where several bridges in the United States collapsed simultaneously due to the aging degradation [4]. Since then, structural engineers have recognized the necessity of practical technology for the assessment of civil structures. A wireless acceleration sensor system, Imote2 (Intel Corp.), is an example of the structural health monitoring system which is commercially available for laboratory use [5]. For more practical use, high-precision but comparatively large velocimeters or accelerometers are commonly used. Such accelerometers are mounted on a highway bridge junction to evaluate the relationship between the traffic load volume and the damage induced into the

bridge junction [6]. A new television tower in China was equipped with accelerometers, and its structural response has been monitored using the accelerometers. The acquired data are widely open on the Internet website [7]. Furthermore, accelerometers were implemented on Shanghai bay bridge to monitor the structural responses during typhoon [8, 9]. Also in Japan, where earthquakes often occur, structural health monitoring attracts much attention, and the eigen frequency or the damping constant of a building is often measured using accelerometers [10, 11]. Currently, such acceleration-based measurement is a matter of necessity rather than a matter of choice although more useful information would be expectedly obtained by directly measuring the displacements, as discussed later.

Figure 1.1 shows the classification of the damage evaluation technology from the view point of the object scale. The system identification which is classified into “macroscopic evaluation” is a method to evaluate the story stiffness and the vibrational mode of whole building structures (Fig.1.1 (a)). However, such macroscopic evaluation is insufficient for detecting damage in the material level. The non-destructive evaluation (NDE) which is classified into “microscopic evaluation” is a method to evaluate the damage induced in the specific element (Fig.1.1 (b)). There are several methods for NDE such as the thermography, the ultrasonic method, and the acoustic-emission technique (AET). Using these methods, the inner defects including the floatage of a concrete structure, flaking off, and the progress of the crack can be evaluated with a high degree of accuracy. However, such microscopic evaluation requires substantial time, and the damage cannot be evaluated in real time. Thus a novel measurement method is strongly

demanded. We focused on the displacement-based measurement for structural health monitoring of a building, which is classified into neither microscopic nor macroscopic evaluation (Fig. 1.1 (c)). Especially, it is expected that the displacement-based measurement makes it possible to identify the damaged element in real time.

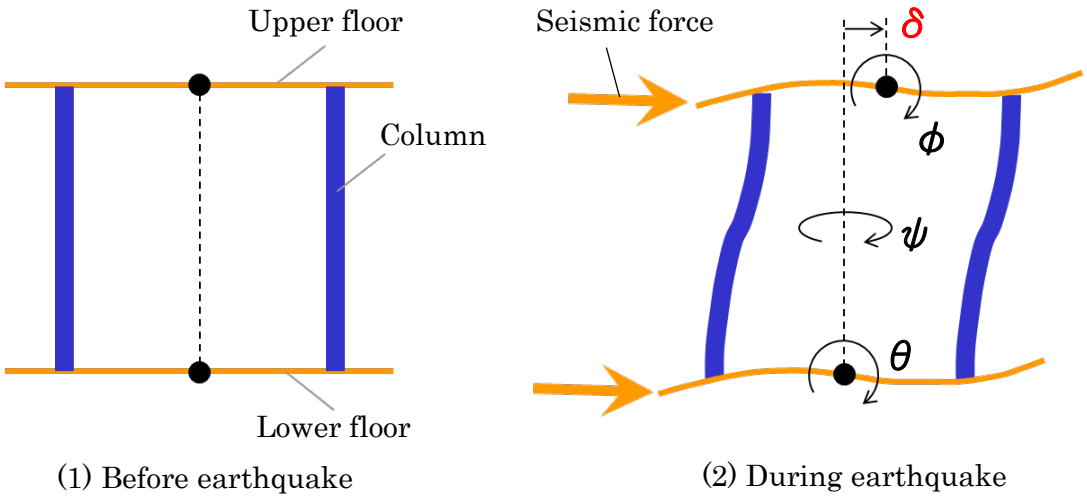

Fig. 1.2 Relative-story displacement of a building induced by seismic force

Earthquakes vibrate every floor of the building laterally, as shown in Fig. 1.2. If the magnitude of the earthquake is small, the floors return to their original position after the earthquake. When the vibration amplitude exceeds the critical level, and the structural elements such as columns or beams are damaged, the vibration center of the floor is displaced, and the floor does not return to its original position. This indicates that measuring the displacement is essential for identifying

building damage. Monitoring the displacements of every floor in real time makes it possible to identify the building elements damaged by the earthquake, and enables us to judge whether the residents need to be evacuated just after the earthquake. Thus, a novel system which is capable of measuring directly the relative-story displacement in real time is required for the health diagnosis of a building structure.

To directly measure the relative-story displacement, two methods have been proposed so far. Hiwatashi and his group proposed a method using a linear potentiometer for measuring the relative-story displacement [12]. In this method, linear potentiometer was fixed on a perfectly rigid tower, and the displacement of the building was measured laterally. However, it would be impractical to construct such a full-scale rigid tower nearby the high-rise building, and also it would be impossible for the rigid tower to exhibit exactly the same movement as the ground at any point of place in the longitudinal direction at any point in time during earthquake. On the other hand, Ooki and his group reported a method using a stainless needle [13]. In this method, a stainless needle was suspended on the end of a wire with the other end fixed on the ceiling, and the movement of the ceiling relative to the floor was recorded by scratching the metal plate on the floor with the suspended stainless needle. This method is quite simple, but the room between the ceiling and the floor is occupied by the suspended needle, and the relative-story displacement measured using the stainless needle contains considerable error.

Generally, a laser distance meter or a supersonic-wave distance meter is utilized for displacement measurement [14, 15]. The distance can be measured by the laser distance meter from the sensor to the object, but the lateral displacement

of the object at a distance cannot be measured by them. A global positioning system (GPS) can measure the lateral displacement, but it suffers from poor resolution [16]. The lateral displacement can be measured by a system using a charge-coupled device (CCD) video camera by scanning the image of a target object, but it requires pixel scanning that is a heavy software task [17]. Thus, these devices cannot be utilized for the relative-story displacement measurement conveniently.

Theoretically speaking, displacement can be estimated from the acceleration data via the double integral process with respect to time. As is widely known among the structural engineers community, however, such a double integral quite often gives the displacement information with some errors involved. Taking account for the above-mentioned technological environments, an innovative instrument which can measure directly the relative displacement would provide us a novel measurement system. Therefore, we opt to develop a novel sensor which enables us to measure the relative-story displacement directly and precisely in real time.

1.2 Overview of this thesis

In this chapter, we have already explained the background and the purpose of this study. In chapter 2, we describe the design of the lateral displacement sensor (LDS) we developed. We describe the data results of both static and dynamic performance tests, and the results prove that the developed LDS fulfills the requirement for both the resolution and the response speed. In chapter 3, the feasibility of the LDS implemented in an actual building is discussed. Several LDSs were implemented in an actual building equipped with an active variable stiffness (AVS) system, and

multi-point measurement was carried out using the LDSs. The building was vibrated with seismic waveforms using an exciter placed on the rooftop. We will show the advantage of using our LDS system for relative-story displacement measurement by comparing with conventional velocimeters. In addition, we will show that the inclination angle of the 2nd floor can be monitored using a pair of LDSs. The results show that the building floor is not a perfectly rigid body but it easily bends during seismic vibration. Eventually, this bending causes error in the relative-story displacement measurement using the LDS system. The method to reduce the error is discussed in the following chapter. We used multiple LDSs in one measurement point so that both the relative-story displacement and the inclination angle due to the floor bending are measured simultaneously. Using a translational stage combined with a rotational stage, both the lateral displacement and the inclination angle were measured simultaneously using the multiple LDSs. The acquired data were verified with the theoretical values. Finally in chapter 6, we will summarize the achievement of this thesis and give the conclusion. Furthermore, we will discuss the future application of the developed LDS system.

Bibliography

[1] K. Suzuki and J. Izumi : "Analysys on the Characteristics of Death Person due to the Hanshin-Awaji Great Earthquake", Papers of the annual conference of the Institute of Social Safety Science, Vol.5, pp.471-478 (1995) (in Japanese)

[2] Ministry of Education, Culture, Sports, Science and Technology Japan : "The results of the earthquake-proof safety investigation of Public School facilities", http://www.mext.go.jp/b_menu/houdou/21/06/1270297.htm (2009) (in Japanese)

[3] R. Kimura, H. Hayashi, S. Tatsuki and Y. Urata : "Clarifying the human behavior of the disaster victims after the Great Hanshin-Awaji earthquake", Journal of social safety science Vol.1, pp.93-102, (1999) (in Japanese)

[4] K. Y. Wong : "Instrumentation and health monitoring of cable supported bridges", Structural Control and Health Monitoring, Vol.11, Iss.2, pp.91-124 (2004)

[5] J. A. Rice, K. Mechitov, S. H. Sim, T. Nagayama, S. Jang, R. Kim, B. F. Spencer Jr., G. Agha and Y. Fujino : "Flexible smart sensor framework for autonomous structural health monitoring", Smart Structures and Systems, Vol.6, No.5-6, pp.423-438 (2010)

[6] J. P. Lynch : "An overview of wireless structural health monitoring for civil structures", Royal Society of London Transactions Series A, Vol.365, Iss.1851, pp.345-372 (2007)

[7] Y. Q. Ni, Y. Xia, W. Y. Liao and J. M. Ko : "Technology Innovation in Developing the Structural Health Monitoring System for Guangzhou New TV Tower", Structural Control and Health Monitoring, Vol.16, Iss.1, pp.73-98 (2008)

[8] K. Y. Wong : "Instrumentation and health monitoring of cable-supported bridges", Structural Control and Health Monitoring, Vol.11, pp.91-124 (2004)

[9] S. N. Pakzad and G. L. Fenves : "Statistical Analysis of Vibration Modes of a Suspension Bridge Using Spatially Dense Wireless Sensor Network", Journal of Structural Engineering, Vol.135, Iss.7, pp.863-872 (2009)

[10] Y. Nitta, A. Nishitani and B. F. Spencer Jr : "Semiactive control strategy for smart base isolation utilizing absolute acceleration information", Structural Control and Health Monitoring, Vol.13, pp.649-659 (2006)

[11] Y. Nitta and A. Nishitani : "Two Stage Based Structural System Identification Utilizing Absolute Acceleration Response Information", Journal of Structural and Construction Engineering, AIJ, No.568, pp.91-97 (2003)

[12] T. Hiwatashi, Y. Shiozaki, H. Fujitani, and S. Soda : "Semi-active base-isolation system by damper utilizing optimal regulator theory", Journal of Structural and Construction Engineering, AIJ, No.567, pp.47–54 (2003) (in Japanese)

[13] Y. Ooki, T. Yamashita, H.Morikawa, S. Yamanda, H. Sakata, H. Yamanaka, K. Kasai, H. Yamanaka, K.Kasai and A. Wada : "Cocrete Approach on Long Term and Dense Monitoring System of Seismically Isolated Tall Building", AIJ Journal of Technology and Design, No.21, pp.73-77 (2005) (in Japanese)

[14] Y. Ohshima, M. Komagari and S. Hasegawa : "Study on a Simple Measurement Method for Bridge Vibration Using Laser Distancemeter", JCOSSAR2007, Vol.6, pp.365-370 (2007) (in Japanese)

[15] M. Okugumo, A. Kimura, M. Ohki, M. Ohkita : "Development Research on High Performance Ultrasound Sensor System", IEEJ Transactions on Electronics, Information and Systems, Vol.128, No.1, pp.55-61 (2008) (in Japanese)

[16] S. Nakamura : "GPS Measurement of Wind-Induced Suspension Bridge Girder Displacements", Journal of Structural Engineering, Vol.126, Iss.12, pp.1413-1419 (2000)

[17] J. J. Lee, Y. Fukuda and M. Shinozuka : "Development and application of a vision-based displacement measurement system for structural health monitoring of civil structures", Smart Structures and Systems, Vol.3, No.3, pp.373-384 (2007)

Chapter 2
Basic performance of the lateral displacement sensor

2.1 Introduction

For measuring the relative-story displacement of an actual building, an array of sensors with high resolution and a wide measurement range is required. In addition, the sensor must be sufficiently compact not to disturb daily living even though the multiple sensors are implemented at the multiple points in the building.

Due to lack of devices that can conveniently measure the lateral displacement of a building, the displacement has not been a physical quantity to be commonly measured and monitored. For the relative-story displacement measurement, the feasibility of an accelerometer, a linear variable differential transformer (LVDT), a laser distance meter, a global positioning system (GPS), and a charge coupled device (CCD) video camera have been examined so far. However, these sensors are not applicable for the relative-story displacement measurement of an actual building. The displacement estimated by double integration of

accelerometer output has a substantial error [1]. A LVDT or a laser distance meter which needs a “gigantic stand” for a fixed point is not suitable for practical use [2]. Although GPS can measure the displacement without a reference, displacement monitoring using the GPS suffers from its poor resolution. The accuracy of GPS is typically ±1 cm in horizontal direction and ±2 cm in vertical direction [3, 4]. A CCD video camera requires additional computational processing such as pixel scanning, object identification and contour definition for evaluating the relative displacement [5, 6].

A position-sensitive detector (PSD) has high potential as a device for the real-time relative-story displacement monitoring, because it has high resolution and high response speed [7-11]. For measuring the lateral position of an object, light emitted from the object must be focused on the photosensitive surface of the PSD. For achieving high resolution with the PSD, the spot light must be irradiated at the central part of the photo sensitive region. In contrast, the spot light must be scanned from one end to the other for achieving a large measurement range. Thus, achieving both high resolution and wide measurement range is difficult, and a novel method to achieve both the requirements needs to be developed.

To achieve both high resolution and a wide measurement range, we propose a lateral-displacement sensor (LDS) composed of a light emitting diode (LED) array, a focusing lens, and a PSD, as shown in Fig. 2.1. The LED array is immobilized on the ceiling whereas the focusing lens is set in front of the PSD and immobilized on the floor together with the PSD. The LED array and the PSD unit can be set up oppositely so that the LED array is immobilized on the floor and the PSD unit on the ceiling. The large displacement between the ceiling and the floor is reproduced

by the movement of the spot light which is emitted from the LED array and focused on the PSD by the lens. This reduced projection makes it possible to achieve both high resolution and a large measurement range.

It was previously reported that the system for the relative-story displacement measurement must fulfill the following requirements [12]:

(1) The accuracy in the displacement measurement should be less than 0.1 mm.

(2) The vibration frequency of 0 to 20 Hz must be monitored.

(3) The measurement range should be greater than 50 mm when the story height is 5.0 m.

(4) The system should be scalable in such a way as to cover multi-point measurements.

(5) A low-costly and small-sized system is preferable.

In this chapter, we investigate the feasibility of our LDS for real-time relative-story displacement monitoring. We measured the lateral displacement between the LED array and the PSD using the LDS, and evaluated the accuracy of the LDS in the displacement measurement. Furthermore, we optimized the LDS for achieving both high resolution and a large measurement range. We discuss the accuracy of the LDS system in the relative-story displacement measurement.

2.2 Design of the lateral displacement sensor

We used a commercially available PSD. There are two criteria to select the PSD. One is that the nonlinearity must be less than 0.1%, and the other is that the cost must be sufficiently low for use of multiple-point sensing. We adopted a

pin-cushion type PSD with low dark current (S2044, 4.7×4.7 mm^2, Hamamatsu Photonics K.K.) [13]. For structural health monitoring, high operation speed is not required, and the response speed of 20 Hz is sufficient because seismic vibration generally contains waves at a frequency of less than 20 Hz. Since reducing the background noise is rather important, reverse-bias voltage which enhances the electrical noise from the power supply was not applied to the PSD junction. The position of the light spot (X, Y) on the PSD is estimated by

$$\mathrm{X} = \frac{L}{2} \cdot \frac{(I_{X2}+I_{Y1})-(I_{X1}+I_{Y2})}{I_{X1}+I_{X2}+I_{Y1}+I_{Y2}} \ , \ \mathrm{Y} = \frac{L}{2} \cdot \frac{(I_{X2}+I_{Y2})-(I_{X1}+I_{Y1})}{I_{X1}+I_{X2}+I_{Y1}+I_{Y2}} \ , \qquad (2.1)$$

where L is the side length of the PSD, and (I_{X1}, I_{X2}, I_{Y1}, I_{Y2}) are the output currents to be detected at four electrodes of the PSD.

The current-voltage (I-V) conversion of the four output currents and the calculation of the Equation (2.1) were carried out using on-board analog computational units (ACUs) as shown in Fig. 2.1 (a). The amplitude of the circuit was set to be 3.0 V mm^{-1}, and the output voltage after the I-V conversion was designed to be greater than 5 V. The electric circuit of the DC power supply was designed so as to eliminate the ripple voltage.

(a)

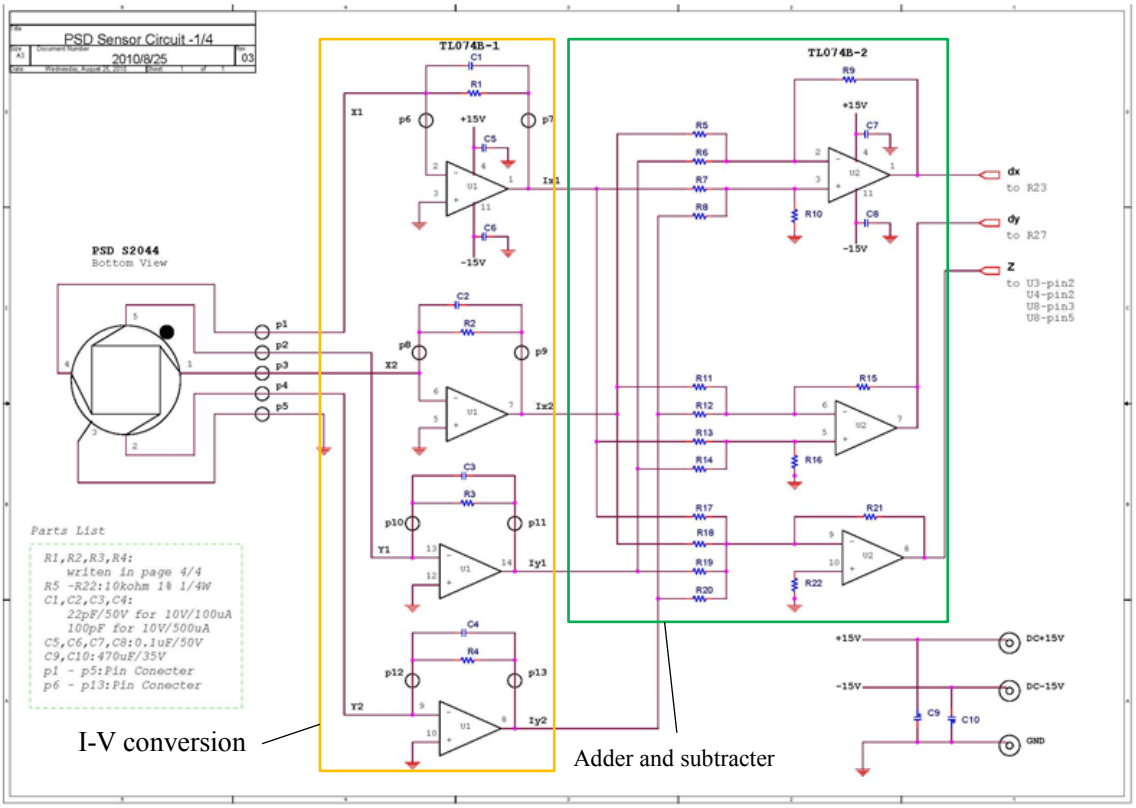
PSD Sensor Circuit -1/4
2010/8/25
TL074B-1
TL074B-2
PSD S2044
Bottom View
Parts List
R1,R2,R3,R4:
writen in page 4/4
R5 -R22:10kohm 1% 1/4W
C1,C2,C3,C4:
22pF/50V for 10V/100uA
100pF for 10V/500uA
C5,C6,C7,C8:0.1uF/50V
C9,C10:470uF/35V
p1 - p5:Pin Conecter
p6 - p13:Pin Conecter
dx
to R23
dy
to R27
Z
to U3-pin2
U4-pin2
U8-pin3
U8-pin5
DC+15V
DC-15V
GND
I-V conversion
Adder and subtracter

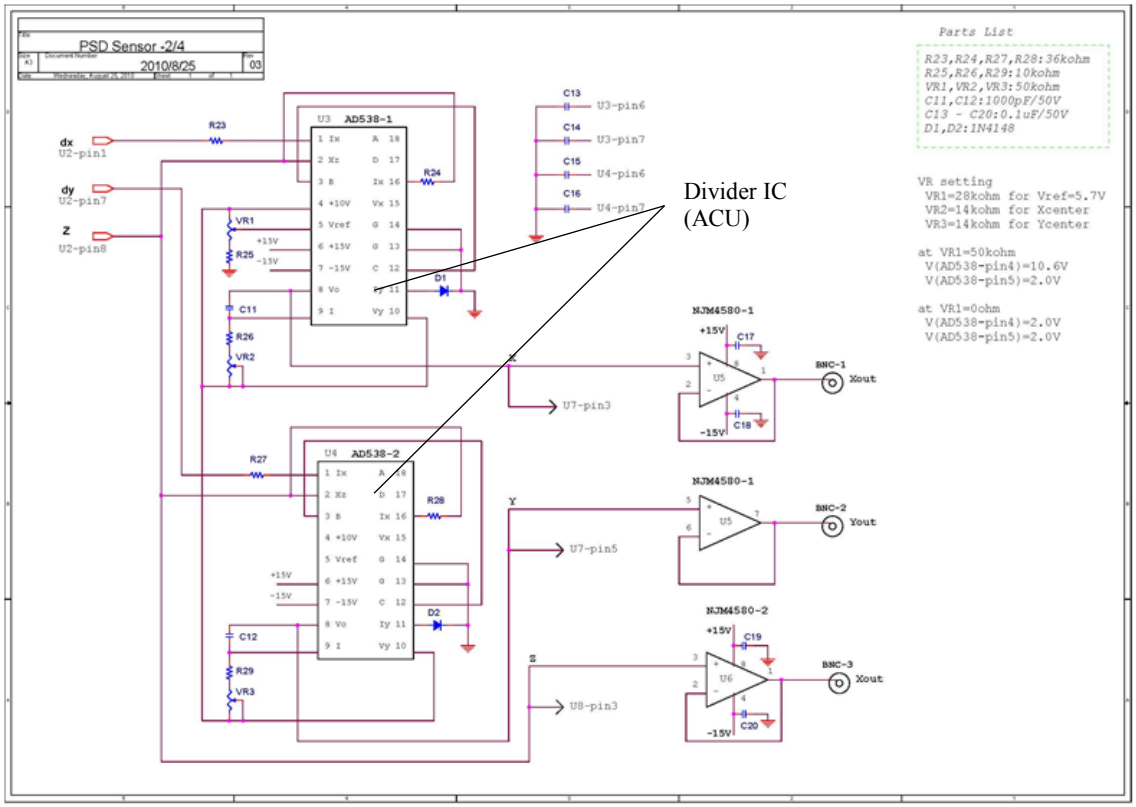
PSD Sensor -2/4
2010/8/25
Parts List
R23,R24,R27,R28:36kohm
R25,R26,R29:10kohm
VR1,VR2,VR3:50kohm
C11,C12:1000pF/50V
C13 - C20:0.1uF/50V
D1,D2:1N4148
VR setting
VR1=28kohm for Vref=5.7V
VR2=14kohm for Xcenter
VR3=14kohm for Ycenter
at VR1=50kohm
V(AD538-pin4)=10.6V
V(AD538-pin5)=2.0V
at VR1=0ohm
V(AD538-pin4)=2.0V
V(AD538-pin5)=2.0V
Divider IC
(ACU)
AD538-1
AD538-2
NJM4580-1
NJM4580-2
Xout
Yout
U7-pin3
U7-pin5
U8-pin3

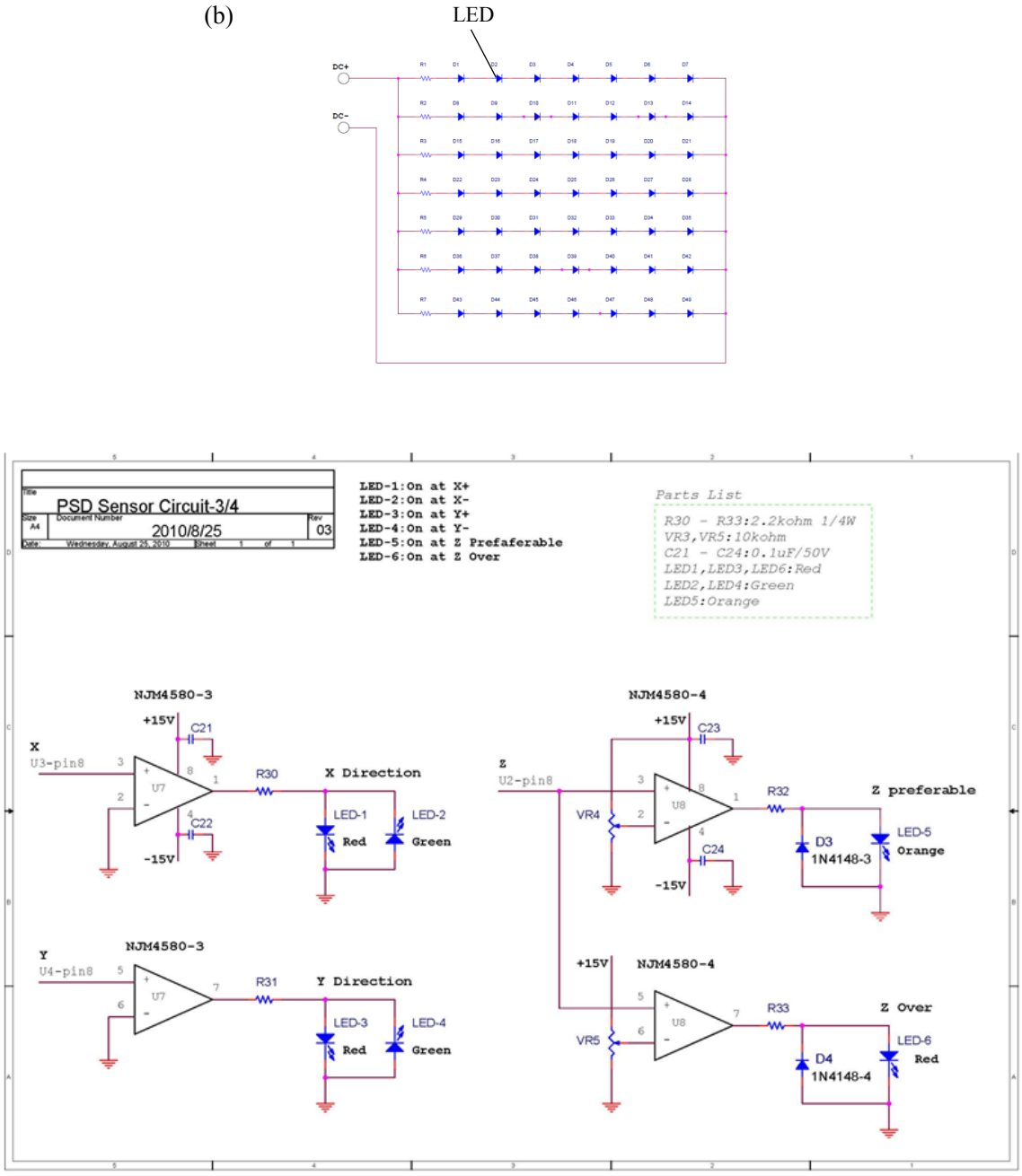

Fig.2.1 Circuit diagram of LDS. (a) PSD circuit, (b) LED array circuit.

A focusing lens (MC CLOSE-UP No.10 KENKO Co., Ltd.) with an aperture diameter of 49 mm and a focal length of 100 mm was utilized as shown in Fig. 2.2 (b). In general, the focal length f is expressed as

$$\frac{1}{a}+\frac{1}{b}=\frac{1}{f}\ , \tag{2.2}$$

$$\frac{[(b/a)+1]^2}{(b/a)}\cdot f = H\ , \tag{2.3}$$

where a is the distance from the light source (object) to the lens, and b is the distance from the lens to the PSD surface. The arrangement of the LED light source, the lens, and the PSD is shown in Fig. 2.2 (c). The optical magnification b/a was designed to be approximately 1/50 by placing the LED array 5 m above the PSD. We utilized an array of red LEDs (OSHR3131P, 625 nm, 25 cd, OptoSupply Ltd.) as a light source instead of a laser. This is because a laser needs a lens with a large numerical aperture, hence the spherical aberration at the outer edges of the lens decreases the accuracy in the position measurement. As shown in Fig. 2.2 (a), the LEDs were aligned to make an 11×11 matrix with the intervals of 4 mm. The image of the light source was focused directly on the central part of the PSD with the lens. By the 1/50 reduced projection, the relative-story displacement of ±50 mm was projected to the PSD surface with the light spot movement of ±1 mm. This reduced projection contributed to increase the accuracy in the position measurement because we could focus the light emitted from the LED array at the central part of the PSD photo-sensitive area and reduced the nonlinearity of the PSD output. The reduced projection contributed also to extending the measurement range [14-16].

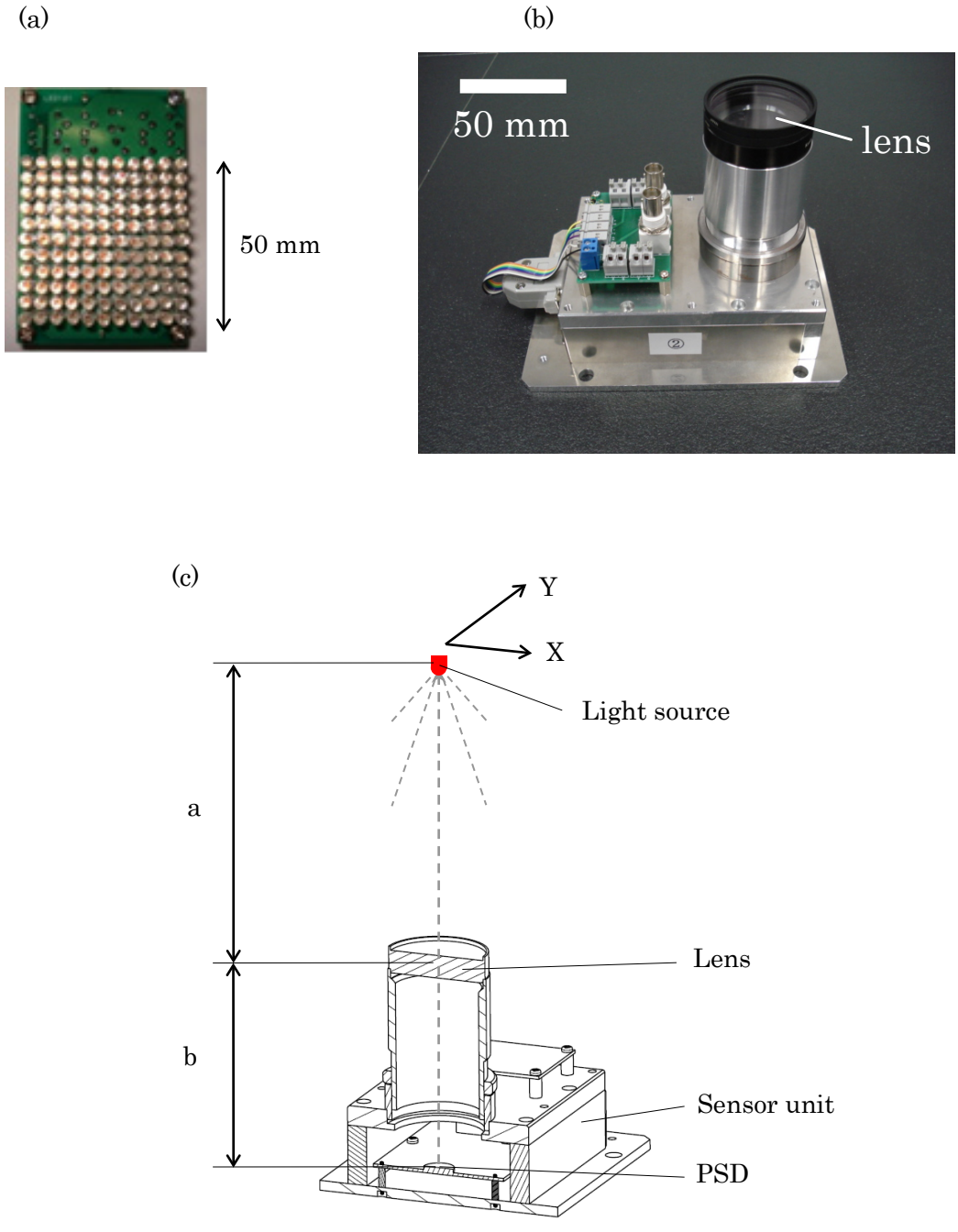

Fig. 2.2 Schematic diagram of LDS. (a) LED array, (b) Sensor unit, (c) Cross-Section diagram.

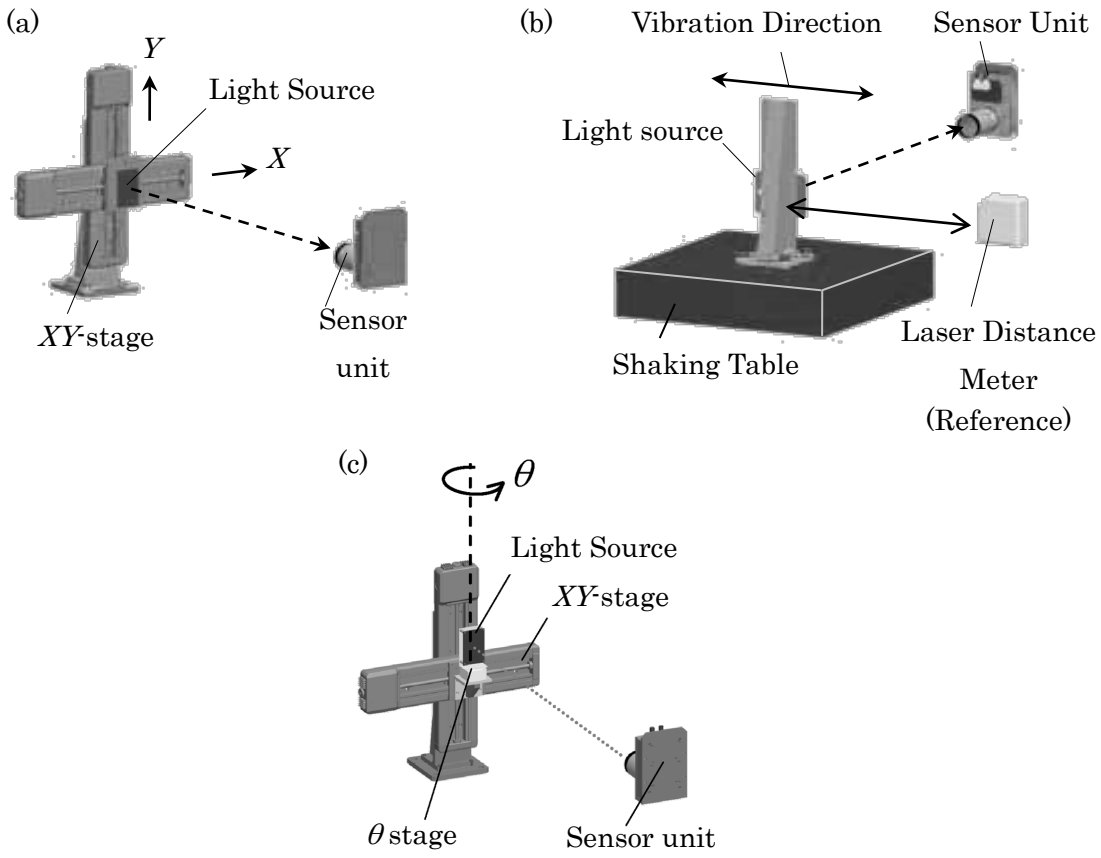

Fig. 2.3 Experimental setup for evaluating the accuracy of LDS. (a) Static experiment. (b) Dynamic response test. (c) Test for effect of the LED rotation.

2.3 Evaluation of the basic performance of the lateral displacement sensor

As shown in Fig. 2.3, for measuring the lateral displacement between the LED array and the sensor unit, we conducted both the static experiments and the frequency response tests. In both experiments, the sensor unit was immobilized at a fixed point, and the light source was displaced by the *XY*-stage or the shaking table.

In the static measurement, the accuracy of the LDS in the lateral displacement measurement was evaluated. The schematic viewgraph of this measurement is illustrated in Fig. 2.3 (a). The position data was investigated

by translating the light source fixed on the *XY*-stage (SGSP26-200XY, ±200 mm, SIGMA KOKI Co., LTD.) in *X* and *Y* directions with a pitch of 0.5 mm and drawing a grid pattern in the *XY* range of ±50 mm. We have paid a special attention to the degradation in the measurement accuracy of the PSD when the PSD is combined with the lens which realizes the reduced projection.

In the frequency response tests, the light source was fixed on the shaking table, and the dynamic response to the sinusoidal vibration of 0.1 to 50 Hz was investigated. A laser distance meter (LK-G405, KEYENCE Corp.) was used as a reference, as shown in Fig. 2.3 (b). The movement of the light source was measured simultaneously by both the laser distance meter and the PSD/lens-combined unit. The position data were recorded with a sampling rate of 20,000 s^{-1}, and a 16-bit data logger was utilized for recording the sampled data.

We investigated also the accuracy of the LDS in the displacement measurement when the LED array was inclined relative to the PSD unit. When the building vibrates in response to earthquakes, it is possible for the LED array and the sensor unit to be inclined with each other since the floor and the ceiling would bend during the seismic vibration. It is conjectured that this inclination affect the measurement accuracy. As shown in Fig. 2.3 (c), the LED array was fixed on a triaxial goniometer composed of a rotational stage (ROTER10 SG, Piezosystem Jena, Inc.) and an *XY*-stage. The PSD unit was immobilized at a fixed point with a distance of 5 m from the LED array. The lateral displacement was measured using the LDS when the LED array was inclined with the angle of 0° to 0.5°, and the error in the displacement measurement was evaluated.

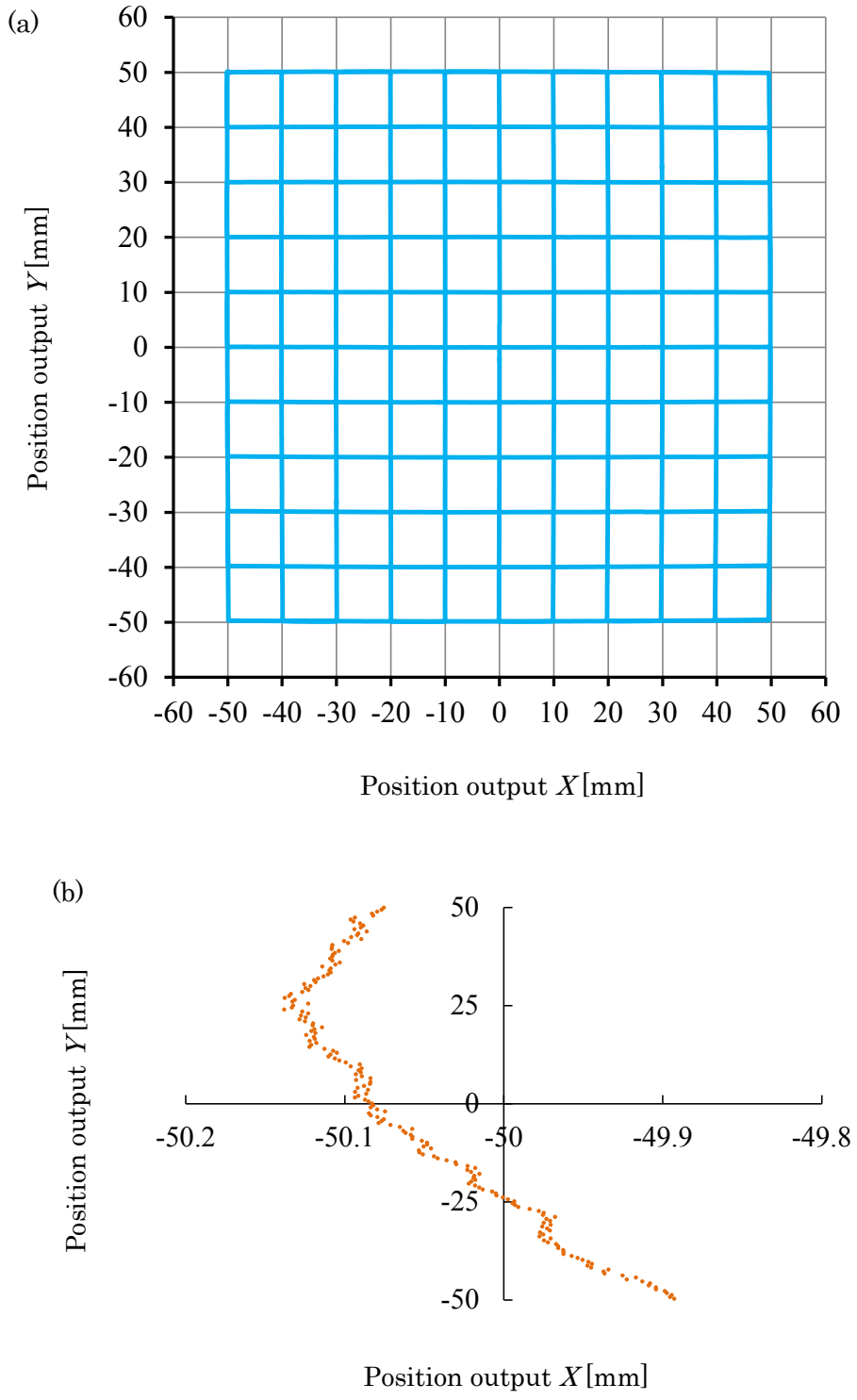

Fig. 2.4 The accuracy of the output from PSD. (a) Two-dimensional grid map of the position output from LDS. (b) The magnified view (X = 50 mm line).

2.4 Results and discussion

Fig. 2.4 shows the two-dimensional (2D) grid map obtained by displacing the LED array laterally to the sensor unit with the *XY*-stage. The maximum deviation evaluated by the grid map is summarized in Table 2.1. The deviation in the static displacement measurement increases with increasing displacement, and the maximum deviation is less than 0.1 mm in the measurement range of ±25 mm. This indicates that the accuracy of the LDS in the displacement measurement is less than 0.1 mm when the measurement distance, *i.e.* the story height, is 5 m and the relative-story displacement is less than ±25 mm.

Table 2.1 Maximum deviation of 2D grid map

Measurement area	Maximum deviation
±10 mm	0.017 mm
±20 mm	0.046 mm
±30 mm	0.10 mm
±40 mm	0.19 mm
±50 mm	0.29 mm

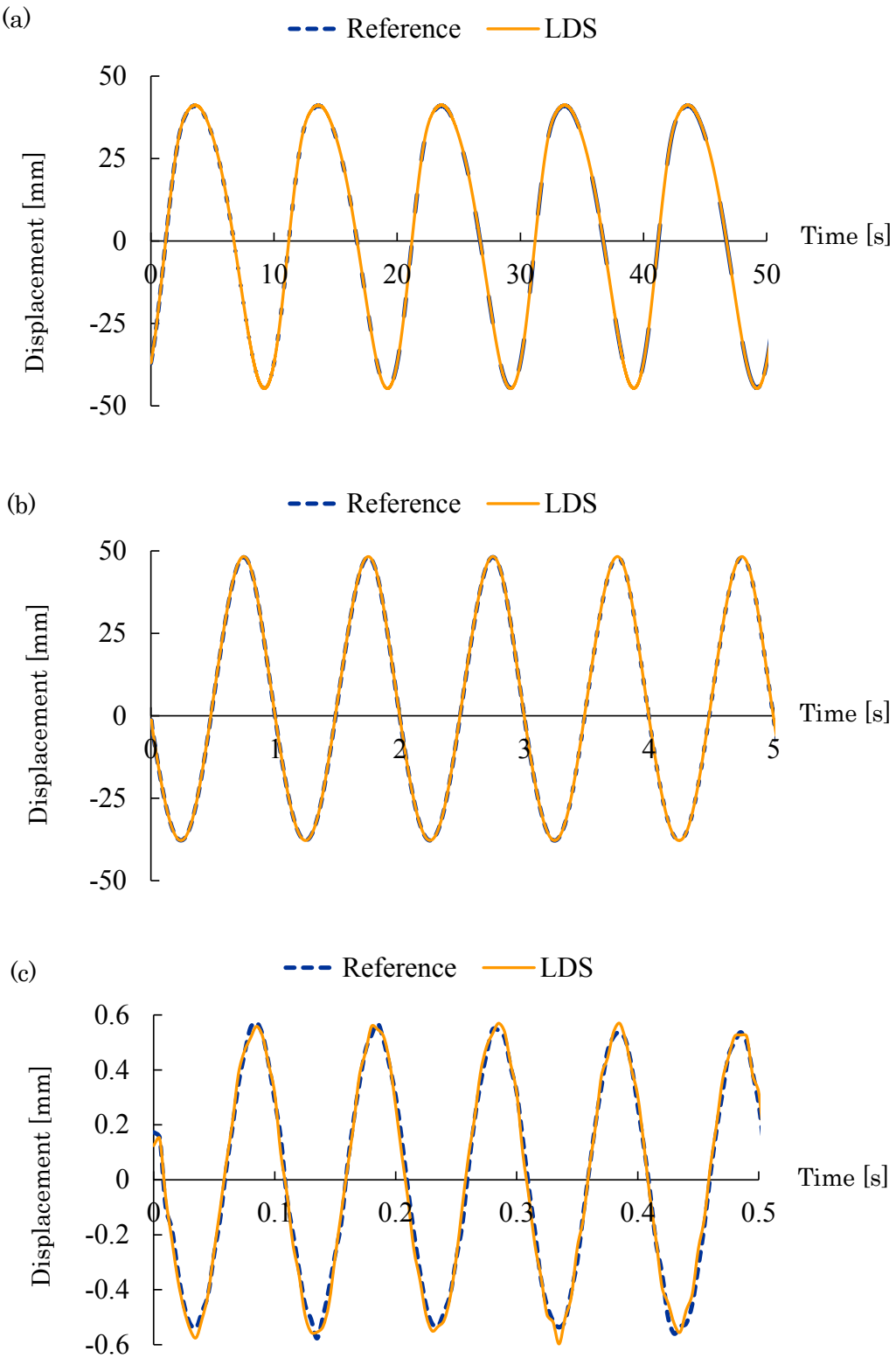
(a)
Reference
LDS
Displacement [mm]
50
25
0
-25
-50
0
10
20
30
40
50
Time [s]
(b)
Reference
LDS
Displacement [mm]
50
25
0
-25
-50
0
1
2
3
4
5
Time [s]
(c)
Reference
LDS
Displacement [mm]
0.6
0.4
0.2
0
-0.2
-0.4
-0.6
0
0.1
0.2
0.3
0.4
0.5
Time [s]

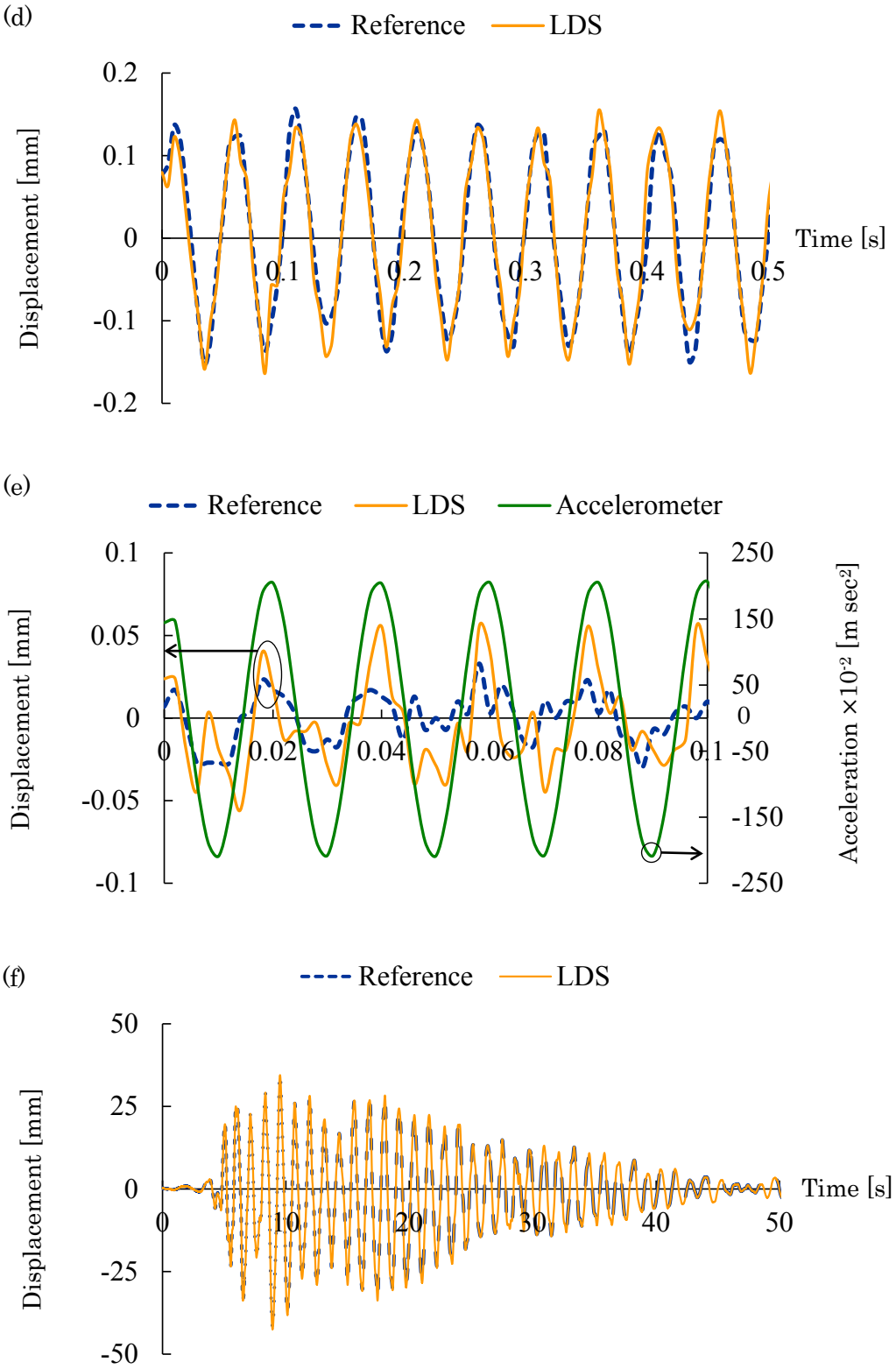

Fig. 2.5 Result of the shaking table tests. (a) 0.1 Hz, (b) 1 Hz, (c) 10 Hz, (d) 20 Hz, (e)50 Hz, (f) The simulated El Centro earthquake.

Figure 2.5 shows the dynamic response of the LDS obtained in the shaking table test. As shown in Fig. 2.5 (a), the data obtained with our LDS almost completely coincide with those with the reference (laser distance meter). As shown in Fig. 2.5 (b), Fig. 2.5 (c) and Fig. 2.5 (d), a good agreement with the reference is observed as well, showing that the error is less than 0.1 mm. Consequently, our LDS fulfills the requirement for the response speed. At frequencies of higher than 50 Hz, as shown in Fig. 2.5 (e), our LDS still follows the original vibration, but some distortion is observed in the measured waveform. The slight distortion of the output waveform are thought to be caused by the rotational motion of the shaking table which is magnified by the 1/50 reduced projection. On the other hand, the conventional laser distance meter completely fails to follow the movement of the shaking table. Eventually this is the limit of the conventional laser distance meter. Finally, we have driven the shaking table with the waveforms of the El Centro earthquake as shown in Fig. 2.5 (f). It is clear that the seismic movement measured with our LDS coincides with the laser distance meter.

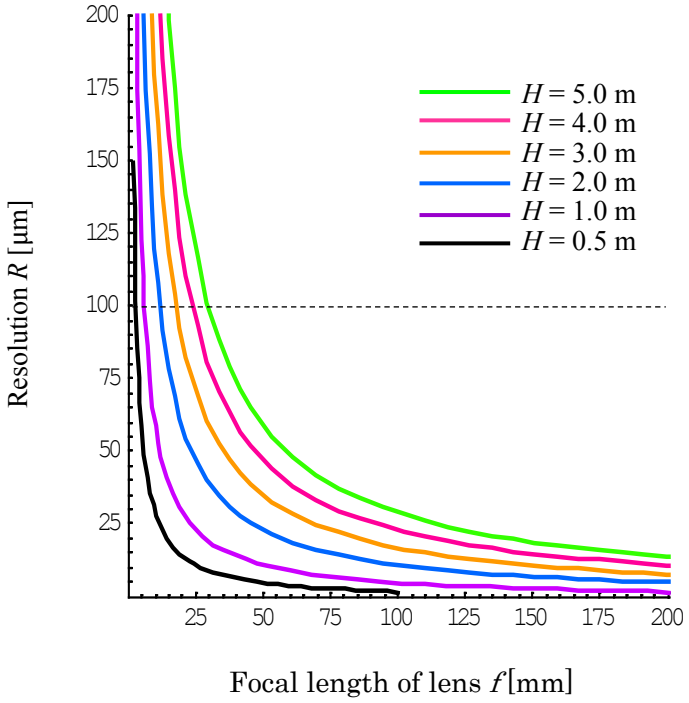

Fig. 2.6 Theoretical resolution of the LDS in the displacement measurement.

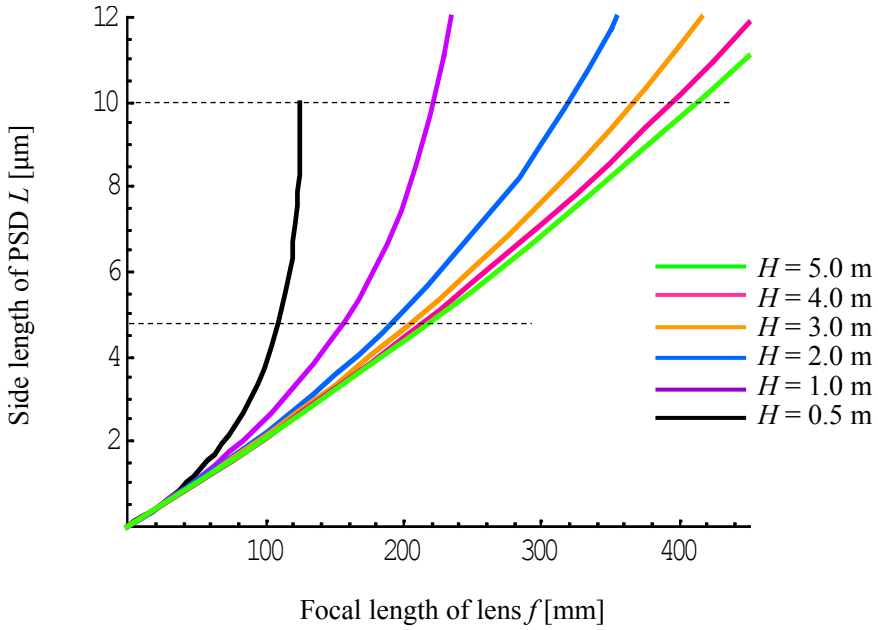

Fig. 2.7 Relationship between the side length of the PSD and focal length of the lens.

We investigated the resolution of the LDS in the displacement measurement theoretically when the focal length of the lens f changes. Using the Equation (2.3), the theoretical resolution of our LDS is expressed as follows.

$$R = \frac{\sigma}{(b/a)} \leqq 100\ \mu m\ , \tag{2.4}$$

where R is the resolution in the displacement measurement in the unit of micrometer and σ is the resolution of the PSD. We assume that σ = 0.6 μm in accordance with the data sheet from the PSD vender. When the story height H is given, the resolution depends on the focal length of the lens according to Equations (2.3) and (2.4). Thus, the optimum focal length of the lens needs to be determined to achieve the resolution of less than 0.1 mm when the story height changes. Figure 2.6 shows the resolution of the LDS in the displacement measurement evaluated theoretically by Equation (2.4). The resolution degrades exponentially with decreasing focal length f, while the resolution degrades gradually with increasing story height H, as shown in Fig. 2.6. To achieve the resolution of less than 0.1 mm for the given story height, Fig. 2.6 indicated that we must use a lens with a longer focal length. Table 2.2 shows the minimum focal length of the lens f_{min} for achieving the resolution of 0.1 mm in the displacement measurement for the given story height H. By using a lens with the focal length of longer than f_{min}, we can achieve the resolution of 0.1 mm. Note that the resolution is improved with increasing focal length but, if we use such a lens, the magnification of the LDS decreases, and the light spot focused on the PSD moves on a wider area. The relationship between the measurement range D and the side length of the PSD L is expressed as follows.

$$D = \frac{L}{2} \cdot \frac{1}{(b/a)} \geqq \frac{H}{100} \quad . \tag{2.5}$$

Equation (2.5) suggests that the PSD with a wide side length L ($\geqq$ $bH/50a$) must be implemented in the LDS, but using such a PSD is distant because the PSD has a limited side length. In Table 2.2, the maximum focal length f_{max} is also shown for the four PSDs with a typical side length. As shown in Table 2.2, by implementing the lens with an optimal focal length in the LDS, the resolution in the displacement measurement of 0.1 mm can be achieved.

Table 2.2 The range of the focal length f for the given story height H.

H [m]	0.5	1.0	1.5	2.0	2.5	3.0	3.5	4.0	4.5	5.0
f_{min} [mm]	2.96	5.93	8.89	11.9	14.8	17.8	20.8	23.7	26.7	29.6
f_{max} [mm] (L = 4.7 mm)	109	154	176	188	196	202	206	210	212	214
f_{max} [mm] (L = 10 mm)	125	222	281	320	347	367	383	395	405	413
f_{max} [mm] (L = 20 mm)	-	250	360	444	510	563	605	640	669	694
f_{max} [mm] (L = 45 mm)	-	-	-	-	623	735	834	922	1000	1070

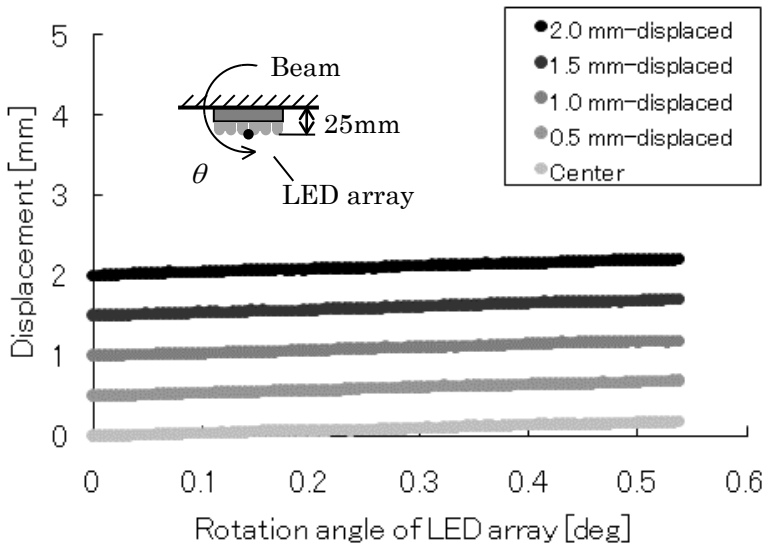

Fig. 2.6 Influence of the rotation angle of the LED array

We investigated also the accuracy of the LDS when the LED array was inclined relative to the PSD unit. Figure 2.6 shows the error of the LDS in displacement measurement when the LED array is inclined relative to the PSD unit using the triaxial goniometer. Figure 2.6 clearly shows that the inclination of the LED array relative to the PSD unit increases the measured displacement value by 0.4 mm deg^{-1}. As shown in the inset of Fig. 2.6, the LED array was fixed on the rotational stage with the distance of 25 mm. Thus, the inclination of θ alters the measured displacement value by $\sin\theta \times 25$ mm, which corresponds to 0.4 mm deg^{-1}, when θ is sufficiently small. The LDS has an accuracy of 60 μm in the displacement measurement; 60 μm corresponds to the angle of 0.15° if the LED array is inclined relative to the PSD unit. Because the rotation angle of the beam is conjectured to be much smaller than 0.15°, we conclude that the inclination of the LED array relative to the PSD unit is negligible.

2.5 Conclusion

We have developed the noncontact-type 2D LDS system that is composed of an LED array, a lens with a fixed focal length, and a pin-cushion type PSD. At a story height of 5 m, the accuracy of the LDS was evaluated to be 0.1 mm in the measurement range of ±25 mm. In the shaking table test, the resolution of the LDS was found to be 0.1 mm when the LED array was vibrated at a frequency of 20 Hz. This response speed of the LDS is sufficient to monitor the seismic displacement in real time, and the LDS can be utilized for the structural displacement monitoring without recourse to the software processing for removing the optical distortion. By implementing the reduced projection and reducing the electrical noise in the electronic circuits, the LDS exhibited the resolution of 60 μm which is sufficiently high for the structural displacement monitoring. We have shown the optimum focal length of the lens by considering both the resolution and the measurement range. If we need the better resolution in the displacement measurement, we should use the lens with a longer focal length and the PSD with a wider side length. Furthermore, we found that the inclination of the LED array relative to the PSD unit was negligible. This verifies the applicability of the proposed LDS for structural health monitoring because the LDS fulfills the requirement of both high resolution and a wide measurement range. These results indicate that the developed LDS is the prime candidate for the measurement of relative-story displacement of buildings.

Bibliography

[1] K. Kusunoki and M. Teshigawara : "A new acceleration integration method to develop a real-time residual seismic capacity evaluation system", Journal of Structural and Construction Engineering, AIJ, No.569, pp.119-126 (2003) (in Japanese)

[2] T. Hiwatashi, Y. Shiozaki, H. Fujitani, and S. Soda : "Semi-active base-isolation system by damper utilizing optimal regulator theory", Journal of Structural and Construction Engineering, AIJ, No.567, pp.47-54 (2003) (in Japanese)

[3] A. Yoshida, Y. Tamura, and S. Ishibashi : "Measurement of wind–induced response of building using RTK-GPS and integrity monitoring", Journal of Structural and Construction Engineering, AIJ, No.571, pp.39-44 (2003) (in Japanese)

[4] A. Niousha and M. Imai : "Displacement measurement of adjacent super high-rise buildings using GPS", AIJ Journal of Technology and Design, No.24, pp.77-82 (2006)

[5] K. Kanda, Y. Miyamoto, A. Kondo, and M. Oshio : "Vision-based measurements for seismic damage monitoring", Journal of Japan Association for Earthquake Engineering, Vol.4, No.1 (2004)

[6] J. J. Lee and M. Shinozuka: "A vision-based system for remote sensing of bridge

displacement" NDT&E International, Vol.39, pp.425-431 (2006)

[7] P. Schaefer, R. D. Williams, G. K. Davis, and R. A. Ross : "Accuracy of position detection using a position-sensitive detector", IEEE Transactions on Instrumentation and Measurement, Vol.47, No.4, pp.914-919 (1998)

[8] A. Mäkynen and J. Kostamovaara : "Accuracy of lateral displacement sensing in atmospheric turbulence using a retroreflector and a position-sensitive detector", Optical Engineering, Vol.36 (11), pp.3119-3126 (1997)

[9] H. J. Woltring : "Single- and dual-axis lateral photodetectors of rectangular shape", IEEE Transactions on Electron Devices, ED-22, pp.581-590 (1975)

[10] R. B. Owen and M. L. Awcock : "One and two dimensional position sensing semiconductor detectors", IEEE Transactions on Nuclear Science, NS-15, No.3, pp.290-303 (1968)

[11] A. Kawasaki and M. Goto : "On the position response of a position-sensitive detector (PSD) irradiated with multiple light beams", Sensors and Actuators A: Physical, Vol.22, pp.534-537 (1989)

[12] A. Nishitani and G. Matsui : "Reinforced Concrete Structures (Revised Edition)", Kajima Publishing Co. (2001)

[13] K. Yamamoto, S. Yamaguchi, and Y. Terada : “New structure of two-dimensional position sensitive semiconductor detector and application”, IEEE Transactions on Nuclear Science, NS-32, No.1 (1985)

[14] I. Matsuya, M. Oshio, R. Tomishi, M. Sato, K. Kanekawa, M. Takahashi, S. Miura, Y. Suzuki, T. Hatada, R. Katamura, Y. Nitta, T. Tanii, S. Shoji, A. Nishitani, and I. Ohdomari : “Noncontact-type relative displacement monitoring system using position sensitive detector”, AIJ Journal of Technology and Design, Vol.16, No.33, pp.469-472 (2010) (in Japanese)

[15] I. Matsuya, R. Tomishi, M. Sato, K. Kanekawa, M. Takahashi, S. Miura, Y. Suzuki, T. Hatada, M. Oshio, R. Katamura, Y. Nitta, T. Tanii, S. Shoji, A. Nishitani, and I. Ohdomari “Development of Noncontact-Type Relative Story Displacement Monitoring System”, The proceedings of the fifth International Workshop on Advanced Smart Materials and Smart Structures Technologies (ANCRiSST 2009), Boston, USA, July 30-31, pp.161-166 (2009)

[16] I. Matsuya, R. Tomishi, M. Sato, K. Kanekawa, Y. Nitta, M. Takahashi, S. Miura, Y. Suzuki, T. Hatada, R. Katamura, T. Tanii, S. Shoji, A. Nishitani and I. Ohdomari : "Development of Lateral-Displacement Sensor for Real-Time Detection of Structural Damage", IEEJ Transactions on Electrical and Electronic Engineering, Vol. 6, No. 3 (accepted for publication in 2011)

Chapter 3
Measurement of relative-story displacement of an actual building using lateral displacement sensor

3.1 Introduction

In this chapter, we show the applicability of the LDS for relative-story displacement measurement of an actual building. We implemented couples of LDSs in an actual three-story building equipped with an active variable stiffness (AVS) system. The building was vibrated with seismic waveforms by an exciter placed on the rooftop, and the relative-story displacement of each layer was monitored by the LDSs in real time.

First, we show the merit of real-time multi-point measurement using the LDSs by comparing with conventional velocimeters. Next, we show that the LDS is able to measure the residual displacement which is difficult to be measured by the conventional velocimeters. To simulate the quasi-damaged state of the building, we utilized the AVS system effectively. The building with the AVS system has

hydraulically actuated braces between every layer and can change the building stiffness can be altered by switching the stiffness of the braces [1-3]. Using the AVS system, we have realized the residual displacement without inducing damage to the building. Finally, based on the relative-story displacement measurement, we show that the rigid beams supporting each floor would bend during the seismic vibration. The LDS was immobilized on the first floor, and another LDS was immobilized on the beam supporting the second floor. These two LDS units were implemented face-to-face so that they measure the displacement between the first and second floor. However, if the second floor bends during the seismic vibration, and the LDS unit on the second floor inclines, the displacement to be evaluated with the LDS must include the error due to the inclination angle [4]. Here, we note that, as mentioned in chapter 1, the inclination of the LED array is negligible, but the inclination of the sensor unit affects the measurement accuracy, as mentioned later. We clarify the effect of the floor bending on the relative-story displacement measurement using the LDS.

3.2 Experimental method

To investigate the feasibility of the LDS as a tool for measuring the relative-story displacement of an actual building, we implemented 5 sets of LDSs in a three-story building equipped with the AVS system, as shown in Fig. 3.1. An exciter with the vibration force of 1.8×10^3 kgf was fixed rigidly on the rooftop. This exciter vibrated the building in the north-south direction, and the vibration force of the exciter corresponded approximately to that of an earthquake with a seismic intensity of 4 on the Japan Meteorological Agency (JMA) scale. The building has

braces on both the east side and the west side. The stiffness of the brace can be controlled by changing the viscosity resistance of the oil damper embedded in the brace. It is known that the resonant frequency of the building is approximately 1.3 Hz when the braces are unlocked, and changes to approximately 2.3 Hz when the braces are locked. Two LDSs were implemented on the west side of the first and the second floor, and one of the LDSs was implemented oppositely so that the PSD unit was fixed on the beam and the LED array was placed on the first floor, as shown in Fig. 3.1 (b). These oppositely arranged LDSs enabled us to measure the inclination angle of the beam relative to the first floor, as discussed later. The displacement of the beam relative to the first floor was measured directly with the LDSs. The displacement was also estimated by integrating the velocity measured with the servo velocimeters which were set up as the reference. Both the displacement data and the velocity data were recorded with a sampling rate of 1,000 samples per second using a 16-bit data logger.

The exciter can vibrate the building with a seismic intensity of up to 4, but it does not induce damage in the building. To simulate the quasi-damaged state of the building, we utilized the AVS system and measured the residual displacement. First, the building was vibrated with a frequency of 1.3 Hz by the exciter placed on the rooftop with all the braces locked. After the vibration reached the steady state, we unlocked all the braces at once, and wait for 10 s until the vibration amplitude increased. This excitation simulates the seismic vibration. Finally, we locked all the braces again during the vibration. The vibration center of the second floor is displaced if we lock all the braces at a moment when the second floor is not located at the vibration center. Thus, taking advantage of the AVS system, we can realize

the residual displacement without inducing damage to the building. We analyzed the lateral displacement of the second floor measured with both the LDS and the servo velocimeter.

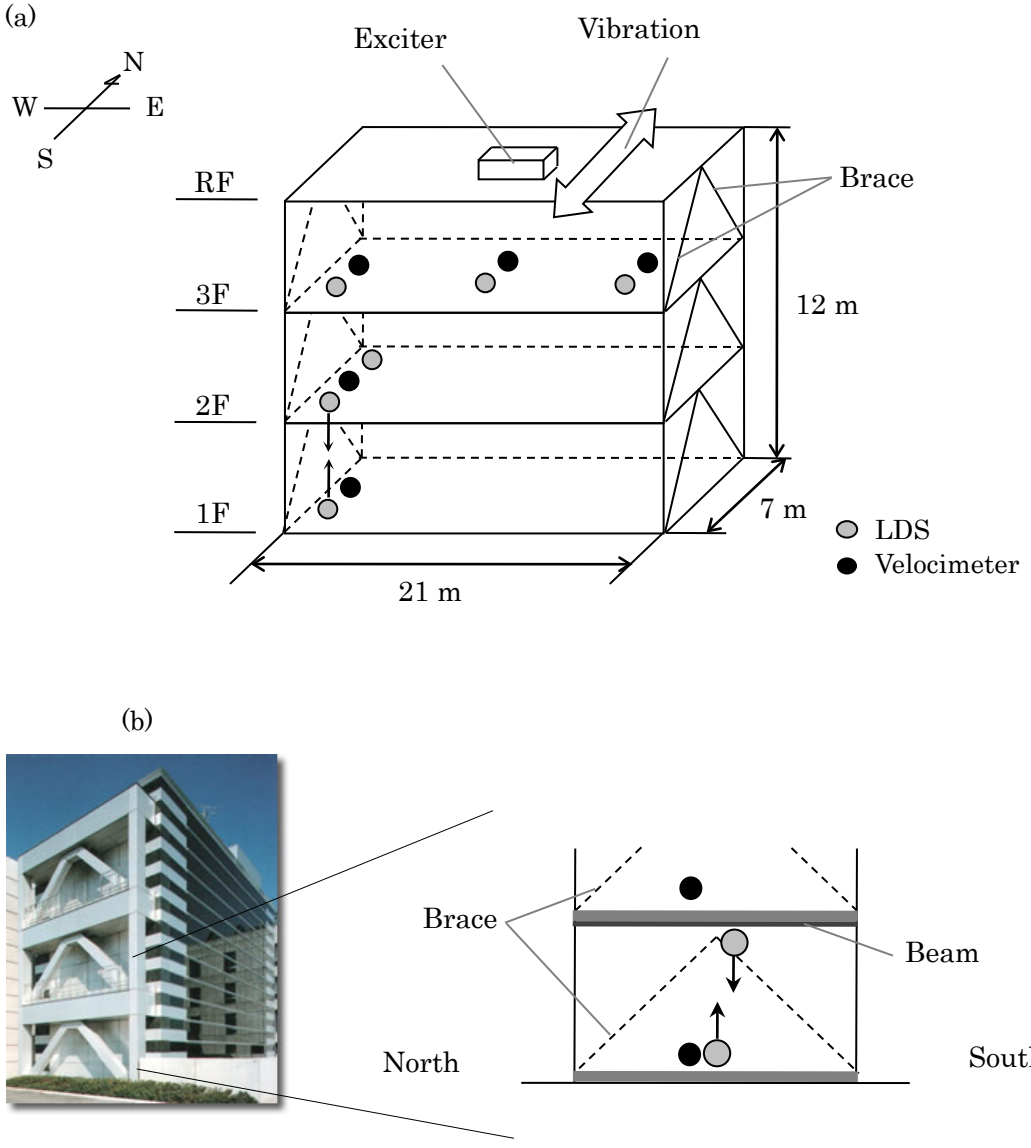

Fig. 3.1 Experimental setup of the LDSs implemented in a three-story building equipped with an AVS system. (a) Birds-eye-view, and (b) View from the west. The arrows from the gray circles indicate the direction of the PSD unit to the LED array.

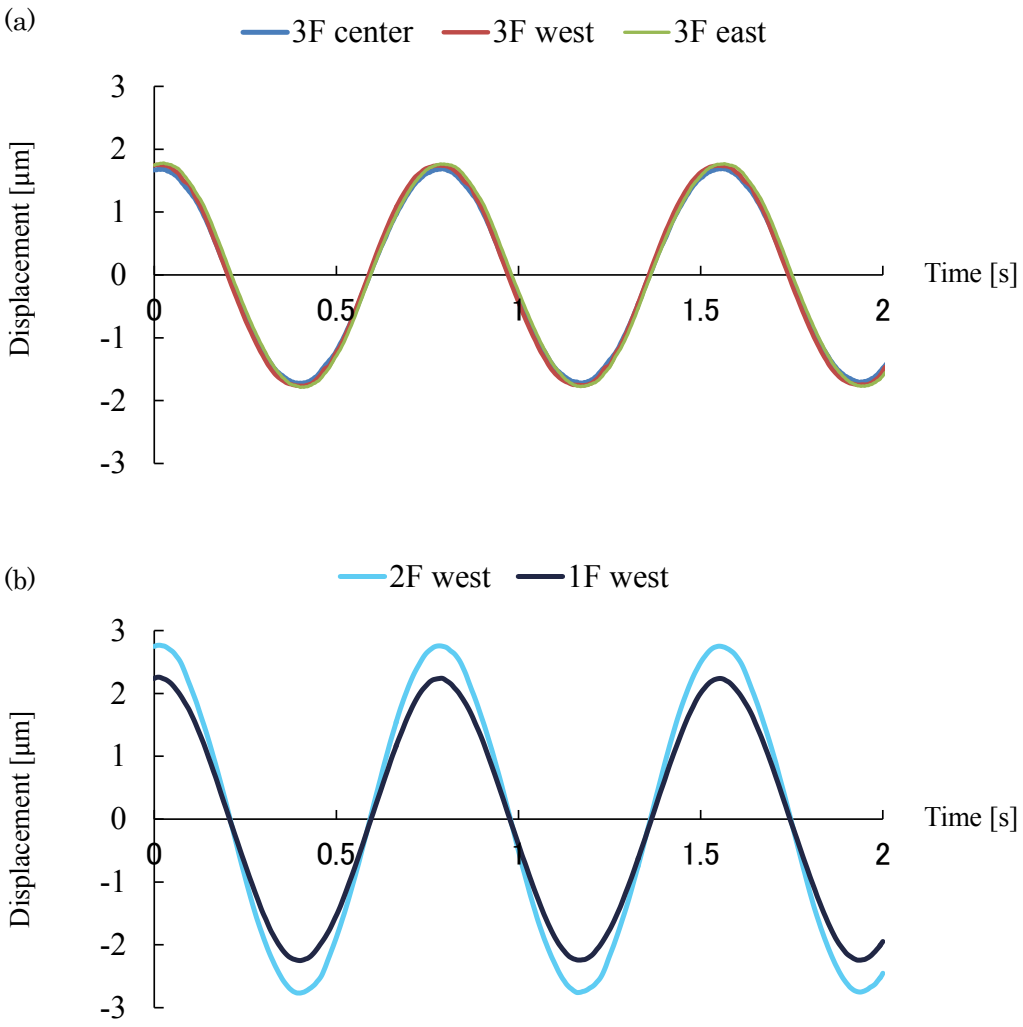

Fig. 3.2 Displacement by LDSs vibrated with the sinusoidal waveform of 1.3 Hz (a) Displacement measured by LDSs on the 3F. (b) Displacement measured by LDSs on 1F and 2F west.

3.3 Results and discussion

First, we evaluated the displacement measured by the LDSs implemented on the third floor. Fig. 3.2 shows the displacement measured by LDSs vibrated with the sinusoidal waveform of 1.3 Hz. As shown in Fig. 3.2 (a), the displacements

measured by the three LDSs coincides with each other with the amplitude of 1.75 mm. This indicates that the building has been vibrated without twisting. Fig. 3.2 (b) shows the displacement of the first floor and that of the second floor. The amplitude of the vibration measured on the first floor to the third floor is in good agreement with amplitude expected in an actual earthquake. In particular, the vibration of the second floor exhibited the highest amplitude, indicating that the excitation from the rooftop simulated the seismic vibration because, in general, the second floor vibrates frenziedly during the earthquake.

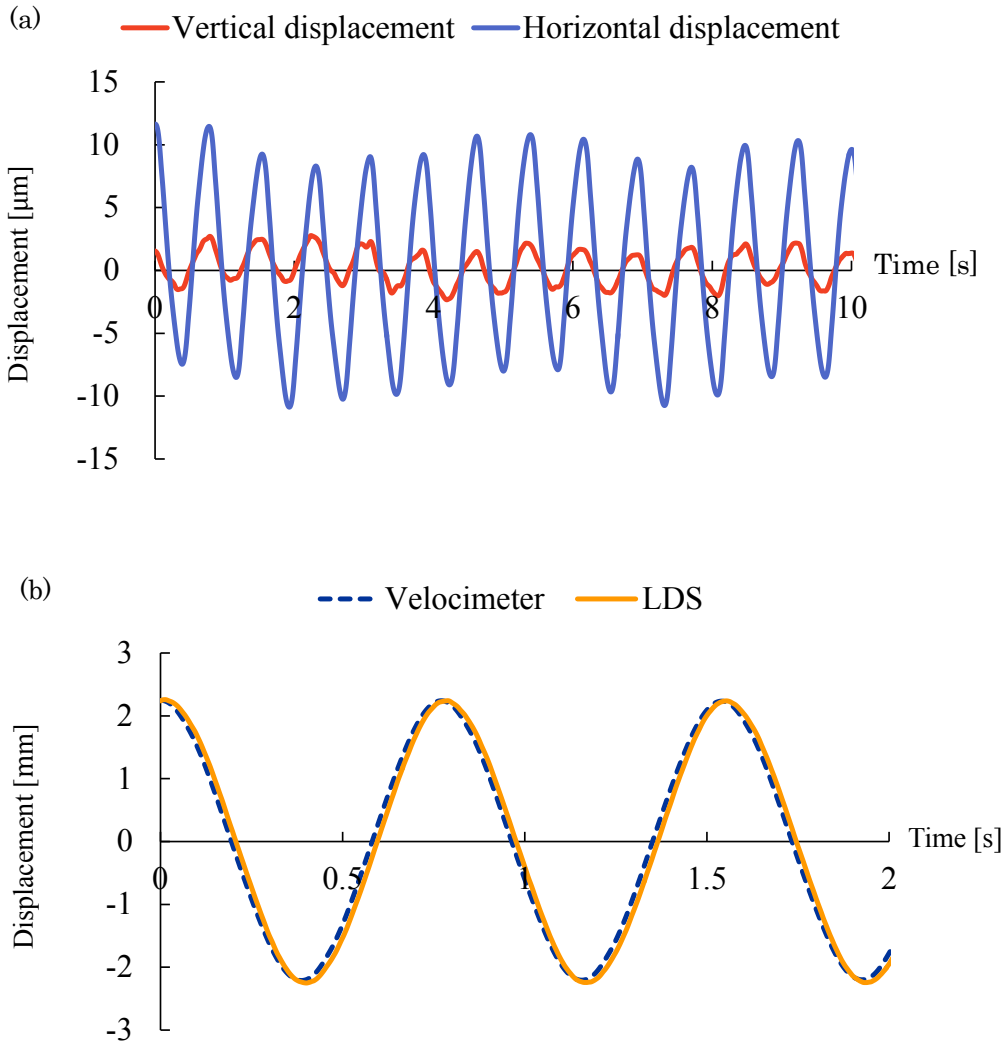

Fig. 3.3 Displacement measured with the LDS and the velocimeter. (a) Displacement of the first floor measured with the velocimeter. (b) Displacement of the second floor relative to the first floor measured with the LDS. The displacement of the second floor estimated with the velocimeter immobilized on the second floor is also depicted.

We also evaluated the displacement of the first floor. Because the first floor is assumed to be the fixed point even when the building is vibrated with the exciter, such a fixed point provides an origin for the displacement measurement. Figure 3.3 (a) shows the displacement of the first floor measured with the volocimeter. The building was vibrated with the sinusoidal waveform of 1.3 Hz. The results show that, although the first floor slightly vibrates both horizontally and vertically, the displacement of the first floor is negligible because the maximum displacement is less than 10 μm, which is much less than the accuracy of the LDS (100 μm). The fact that the displacement of the first floor is negligible indicates that we can measure the displacement of the second floor with the velocimeter placed on the second floor. The integral of the velocity measured with the velocimeter on the second floor gives the lateral displacement of the second floor relative to the first floor. Figure 3.3 (b) shows the displacement of the second floor measured with the velocimeter. The displacement between the first floor and the beam measured with the LDS is also depicted in Fig. 3.3 (b). Because the beam is fixed to the second floor, we can compare the two displacements. The displacement measured with the LDS indicates that the second floor vibrates with the amplitude of 2.26 mm, whereas that measured with the velocimeter indicates that the vibration amplitude is 2.23

mm. We have compared the displacement measured with the LDS and that measured with the velocimeter when the building was vibrated with a sinusoidal waveform of 1.3 Hz with the vibration force of 0.3×10^3 kgf to 1.8×10^3 kgf. The displacements measured with the LDS coincided with those measured with the velocimeter within the error of 60 μm (data not shown). The discrepancy of 60 μm is within the permissible range for structural health monitoring.

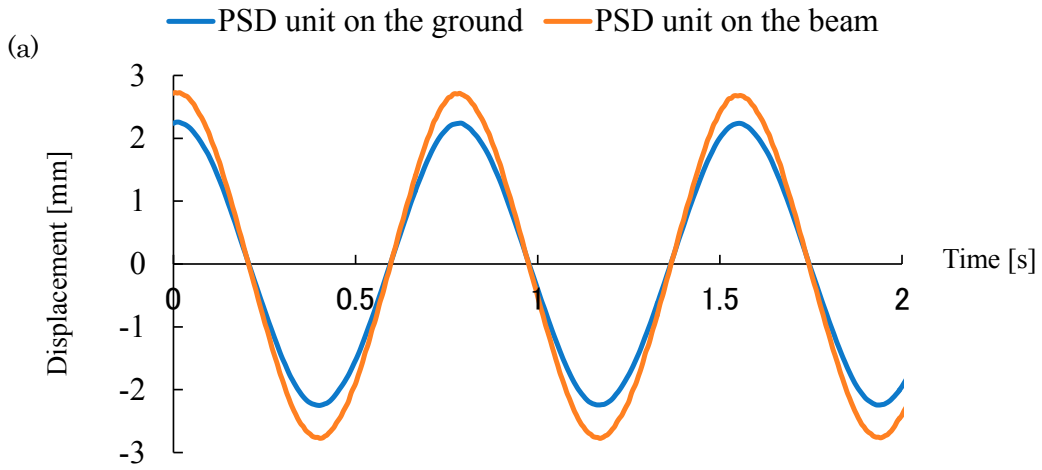

Fig. 3.4 The local inclination angle and the torsion angle of the building measured with the LDSs. Relative displacement between first floor and the second floor measured with two LDSs arranged oppositely. The discrepancy in the displacement indicates the inclination of the second floor relative to the first floor.

Next, we evaluated the inclination angle of the beam using two LDSs. Figure 3.4 shows the displacement between the first floor and the beam. When the

displacement of the LED array fixed on the beam was measured with the PSD unit placed on the first floor, the vibration amplitude of the beam was evaluated to be 2.26 mm. When the displacement of the LED array placed on the first floor was measured with the PSD unit fixed on the beam, the first floor seemed to have vibrated with the amplitude of 2.76 mm. This discrepancy of 0.5 mm can be explained as follows. The displacement can be measured correctly even when the LED array is inclined relative to the PSD unit, as mentioned in chapter 2. This is true if the PSD unit is immobilized on the immobile first floor. However, if the PSD unit is fixed on the inclinable beam, the inclination of the PSD unit affects the accuracy of the displacement measurement. Namely, if the PSD unit is inclined by θ, the LED array appears to be displaced laterally by $(1 / 50) \times H \tan\theta$, where H is the distance between the beam and the first floor. Thus, by using two LDSs that are oppositely arranged between the first floor and the beam, we can evaluate the inclination angle of the beam. The maximum inclination angle is estimated to be ±0.008° when the distance between the first floor and the beam is 3.5 m. Because the accuracy of the LDS in the displacement measurement is 60 μm, the accuracy of the inclination angle measurement is evaluated to be ±0.001°.

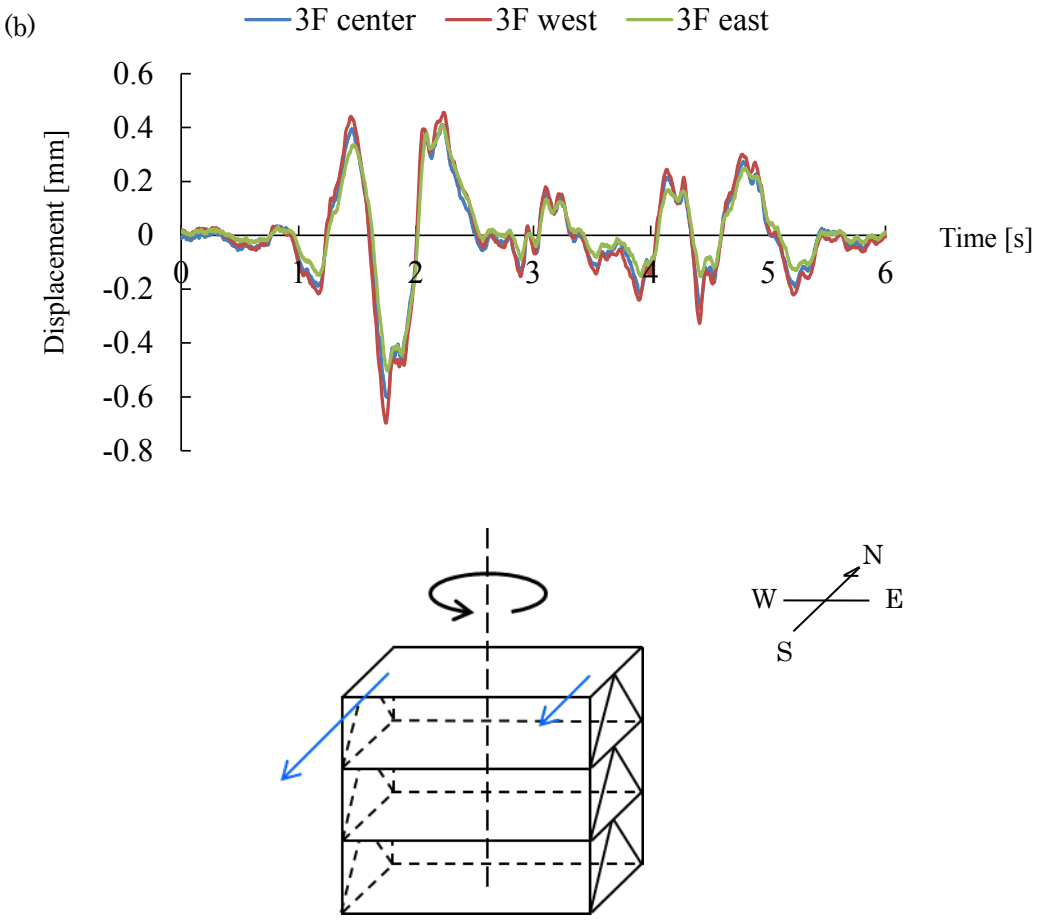

Fig. 3.5 The torsion of the building. (a) Displacement measured with three LDSs on the third floor vibrated with El Centro NS waveform. (b) The torsion angle estimated from the three-PSD outputs.

We also evaluated the torsion angle of the third floor by using three LDSs on the third floor. Figure 3.5 (a) shows the displacement measured by three LDSs on the third floor vibrated with the simulated El Centro NS waveform. The maximum displacements measured by the LDSs are -0.72 mm in the west, -0.65 mm in the center and -0.56 mm in the east, respectively. As compared with Fig.

3.2 (a) and Fig. 3.5 (a), the difference clearly shoes that the building vibrated with the El Centro NS waveform has twisted. Namely, the amplitude of the west-side was higher than that of the east-side, as shown in Fig. 3.5 (b). This is totally different from the pure sinusoidal waveform of 1.3 Hz, as shown in Fig. 3.2 (a).

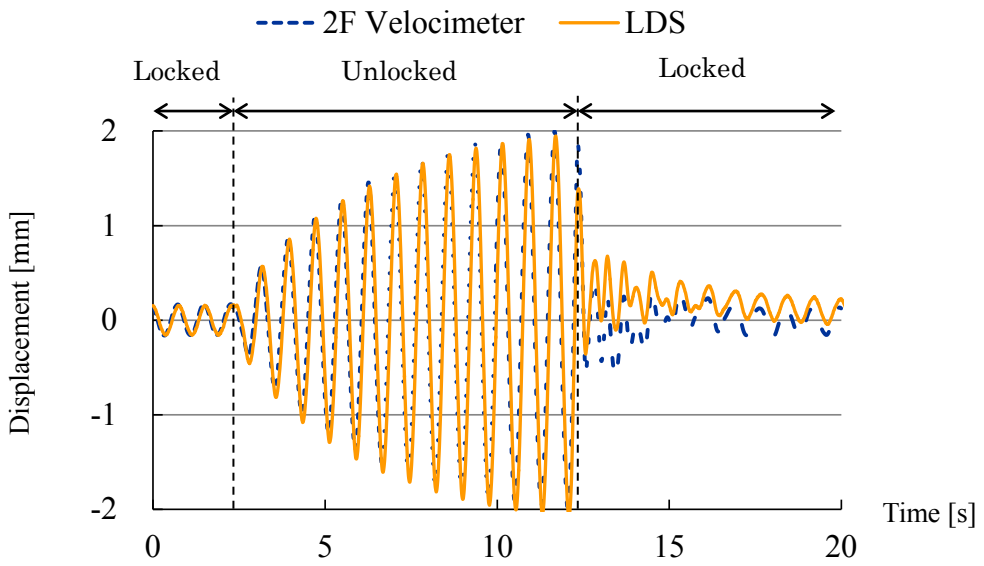

Fig. 3.6 Residual displacement of second floor measured both with the LDS and the servo velocimeter. The residual displacement was realized by controlling the displacement of the second floor using the AVS system.

Finally, we measured the residual displacement between the first floor and the second floor. Because the residual displacement is evidence that the building has incurred damage [5]. Figure 3.6 shows the residual displacement measured with the LDS. We measured the displacement of the beam relative to the floor by

fixing the LED array on the beam and immobilizing the PSD unit on the first floor. The displacement between the first floor and the second floor was estimated also with the velocimeter that was immobilized on the second floor. The displacements exhibited sinusoidal vibration with small amplitude when we vibrated the building with a frequency of 1.3 Hz with all braces locked. During vibration, the displacement measured with the LDS and that measured with the velocimeter were in good agreement. When the braces were unlocked, the displacements increased with time, since the excitation frequency was controlled to be equivalent to the resonant frequency of the building. After we locked all the braces again during the resonant vibration, the vibration amplitude became small, but there was a discrepancy between the displacement measured with the LDS and that measured with the velocimeter. The vibration center measured with the LDS was displaced by 0.15 mm while the vibration center measured with the velocimeter remained at the original point. Because the second floor was not located at the vibration center at the moment when the braces were locked, the vibration center must have been displaced after the braces were locked. Thus, the displacement measured with the LDS is correct. In contrast, the displacement estimated by integrating the velocity did not follow the actual movement of the second floor. These results clearly indicate that the residual displacement cannot be evaluated correctly by a method that requires integration. A differential quantity is measured by the accelerometer and the velocimeter, and the residual displacement is eliminated when the displacement is differentiated. In other words, only a direct method of measuring displacement can provide the integral constant that corresponds to the residual displacement because the low-frequency constituent of the displacement is

eliminated owing to the property of the velocimeter [6]. This is the advantage of using the LDS for structural-health monitoring. Statistical analyses of displacements measured using an array of LDSs would provide more information about the health of a building, such as the state of damage-sensitive elements and the seismic capacity of the building, but these analyses are beyond the scope of this chapter. We emphasize that in the near future, the advanced LDS would be sufficiently small and suitable for the real-time multipoint measurement of relative story displacement.

3.4 Conclusion

Taking advantage of the AVS system implemented in the building, residual displacement was realized without inducing damage to the building. We measured the residual displacement induced in the second floor of the building using the LDS in real time, while the conventional velocimeter immobilized on the second floor could not provide a correct measurement of the residual displacement. These results indicate that the developed LDS is more useful than conventional method for the health diagnosis of a building structure in real time.

The remained problem is the bending of each floor during seismic vibration. This floor bending inclines the PSD unit and affects the accuracy in the relative-story displacement measurement. In the following chapter, we show the alternative method to measure the relative-story displacement and the inclination angle at the same time.

Bibliography

[1] M. Takahashi, T. Kobori, T. Nasu, and A. Kunisue : "Study on control characteristics of active variable stiffness system applied to a high-rise building", J. Struct. Constr. Eng., AIJ, No.531, pp.79-86 (2000) (in Japanese)

[2] T. Nasu, T. Kobori, K. Ishii, M. Takahashi, Y. Matsunaga, N. Tanba, and K. Ogasawara : "Development of active variable stiffness system (part-1) outline of the applied building and composition of the AVS system", Summaries of technical papers of Annual Meeting AIJ. B, Structures I pp.1065-1066 (1991) (in Japanese)

[3] S. Hiehata, T. Kobori, M. Takahashi, J. Hirai, T. Nasu, J. Tanoue, S. Kurata, and T. Mizuno : "Development of active variable stiffness system (part-2) forced vibration and stiffness changing test of the building with the AVS system", Summaries of technical papers of Annual Meeting AIJ. B, Structures I, pp.1067-1068 (1991) (in Japanese)

[4] J.W. Park, H.J. Jung and J.J. Lee : "Vision-based displacement measurement method for high-rise building structures using partitioning approach", The proceedings of the fifth international workshop on advanced smart structures technology (ANCRiSST 2009), Boston, USA, July 30-31, pp.122-129 (2009)

[5] K. Kusunoki and M. Teshigawara : “A new acceleration integration method to develop a real-time residual seismic capacity evaluation system”, Journal of

Structural and Construction Engineering, AIJ, No.569, pp.119-126 (2003) (in Japanese)

[6] I. Matsuya, R. Tomishi, M. Sato, K. Kanekawa, Y. Nitta, M. Takahashi, S. Miura, Y. Suzuki, T. Hatada, R. Katamura, T. Tanii, S. Shoji, A. Nishitani and I. Ohdomari : "Development of Lateral-Displacement Sensor for Real-Time Detection of Structural Damage", IEEJ Transactions on Electrical and Electronic Engineering, Vol. 6, No. 3 (accepted for publication in 2011)

Chapter 4
Simultaneous measurement of relative-story displacement and inclination angle using multiple lateral displacement sensors

4.1 Introduction

In chapter 4, we propose a method to measure both the relative-story displacement and the inclination angle of the floor using multiple lateral displacement sensors (LDSs). As discussed in chapter 3, the building floor is not a perfectly rigid layer, but it bends during seismic vibration. This floor bending causes error in the relative-story displacement measurement because the PSD unit is inclined due to bending floor. Thus, in practical use, the LDS system must be improved so as to accurately measure the relative-story displacement even though the PSD unit is inclined.

As shown in Fig. 4.1, the local rotation angle ϕ, θ, and the torsion angle ψ must be measured as well as the relative-story displacement δ. Especially, to accurately measure the relative-story displacement δ, measuring the local

inclination angle θ is important. The similar measurement has been already realized in the image stabilizer of a digital camera where the captured image is automatically stabilized against unstable handling using the embedded gyro sensor [1]. However, such a gyro sensor does not work in case of seismic vibration because the frequency of the seismic motion is too low (from DC to 20 Hz), and also the inclination angle is too small (approximately 0.001 degree). Olaszek developed a novel system called the additional reference system which stabilizes the image using two reference points [2]. Although they could stabilize the captured image when the camera was vibrated in the vertical direction at a low frequency, they could not stabilize the image if the camera was inclined to the two reference points. Thus, the additional reference system is not applicable to the relative-story displacement measurement. Park and his group proposed a method called the partitioning approach which can measure the relative-story displacement and the inclination angle of the floor by implementing two video cameras on every floor [3]. Myung and his group also proposed the similar method [4]. However, as mentioned in chapter 2, a video camera requires additional computational image processing such as pixel scanning, object identification, and contour definition, and is not suitable for our purpose. Moreover, in the partitioning approach, the cameras must be set up in the open ceiling space to monitor the motion of both the upper layer and the two-story-upper layer using the two cameras. Thus, the partitioning approach is not a convenient method for the relative-story displacement measurement. With these points in mind, we opted to develop a novel method that can simultaneously measure the relative-story displacement and the inclination angle of the floor.

In this chapter we propose a new method using a pair of lateral displacement sensors (LDSs). We call a pair of LDSs installed in one place as the combined LDS system. First, we show that, using the combined LDS system, the relative-story displacement δ and the local rotation angle θ can be measured independently. Next, we evaluate the performance of the combined LDS system using the results of static and dynamic response tests. In the static response test, the Jacobian matrix for transforming the XY-coordinate of the two PSD units (X_1, X_2) to the (δ_x, θ_y) coordinate was introduced theoretically and was compared with the experimental data. In the dynamic response test, the LED arrays were displaced in δ_x direction using a shaking table, and the combined LDS system was inclined with the inclination angle of θ_y using a θ-stage. The displacement δ_x and the inclination angle θ_y were measured directly in real time. Finally, we discuss the response speed and the resolution of the combined LDS system.

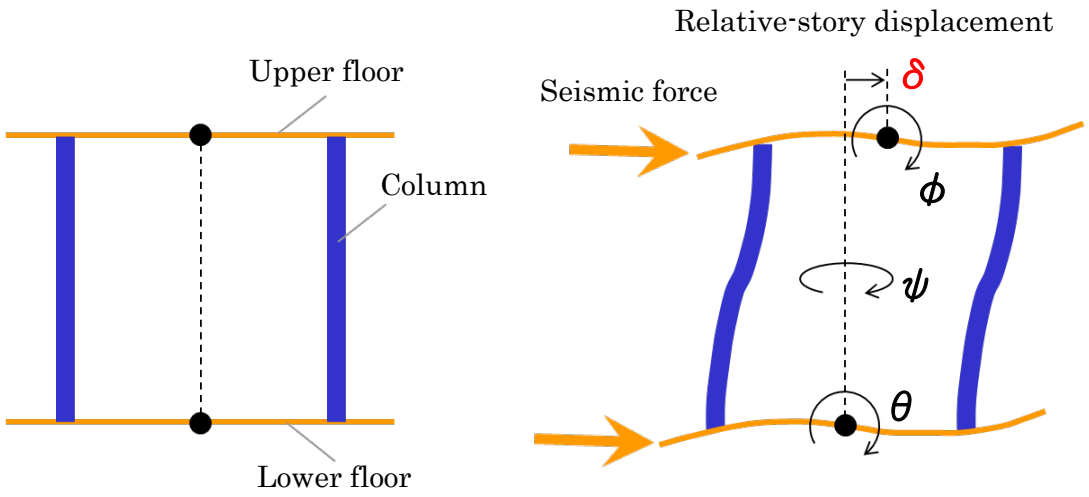

(1) Before earthquake (2) During earthquake

Fig. 4.1 Deformation of a building during seismic vibration.

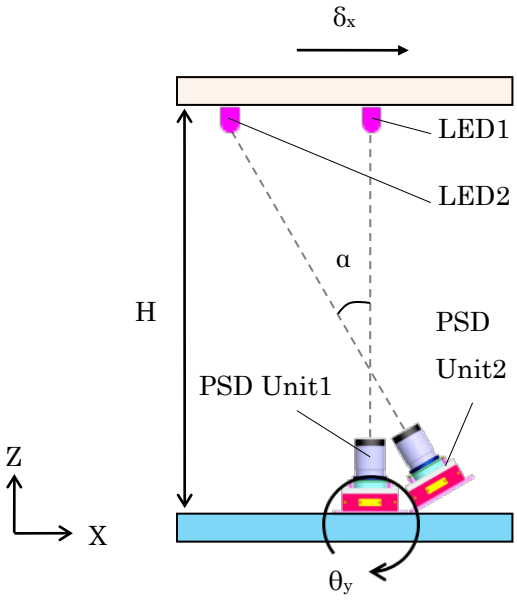

Fig. 4.2 Schematic diagram of the combined LDS system for measuring the relative-story displacement and the inclination angle.

4.2 Theoretical model

Figure 4.2 shows the schematic diagram of the combined LDS system. The position of two light sources immobilized on the ceiling is located at (0, 0, H) and (-d_0, 0, H) respectively. The PSD unit 1 is at the original position (0, 0, 0), and the PSD unit 2 is located at (l_0, 0, 0). The PSD unit 2 is installed with an inclination angle α so that the PSD unit 2 faces the LED 2. Moreover, the PSD unit 1 and the PSD unit 2 are rigidly connected with each other and immobilized on the floor. In accordance with the arrangement of the PSD unit 1 and the LED 1, the distance between the ceiling and the floor H is expressed as

$$\frac{[(b/a)+1]^2}{(b/a)} \cdot f = H, \tag{4.1}$$

where, a is the distance from the lens to the ceiling, b (= $H - a$) is the distance from the PSD 1 to the lens, and f is the fixed focal length of the lens. In Equation (4.1), the ratio b/a represents the magnification of the PSD unit 1. In this arrangement, the position of the light spot (X_1, Y_1) focused on the PSD 1 is expressed as

$$X_1 = \frac{\mathrm{b}}{a}(-\delta_x + H\theta_y), \tag{4.2}$$

$$Y_1 = \frac{\mathrm{b}}{a}(-\delta_y - H\theta_x), \tag{4.3}$$

where (δ_x, δ_y) is the lateral displacement of the LED 1, and (θ_x, θ_y) is the inclination angle of the PSD unit 1 [1, 5]. Similarly, the position of the light spot (X_2, Y_2) focused on the PSD 2 is expressed as

$$X_2 = \frac{b'}{a'}[-\cos\alpha \cdot \delta_x + (\frac{H}{\cos\alpha} - l_0 \sin\alpha)\theta_y], \tag{4.4}$$

$$Y_2 = \frac{b'}{a'}\left(-\delta_y - H\theta_x\right) - l_0\psi, \tag{4.5}$$

where (δ_x, δ_y) is the lateral displacement of the LED 2, and the ratio b'/a' is the magnification of the PSD unit 2. Since the PSD unit 2 is inclined with respect to the vertical line, the distance from the PSD 2 to the LED 2 differs from the story height H, and the magnification of the PSD unit 2 b'/a' differs from that of the PSD

unit1 (b / a). In Equations (4.2) to (4.5), we assume that the inclination angles of θ_x and θ_y are positive when they are clockwise rotated, and that the center of rotation is the original point. We show the Jacobian matrix for our experimental setup in the following section.

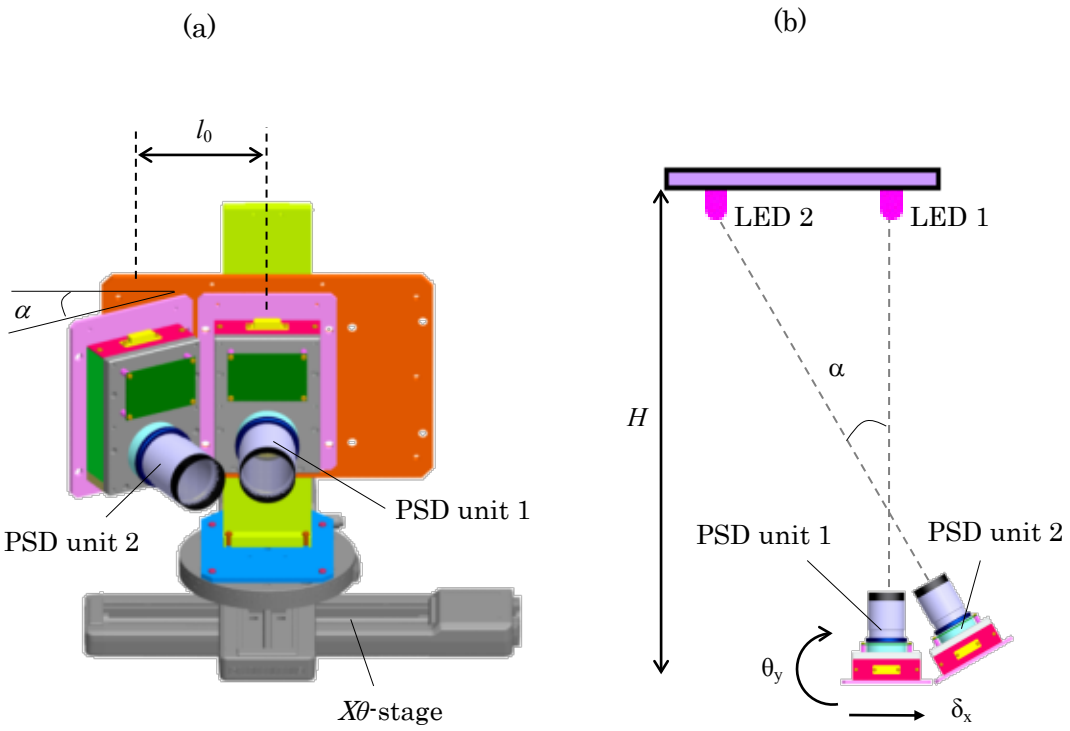

Fig. 4.3 Experimental setup for measuring the relative-story displacement and the inclination angle using two LDSs. (a) Birds eye view of two LDSs, (b) *XZ*-plane view.

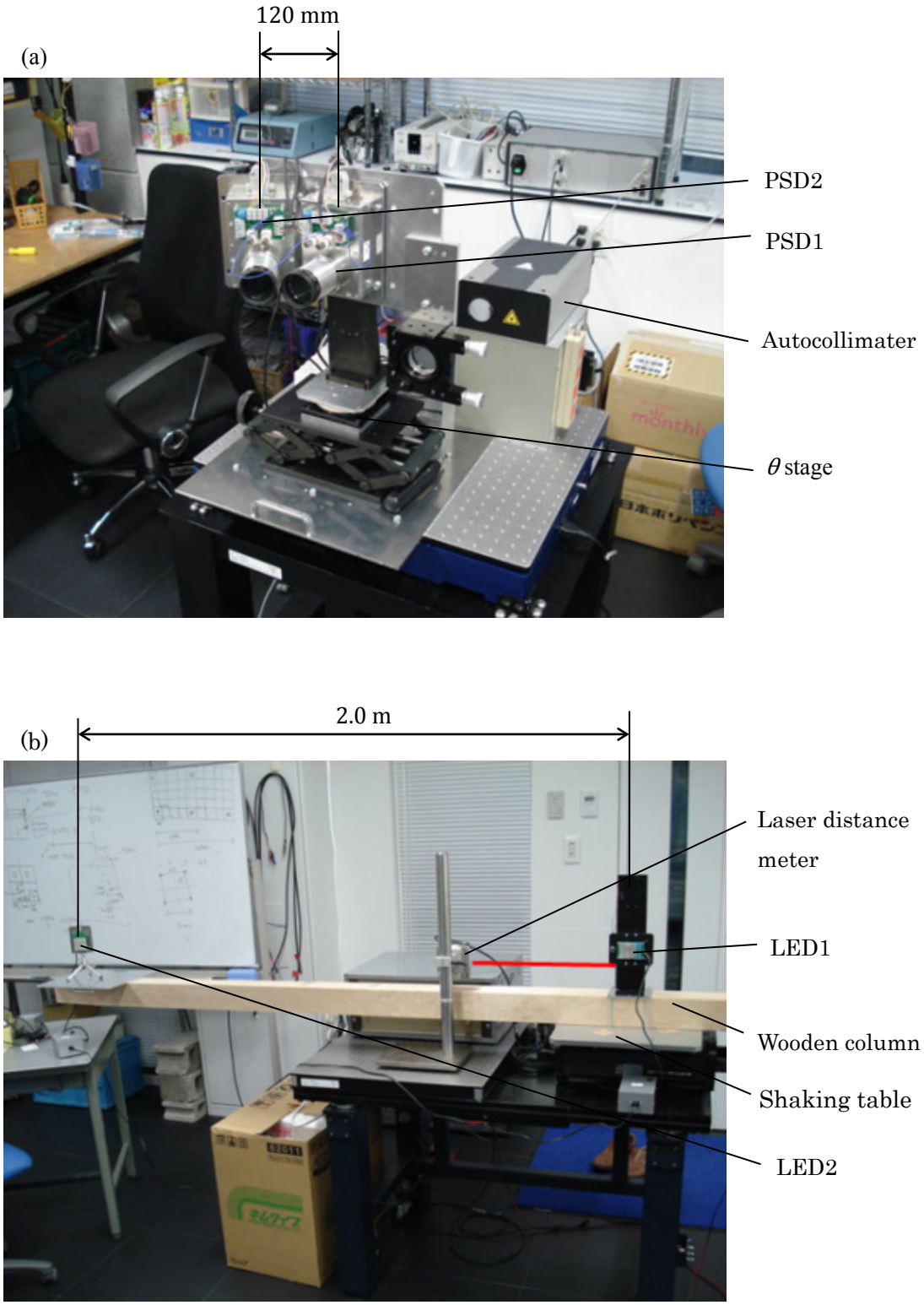

Fig. 4.4 Pictures of the experimental setup. (a) Two LDSs, (b) Two LEDs.

4.3 Experimental setup

As shown in Fig. 4.3 and Fig. 4.4, two pairs of LED arrays and PSD units were set up horizontally at a distance of 3.5 m. Using this combined system, we measured the relative-story displacement δ_x and the inclination angle θ_y. The two pairs of PSD units were immobilized on the $X\theta$-stage with an interval of 120 mm, and the PSD unit 2 was connected with the PSD unit 1 with an inclination angle of 30°. Two LED arrays were immobilized on a wooden column with an interval of approximately 2 m. The wooden column was mounted on the shaking table so that the immobilized LED arrays were vibrated only in X-direction. A laser distance meter was set up nearby the shaking table so as to measure the displacement of the shaking table, and an autocollimator was set up in the back of the combined LDS system to measure the inclination angle.

In the static measurement, the shaking table was fixed, and the PSD units were displaced using the X-stage. The translational movement of ±30 mm in X-direction and the rotational movement of ±1.7 mrad in θ_y-direction were measured using the PSD unit 1 and the PSD unit 2. In this experiment, the values (δ_x, θ_y) measured by the laser distance meter and the autocollimator were used as the reference. The accuracy of this two-pair-combined LDS system was investigated by comparing the outputs with the reference.

In the dynamic response test, the X-stage was fixed, and the wooden column was vibrated using the shaking table. The inclination angle θ_y and the displacement δ_x were simultaneously measured in real time using the PSD unit 1 and the PSD unit 2 when the shaking table and the θ-stage were moved simultaneously. The shaking table was controlled to be vibrated with amplitude of

±10 mm and the frequency of 0.5 Hz. The θ-stage was controlled to be rotated with an inclination angle of ±1.7 mrad (0.1°) and the frequency of 0.9 Hz. The fixed focal length f of both the PSD unit 1 and the PSD unit 2 was fixed at 100 mm.

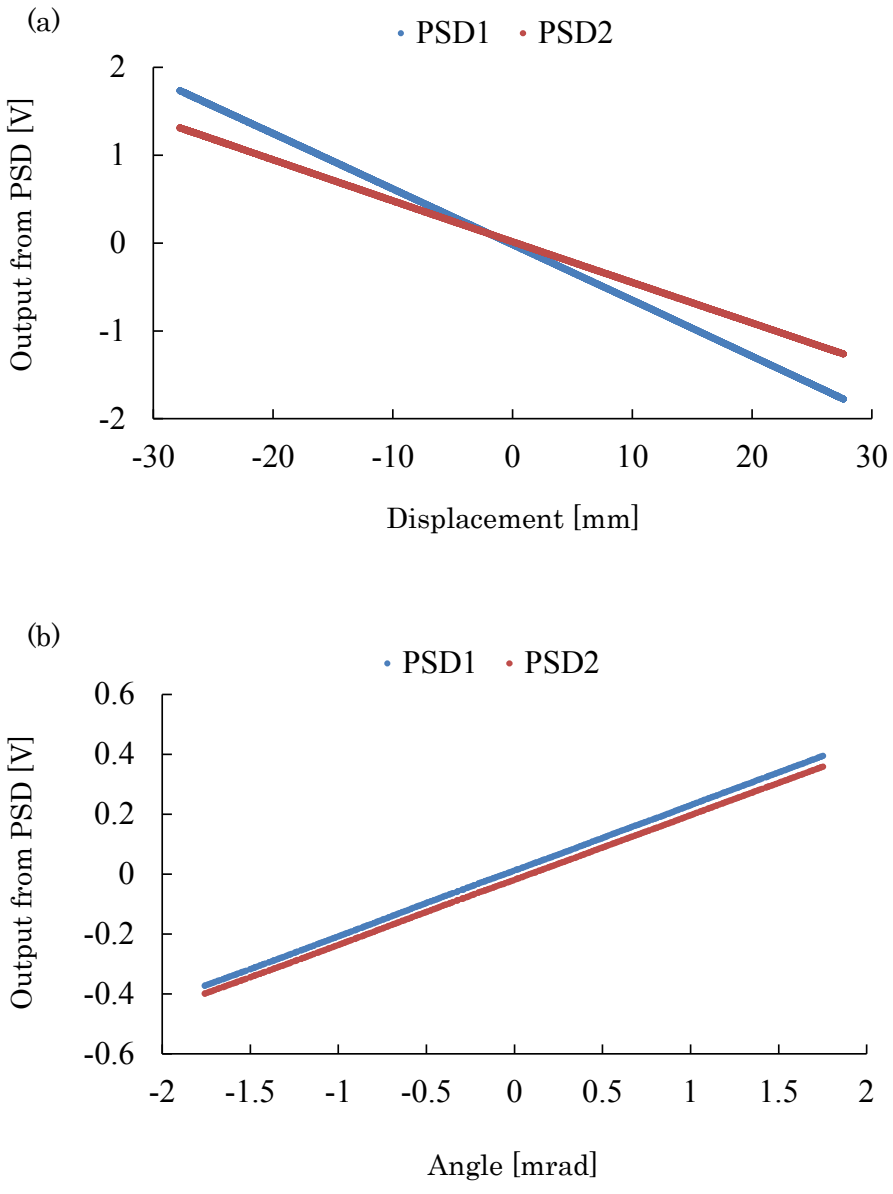

Fig. 4.5 Output voltages from the PSD units according to (a) the lateral displacement δ_x and, (b) the inclination angle θ_y in the static experiments

4.4. Results and Discussion

Fig. 4.5 shows the results of the static experiments. Figure 4.5 (a) shows the output voltages from the PSD unit 1 and the PSD unit 2 by the relative displacement of the combined LDS unit to the light source. In this experiment, only the *X*-stage was displaced, and the θ-stage was fixed. Fig. 4.5 (b) shows the output voltages from the PSD unit 1 and the PSD unit 2 by the rotational movement of the θ-stage. In this experiment, the *X*-stage was fixed and only the θ-stage was rotated. As shown in Fig. 4.5 (a), both two lines exhibit linearity with respect to the displacement of the *X*-stage. Similarly, as shown in Fig. 4.5 (b), the two lines exhibit linearity with respect to the rotational motion of the θ-stage. From these results, following equation is obtained.

$$\begin{pmatrix} V_1 \\ V_2 \end{pmatrix} = \begin{pmatrix} -0.06340 & 218.7 \\ -0.04647 & 216.2 \end{pmatrix} \begin{pmatrix} \delta_x \\ \theta_y \end{pmatrix}, \tag{4.6}$$

where V_1 and V_2 are the output voltages from PSD 1 and PSD 2 in the unit of volt, δ_x is the lateral displacement of the *X*-stage in the unit of millimeter, and θ_y is the inclination angle of the θ-stage in the unit of milliradian. The conversion coefficients from the output voltage to the position of the light spots on PSDs are 0.473 mm/V for the PSD unit 1 and 0.484 mm/V for the PSD unit 2. Using these conversion coefficients, Equations (4.6) can be transformed into the following equation.

$$\begin{pmatrix} X_1 \\ X_2 \end{pmatrix} = \begin{pmatrix} -0.0300 & 103.3 \\ -0.0225 & 105.9 \end{pmatrix} \begin{pmatrix} \delta_x \\ \theta_y \end{pmatrix}. \tag{4.7}$$

Thus, the (δ_x, θ_y) can be transformed to (X_1, X_2). Note that (X_1, X_2) is expressed in

the unit of millimeter, but (X_1, X_2) involves the rotation as well as the displacement. The matrix for transforming the (X_1, X_2) coordinate into the (δ_x, θ_y) coordinate can be determined as the inverse of the transformation matrix in Equation (4.7).

We investigated the resolution which was the most important performance of the combined LDS system. The resolution of the combined system can be derived from the experimentally obtained Jacobian matrix [6-8]. The resolution is given by the following equations.

$$\begin{pmatrix}\Delta X_1\\ \Delta X_2\end{pmatrix} = \mathrm{J}\cdot\begin{pmatrix}\Delta\delta_x\\ \Delta\theta_y\end{pmatrix},\ \mathrm{J} = \begin{pmatrix}\frac{\partial X_1}{\partial\delta_x} & \frac{\partial X_1}{\partial\theta_y}\\ \frac{\partial X_2}{\partial\delta_x} & \frac{\partial X_2}{\partial\theta_y}\end{pmatrix}. \tag{4.8}$$

Equation (4.8) represents the differential of the Equation (4.7), but the differential matrix J in Equation (4.8) is equivalent to the transformational matrix in Equation (4.7) since, as shown in Fig 4.5, all the lines are the straight lines from the origin, and the differential coefficients do not change. Thus, we can write the differential matrix J as follows.

$$J = \begin{pmatrix}-0.0300 & 103.3\\ -0.0225 & 105.9\end{pmatrix}. \tag{4.9}$$

Using the inverse matrix of J^1, the resolution of the combined LDS system can be calculated as follows.

$$J^{-1} = \begin{pmatrix}-109.33 & 116.41\\ -0.02536 & 0.034179\end{pmatrix}, \tag{4.10}$$

$$R_i = \sqrt{\sum \left({J^{-1}}_{ij} \cdot \sigma_j \right)^2} \ , \ (\mathrm{i,j} = 1, 2) \ , \qquad (4.11)$$

where R_1 is the resolution of the combined LDS unit in the displacement measurement, R_2 is that in the inclination angle measurement, and σ_1 and σ_2 are the resolution of the PSDs. We assume that $\sigma_1 = \sigma_2 = 0.6$ μm in accordance with the performance guarantee by the manufacturer. From Equations (4.10) and (4.11), the resolution for each axis is calculated as follows:

$$R_1 = \sqrt{(-109.33 \times 0.6)^2 + (-116.41 \times 0.6)^2} = 95.8 \ [\mu\mathrm{m}] \ , \qquad (4.12)$$

$$R_2 = \sqrt{(-0.02536 \times 1)^2 + (-0.034179 \times 1)^2} = 25.5 \ [\mu\mathrm{rad}] \ . \qquad (4.13)$$

As a result, the resolution for both δ_x and θ_y fulfills the requirement for the structural health monitoring, as discussed in chapter 2.

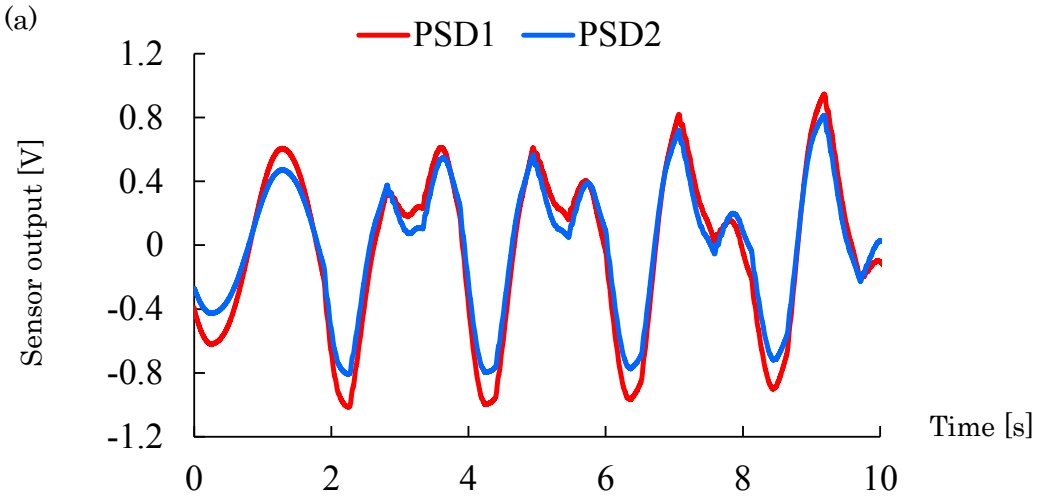
(a)
PSD1
PSD2
Sensor output [V]
1.2
0.8
0.4
0
-0.4
-0.8
-1.2
0
2
4
6
8
10
Time [s]

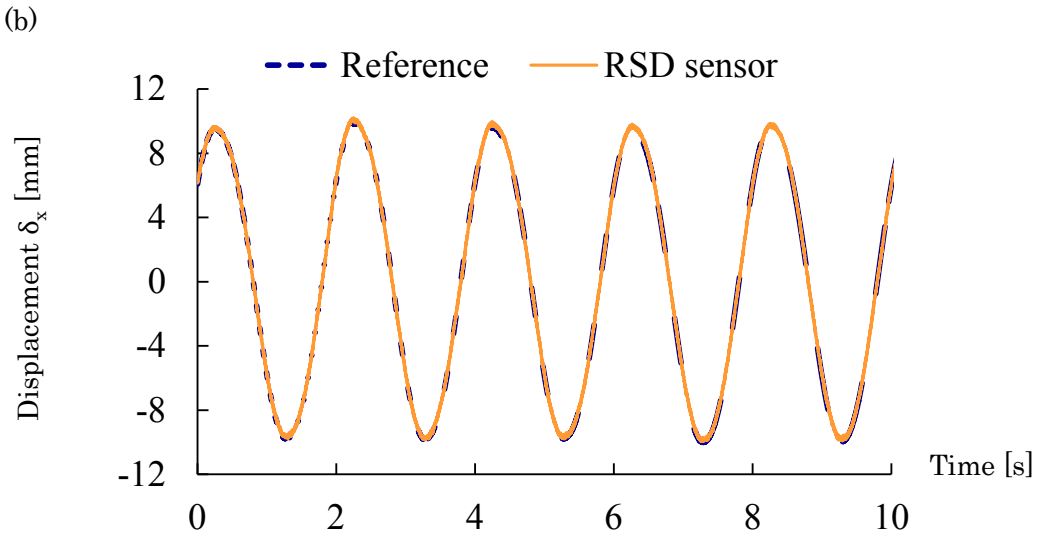
(b)
Reference
RSD sensor
Displacement δ_x [mm]
12
8
4
0
-4
-8
-12
0
2
4
6
8
10
Time [s]

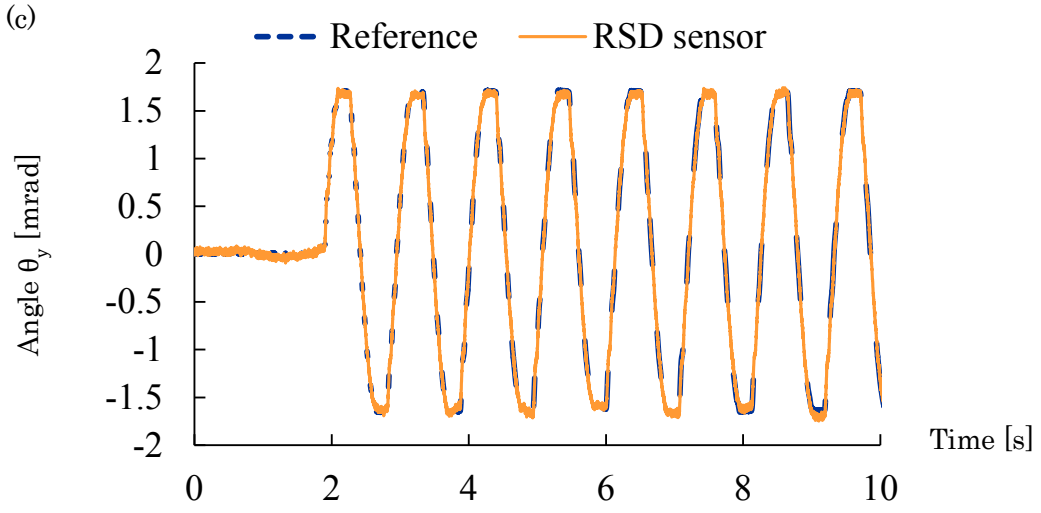
(c)
Reference
RSD sensor
Angle θ_y [mrad]
2
1.5
1
0.5
0
-0.5
-1
-1.5
-2
0
2
4
6
8
10
Time [s]

Fig.4.6 The results of the dynamic experiments by using the shaking table and the θ-stage. (a) The output voltages from PSDs, (b) the calculated displacement δ_x, and (c) the calculated angle θ_y.

Fig. 4.6 shows the results of the dynamic experiment. In this dynamic experiment, the inclination angle θ_y and the displacement δ_x were simultaneously measured in real time using the PSD unit 1 and the PSD unit 2 when the shaking table and the θ-stage were moved independently. The outputs from the PSD unit 1 and the PSD unit 2 exhibit the mixed motion, as shown in Fig. 4.6 (a). The displacement and the inclination angle were calculated using Equations (4.6), and the calculated displacement and inclination angle were depicted in Fig. 4.6 (b) and Fig. 4.6 (c), respectively. The outputs of calculated displacement and angle by combined LDS system coincided with the references, as shown in Fig.4.6 (b) and Fig. 4.6 (c). The accuracy was evaluated to be approximately 0.15 mm in the relative displacement and 0.1 mrad in the inclination angle. The values are in good agreement with the resolution of the combined LDS system estimated in Equations (4.12) and (4.13), indicating that our theoretical model proposed in section 4.2 is applicable for the experimental analysis. The results show that the proposed method can measure the relative-story displacement and the inclination angle of the floor correctly.

4.5 Conclusion

The method to eliminate the angular error caused by the inclination of the LDS detector unit was developed. A pair of the lateral-displacement sensor was used for measuring the relative-story displacement and the inclination angle of the floor simultaneously. For verification, laboratory tests have been carried out using an $X\theta$-stage and a shaking table. In the static experiment, it is verified that the inclination angle of the detector itself can be measured as well as the displacement by means of the proposed method. Theoretically, the resolution of the combined LDS system in the displacement measurement was evaluated to be 0.0958 mm, and that in the inclination angle measurement was evaluated to be 25.5 μrad. The accuracy of the LDS system was experimentally evaluated to be approximately 0.15 mm in the relative displacement measurement and 0.1 mrad in the inclination angle measurement. These results indicate that the developed method achieved enough accuracy for the measurement of relative-story displacement and inclination angle, and the combined LDS system can resolve the angular error problem.

Bibliography

[1] M. Oshima : "Research on Core Technologies for the Improvement of Vulnerabilities in Video Systems", doctoral thesis of Waseda University (2006)

[2] P. Olaszek : "Investigation of the dynamic charactteristic of bridge structures using a computer vision method", Measurement Vol. 25, pp.227-236 (1999)

[3] J. W. Park, H. J. Jung and J. J. Lee : "Vision-Based Displacement Method for High-Rise Building Structures using Partitioning Approach", Proceedings of the fifth international workshop on advanced smart structures technology (ANCRiSST 2009), Boston, USA, pp.122-129 (2009)

[4] H. Myung, S. Lee and J. Jung : "A Robotic Approach to Structural Health Monitoring", Proceedings of the fifth international workshop on advanced smart structures technology (ANCRiSST 2009), Boston, USA, pp.761-768 (2009)

[5] S. Kiyoshige : "Review of the Vibration Reduction Technology in the Digital Single-Lens Reflex Camera System(<Special Edition> Digital Single-Lens Reflex Camera)", The journal of the Institute of Image Information and Television Engineers Vol.61, No.3, pp.279-283 (2007)

[6] J. A. Kim, E. W. Bae, S. H. Kim and Y. K. Kwak : "Application of sensitivity analysis for design of six-degree-of-freedom measurement system", Optical Engineering, Vol.40, No.12, pp.2837-2844 (2001)

[7] J. A. Kim, E. W. Bae, S. H. Kim and Y. K. Kwak : "Design methods for six-degree-of-freedom displacement measurement systems using cooperative targets", Precision Engineering, Vol.26, pp.99-104 (2002)

[8] K. Kwon, J. J. Park and N. Cho: "A highly sensitive multi-dimensional motion measurement system using a spherical reflector", Measurement Science and Technology Vol.17, pp.24210-2429 (2006)

Chapter 5
Relative-story displacement sensor capable of five-degree-of-freedom measurement

5.1 Introduction

As reported in chapter 4, we have developed an optical sensor for simultaneously measuring the relative-story displacement and the inclination angle. Using the sensor system, we have succeeded in measuring the relative-story displacement and the local inclination angle of the floor. However, the laboratory test explained in chapter 4 assumed the vibration with the one-dimensional displacement δ_x, and the one-dimensional inclination θ_y. As shown in Fig. 5.1, however, the sensor unit rotates in θ_x-, θ_y-, and ψ-direction according to the floor bending. The possible way to eliminate the measurement error due to the three-axis rotation is to monitor the inclination angle (θ_x, θ_y) and the torsion angle ψ as well as the horizontal displacement (δ_x, δ_y), and estimate the true value.

Such multi-degree-of-freedom measurement methods were reported previously [1-6]. In these methods, the displacement of the object was measured

using a reference point outside of the sensor system. When employed to measure the movement of a building, the reference point must be viewable and referable from any place in the building. However, it is impossible to construct such a reference point outside the builaing. Therefore, the alternative method is required for measuring the five-degree-of freedom (5-DOF) movement of the building.

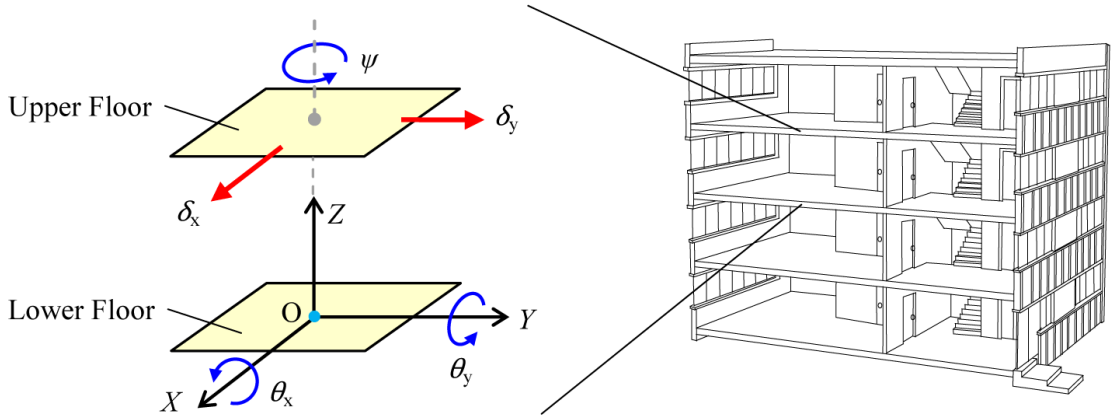

Fig. 5.1 Schematic diagram of the 5-DOF movement of building layers. Here, (δ_x, δ_y) shows the relative-story displacement, ψ shows the torsion angle of the upper layer relative to the lower layer, (θ_x, θ_y) shows the inclination angle of the lower layer.

In this chapter, we propose a novel sensor system capable of measuring the 5-DOF movement of two adjacent building layers utilizing three pairs of infrared-light emitting diode (IR-LED) arrays and position-sensitive detector (PSD) units. The three LED arrays were fixed on the ceiling as the measurement target, and the three PSD units were installed in one place on the lower floor so that each PSD captures the motion of the corresponding LED array target. First, we show the

theory of the 5-DOF movement measurement. Next, we show the result from the dynamic performance tests of the sensor system. The three PSD units were vibrated and rotated using a shaking table, a motorized micrometer, and a rotation stage. The optimum configuration of the sensor system was figured out by calculating the ideal resolution theoretically. Finally, from the viewpoint of the configuration and the accuracy, we discuss the feasibility of this sensor system for structural health monitoring of a building.

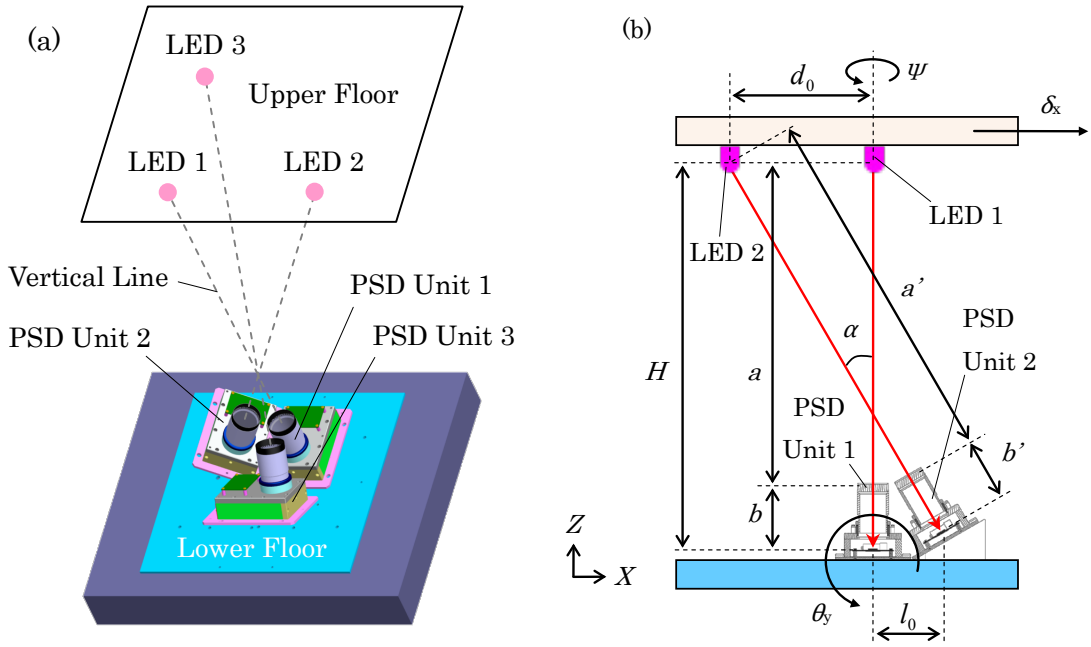

Fig.5.2 Schematic diagram of the relative-story displacement sensor capable of 5-DOF measurement. (a) Birds eye view. (b) Cross-section view.

5.2 Measurement theory and principal

Fig. 5.2 shows the schematic diagram of the sensor system. The specifications of the single PSD unit were reported in chapter 2. As shown in Fig. 5.2, the PSD unit 1 is located in the original position (0, 0, 0). The PSD unit 2 and the PSD unit 3 are located at (l_0, 0, 0) and (0, l_0, 0), respectively. The position of three LED light targets fixed on the ceiling is located at (0, 0, H), ($-d_0$, 0, H), and (0, $-d_0$, H), respectively. The PSD unit 2 is installed with an inclination angle α so that the PSD unit 2 faces the LED 2. The PSD unit 3 is also inclined with the angle α and faces the LED 3. Moreover, the three PSD units are rigidly connected with each other and immobilized in one place on the floor. In accordance with the arrangement of the PSD units and the LEDs, the story height H is expressed as

$$H = a + b = (a' + b')cos\alpha \ , \tag{5.1}$$

$$H = \frac{[(b/a)+1]^2}{(b/a)} \cdot f = \frac{[(b'/a')+1]^2}{(b'/a')} \cdot f cos\alpha \ , \tag{5.2}$$

where a is the distance from the lens to the upper floor, b is the distance from the PSD 1 to the lens, and f is the fixed focal length of the lens. Equally, a' is the distance from the lens of the PSD unit 2 to the LED 2, b' is the distance from the PSD 2 to the lens of the PSD unit 2. Equation (5.2) is derived from Equation (5.1) and the Gaussian lens formula. In Equation (5.2), the ratio b/a represents the magnification of the PSD unit 1, and the ratio b'/a' represents the magnification of the PSD unit 2 and the PSD unit 3. In this arrangement, the position of the light spots focused on each PSD is expressed as follows [7].

$$X_1 = \frac{\mathrm{b}}{a}(-\delta_x + H\theta_y) \ , \tag{5.3}$$

$$Y_1 = \frac{\mathrm{b}}{a}(-\delta_y - H\theta_x) \ , \tag{5.4}$$

$$X_2 = \frac{b'}{a'}[-\cos\alpha \cdot \delta_x + (\frac{H}{\cos\alpha} - l_0 \sin\alpha)\theta_y] \ , \tag{5.5}$$

$$Y_2 = \frac{b'}{a'}\left(-\delta_y - H\theta_x\right) - l_0\psi \ , \tag{5.6}$$

$$X_3 = \frac{b'}{a'}\left(-\delta_x + H\theta_y\right) + l_0\psi \ , \tag{5.7}$$

$$Y_3 = \frac{b'}{a'}[-\cos\alpha \cdot \delta_y - (\frac{H}{\cos\alpha} - l_0 \sin\alpha)\theta_x] \ . \tag{5.8}$$

In this equation, (δ_x, δ_y) is the relative-story displacement between the ceiling and the floor, (θ_x, θ_y) is the inclination angle of the PSD units around X- and Y-axes, ψ is the torsion angle of the ceiling around the Z-axis. We assume that in Equations (5.3) to (5.8), the inclination angles θ_x, θ_y and the torsion angle ψ are positive when they are clockwise rotated, and the center of the rotation is the original point. Here we note that solving the simultaneous equations of (5.3) to (5.8) is not categorized as a six-degree-of-freedom problem but as a five-degree-of- freedom problem although six variables of (X_1, Y_1, X_2, Y_2, X_3, Y_3) are included. Namely, for solving these simultaneous equations, Equation (5.6) need not to be taken into account because

Y_2 can be determined using other valuables. Thus, the solution is to be given by the Jacobian matrix transforming (X_1, Y_1, X_2, X_3, Y_3) to (δ_x, δ_y, θ_x, θ_y, ψ) coordinate without Y_2.

$$\begin{pmatrix} X_1 \\ X_2 \\ X_3 \end{pmatrix} = \begin{bmatrix} -\frac{b}{a} & \frac{b}{a}H & 0 \\ -\frac{b'}{a'}cos\alpha & \frac{b'}{a'}(\frac{H}{cos\alpha} - l_0 sin\alpha) & 0 \\ -\frac{b'}{a'} & \frac{b'}{a'}H & l_0 \end{bmatrix} \begin{pmatrix} \delta_x \\ \theta_y \\ \psi \end{pmatrix}, \tag{5.9}$$

$$\begin{pmatrix} Y_1 \\ Y_3 \end{pmatrix} = \begin{bmatrix} -\frac{b}{a} & -\frac{b}{a}H \\ -\frac{b'}{a'}cos\alpha & \frac{b'}{a'}(\frac{H}{cos\alpha} - l_0 sin\alpha) \end{bmatrix} \begin{pmatrix} \delta_y \\ \theta_x \end{pmatrix}. \tag{5.10}$$

Equations (5.9) and (5.10) indicate that (X_1, X_2, X_3) and (Y_1, Y_3) can be calculated independently. Namely, (X_1, X_2, X_3) can be calculated using (δ_x, θ_y, ψ), whereas (Y_1, Y_3) can be calculated using (δ_y, θ_x). Equations (5.9) and (5.10) show that the relationship between (X_1, X_2) and (δ_x, θ_y) is same as that between (Y_1, Y_3) and (δ_y, θ_x) hence, in the following experimental setup, we focus on evaluating the relationship between (X_1, X_2, X_3) and (δ_x, θ_y, ψ) using Equation (5.9).

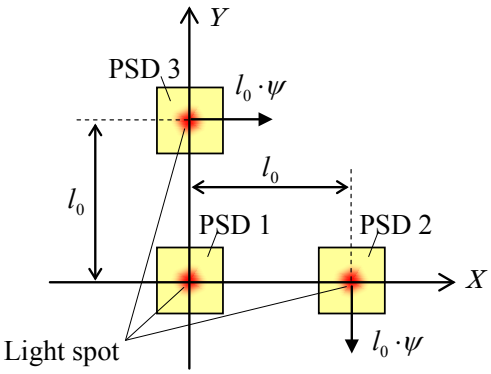

Fig. 5.3 Displacement of the light spot which comes from the LED and is focused on the PSD surface by the lens in response to the torsional motion of the ceiling. The schematic shows the *XY*-plane. The original point for the torsional motion is located at the center of the PSD 1. If the ceiling was counterclockwise rotated with the angle ψ, the light spot on the PSD 3 displaces by $l_0 \cdot \psi$ in *X*-direction, and the light spot on the PSD 2 displaces by $l_0 \cdot \psi$ negatively in *Y*-direction.

(a)

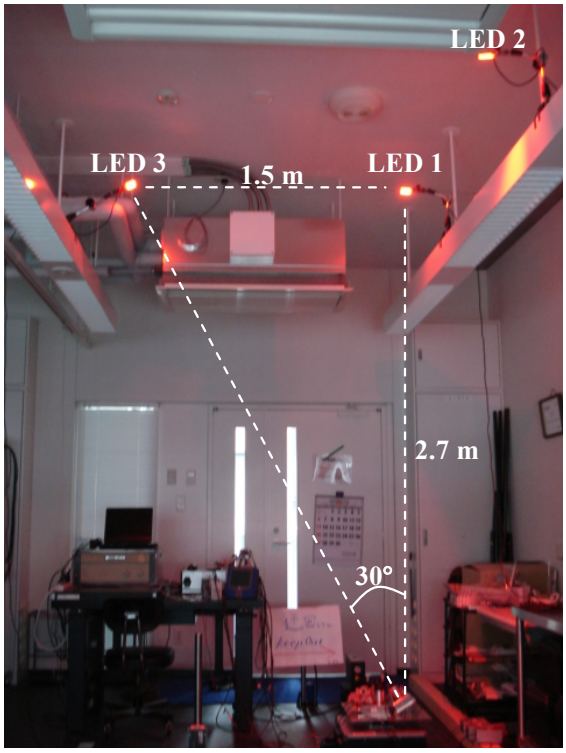

(b)

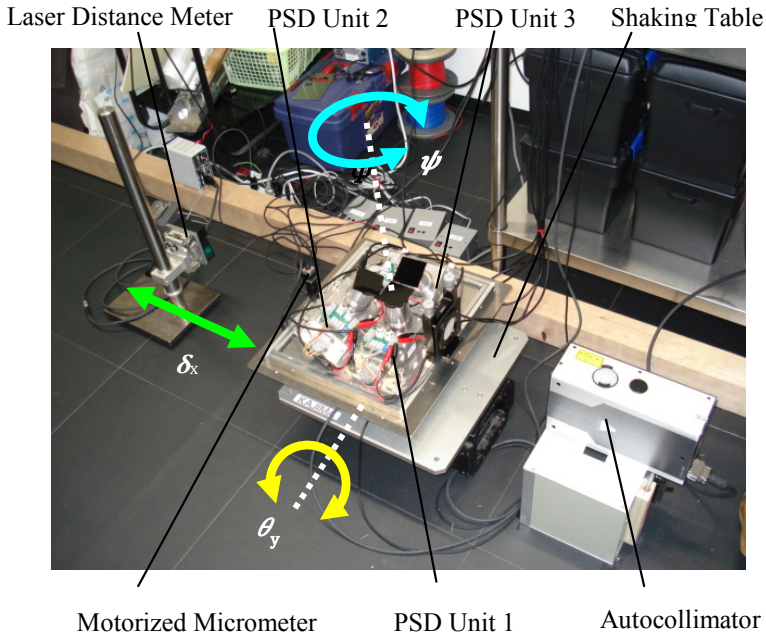

(c)

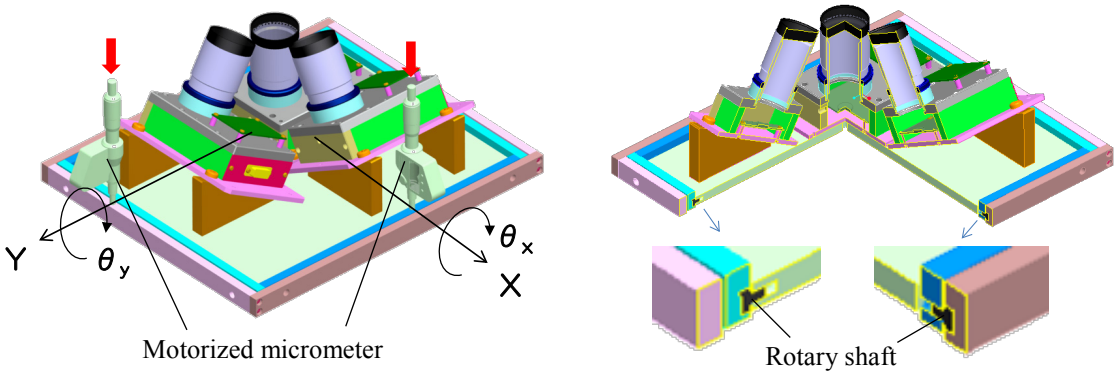

Fig. 5.4 The experimental setup for the verification of 5-DOF measurement. (a) Arrangement of three pairs of the LED arrays and the PSD units. Although the IR-LEDs which are invisible were used in this experiment, the infrared light is visualized as the red light in the photograph. (b) Close-up view of the PSD units. The rotation stage was hidden under the PSD units. (c) The controller unit introducing θ_x and θ_y.

5.3 Experimental Setup

Fig. 5.4 shows the experimental setup for measuring the relative displacement δ_x, the inclination angle θ_y, and the torsion angle ψ. Three pairs of IR-LED arrays and PSD units were set up on the ceiling and the floor, respectively. The story height was 2.7 m. As shown in Fig. 5.4, the three PSD units were immobilized on the rotation stage to be rotated in ψ direction, and the rotation stage was fixed on the shaking table to be displaced in X-direction. The inclination angle θ_y was controlled by pushing up the basal plate where the three PSD units were fixed using the motorized micrometer. The PSD unit 2 and the PSD unit 3 were connected with the PSD unit 1 with an interval of 120 mm (l_0 = 120 mm) and were inclined with the angle of 30° (α = 30°). Three LED arrays were immobilized on the ceiling with an interval of 1.5 m. As shown in Fig. 5.4 (c), the inclination angle (θ_x, θ_y) was controlled by the local inclination angle controller unit which can rotate around 8.5 mm above the ground in both θ_x- and θ_y-direction. A laser distance meter was set up nearby the shaking table so as to measure the relative displacement δ_x, and an autocollimator was set up nearby the combined PSD unit system to measure the inclination angle θ_y and the torsion angle ψ. The laser distance meter and the autocollimator were used as the reference.

The first experimental step is to move the PSD units by δ_x, θ_y, and ψ independently and calculate the inverse matrix of Equation (5.9). Namely, the movement of the PSD units (δ_x, θ_y, ψ) must be estimated from the PSD outputs (X_1, X_2, X_3). For this purpose, we have conducted the static experiment. In the static experiment, the translational movement of ±5 mm in X-direction, the inclination movement of ±2 mrad in θ_y-direction, and the torsion of ±1.5 mrad in ψ-direction

were introduced independently, and the relationship between (δ_x, θ_y, ψ) and (X_1, X_2, X_3) was evaluated using the reference.

In the dynamic response experiment, the three PSD units were vibrated using the shaking table, the motorized micrometer, and the rotation stage. The movement of the PSD units was calculated using the output from the PSD units and the inversion matrix of Equation (5.9) which was obtained in the static experiment. The experimentally obtained values were compared with the reference. The vibration amplitude and the frequency of the translational movement were ±5 mm and 0.6 Hz, respectively. The inclination angle and the frequency were ±2 mrad and 0.4 Hz, respectively. The torsion angle and the frequency were ±1.7 mrad and 0.8 Hz, respectively. The fixed focal length of the lens of all the PSD units was 100 mm.

5.4 Results and discussion

Fig. 5.5 shows the results of the static experiments. Fig. 5.5 (a) shows the output voltages from three PSD units according to the displacement of the PSD units relative to the LED arrays. In this experiment, only the shaking table was displaced, whereas the motorized micrometer and the rotation stage were fixed. Fig. 5.5 (b) shows the output voltages from three PSD units according to the inclination. In this experiment, the shaking table and the rotation stage were fixed, and only the motorized micrometer was moved. Fig. 5.5 (c) shows the output voltages from three PSD units according to the torsion of the PSD units to the LED arrays. In this experiment, only the rotation stage was moved, whereas the shaking table and the motorized micrometer were fixed. As shown in Fig. 5.5 (a), the three lines exhibit linearity with respect to the displacement of the shaking table. Similarly, as shown

in Figs. 5.5 (b) and (c), the three lines exhibit linearity with respect to the inclination angle or the torsion angle. From these results, the matrix of these conversion coefficients is expressed as follows.

$$\begin{pmatrix} V_{x1} \\ V_{x2} \\ V_{x3} \end{pmatrix} = \begin{bmatrix} -0.0790 & 0.2174 & -0.0012 \\ -0.0599 & 0.2073 & -0.0028 \\ -0.0656 & 0.1841 & 0.1000 \end{bmatrix} \begin{pmatrix} \delta_x \\ \theta_y \\ \psi \end{pmatrix}, \tag{5.11}$$

where V_{x1}, V_{x2} and V_{x3} are the output voltages from PSD 1, PSD 2 and PSD 3 in the unit of volt, δ_x is the relative displacement in the unit of millimeter, θ_y is the inclination angle in the unit of milliradian, and ψ is the torsion angle in the unit of milliradian. The conversion coefficients from the output voltage to the position of the light spots on the PSDs are 1.962 V/mm for the PSD unit 1, 1.898 V/mm for the PSD unit 2, and 1.937 V/mm for the PSD unit 3, respectively. Using these conversion coefficients, Equation (5.11) can be transformed into the following equation.

$$\begin{pmatrix} X_1 \\ X_2 \\ X_3 \end{pmatrix} = \begin{bmatrix} -0.0403 & 0.1108 & -0.0006 \\ -0.0316 & 0.1092 & -0.0015 \\ -0.0339 & 0.0950 & 0.0516 \end{bmatrix} \begin{pmatrix} \delta_x \\ \theta_y \\ \psi \end{pmatrix}, \tag{5.12}$$

where (X_1, X_2, X_3) is the position of the light spots focused on the corresponding PSD surface. We investigated the resolution which was the most important performance of the combined PSD unit system. The resolution is defined by the following equations [8].

$$\begin{pmatrix} \Delta X_1 \\ \Delta X_2 \\ \Delta X_3 \end{pmatrix} = J \cdot \begin{pmatrix} \Delta\delta_x \\ \Delta\theta_y \\ \Delta\psi \end{pmatrix} = \begin{bmatrix} \frac{\partial X_1}{\partial \delta_x} & \frac{\partial X_1}{\partial \theta_y} & \frac{\partial X_1}{\partial \psi} \\ \frac{\partial X_2}{\partial \delta_x} & \frac{\partial X_2}{\partial \theta_y} & \frac{\partial X_2}{\partial \psi} \\ \frac{\partial X_3}{\partial \delta_x} & \frac{\partial X_3}{\partial \theta_y} & \frac{\partial X_3}{\partial \psi} \end{bmatrix} \begin{pmatrix} \Delta\delta_x \\ \Delta\theta_y \\ \Delta\psi \end{pmatrix} , \quad (5.13)$$

$$R_i = \left[\sum_{j=1}^{3} (J^{-1}{}_{ij} \cdot \sigma_j)^2\right]^{\frac{1}{2}} \quad (i = 1,2,3) \ , \quad (5.14)$$

where J is the Jacobian matrix, R_1 is the resolution in the displacement measurement, R_2 is that in the inclination angle measurement, and R_3 is that in the torsion angle measurement. The resolution of the combined PSD units depends also on the original resolution of the three PSDs embedded in the PSD units. The resolution of the PSDs was denoted as σ_1, σ_2 and σ_3, respectively. We can write the matrix J using Equation (5.12) and the inverse matrix J^{-1} as follows.

$$J = \begin{bmatrix} -0.0403 & 0.1108 & -0.0006 \\ -0.0316 & 0.1092 & -0.0015 \\ -0.0339 & 0.0950 & 0.0516 \end{bmatrix} , \quad (5.15)$$

$$J^{-1} = \begin{bmatrix} -123.1 & 123.0 & 2.145 \\ -35.82 & 44.73 & 0.8839 \\ -14.91 & -1.542 & 19.16 \end{bmatrix} . \quad (5.16)$$

Using this inverse matrix J^{-1}, the resolution of the combined PSD unit system was calculated. We assume that $\sigma_1 = \sigma_2 = \sigma_3 = 0.6$ μm in accordance with the data sheet from the PSD vender [13]. From Equations (5.14) and (5.16), the resolution was calculated as follows.

$$R_1 = \sqrt{(-123.1 \times 0.6)^2 + (123.0 \times 0.6)^2 + (2.145 \times 0.6)^2}$$
$$= 104.4\ [\mu m]\ , \quad (17)$$

$$R_2 = \sqrt{(-35.82 \times 0.6)^2 + (44.73 \times 0.6)^2 + (0.8839 \times 0.6)^2}$$
$$= 34.39\ [\mu rad]\ , \quad (18)$$

$$R_3 = \sqrt{(-14.91 \times 0.6)^2 + (-1.542 \times 0.6)^2 + (19.16 \times 0.6)^2}$$
$$= 14.60\ [\mu rad]\ , \quad (19)$$

where R_1 is the resolution of the sensor system in the displacement measurement, R_2 is that in the inclination angle measurement, and R_3 is that in the torsion angle measurement. Since the resolution of less than 0.1 mm is the requirement for structural health monitoring of a building, the resolution obtained in the relative-displacement measurement was evaluated to be sufficiently high, as shown in Equation (5.17). We conjecture that using our sensor system, even a minute crack in the concrete and the small residual displacement can be monitored in real time. The resolution in the inclination angle measurement evaluated by Equation (5.18) is also sufficiently high because, if we assume that the story height is 2.7 m, the inclination of 34.39 μrad is equivalent to the relative-story displacement of 2.7 m × tan[34.39 μrad] = 0.093 mm. Similarly, the resolution in the torsion angle measurement evaluated by Equation (5.19) is also enough high for the structural health monitoring.

(a)

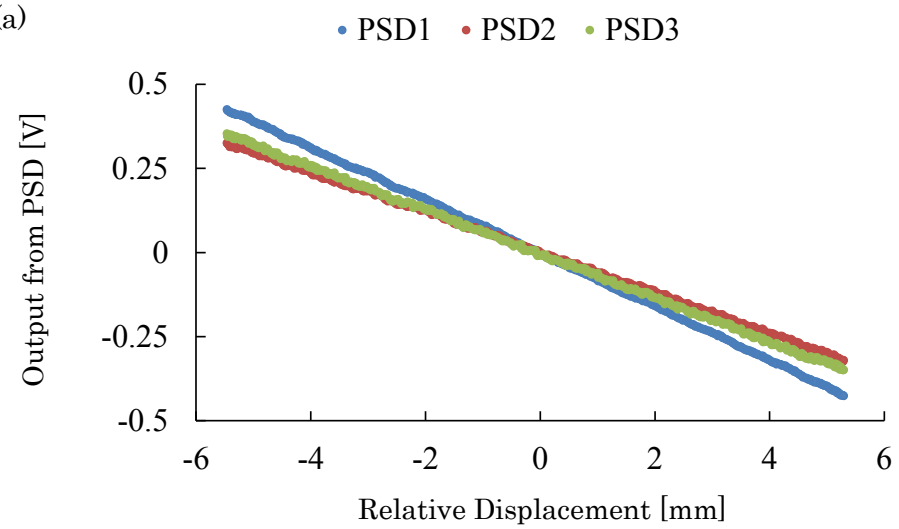
PSD1
PSD2
PSD3
Output from PSD [V]
0.5
0.25
0
-0.25
-0.5
-6
-4
-2
0
2
4
6
Relative Displacement [mm]

(b)

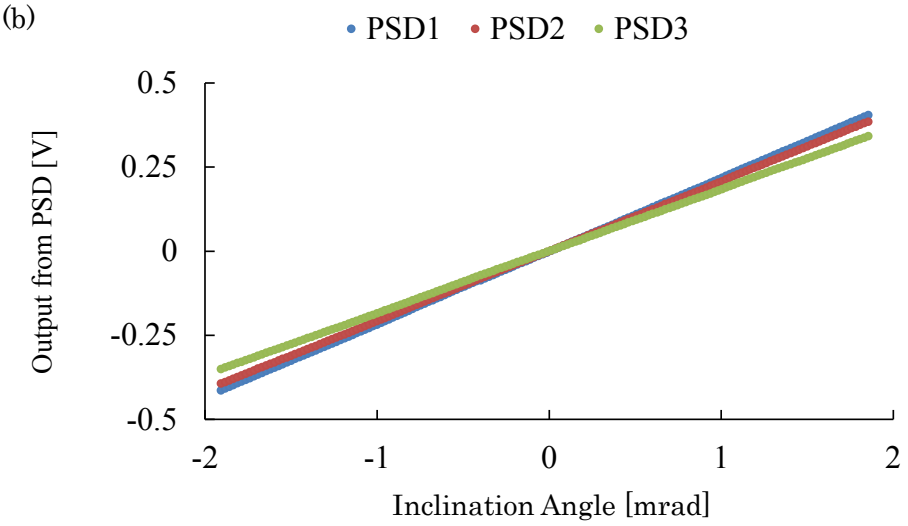
PSD1
PSD2
PSD3
Output from PSD [V]
0.5
0.25
0
-0.25
-0.5
-2
-1
0
1
2
Inclination Angle [mrad]

(c)

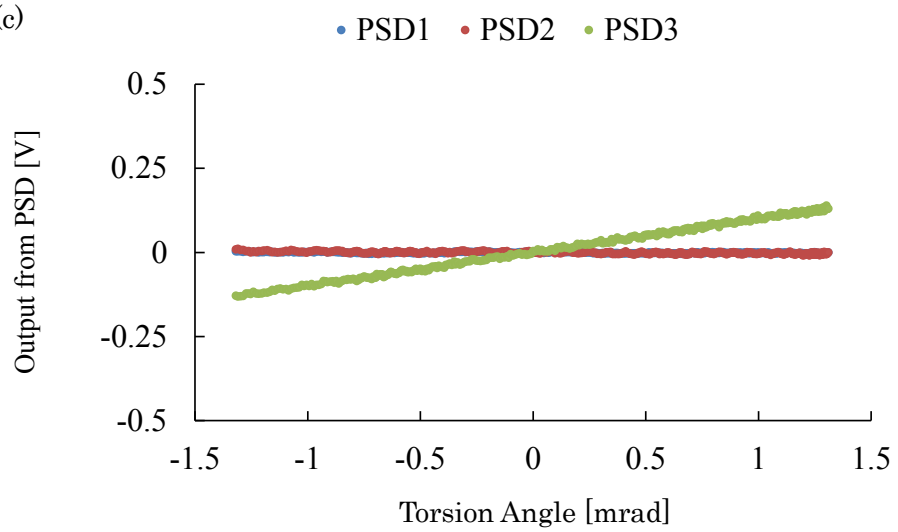
PSD1
PSD2
PSD3
Output from PSD [V]
0.5
0.25
0
-0.25
-0.5
-1.5
-1
-0.5
0
0.5
1
1.5
Torsion Angle [mrad]

Fig. 5.5 Results from the static experiments. (a) Output voltages from PSD units when the PSD units were displaced by δ_x. (b) Output voltages from PSD units when the PSD units were inclined by θ_y. (c) Output voltages from PSD units when the PSD units were rotated by ψ.

Fig. 5.6 shows the results from the dynamic experiment. In this experiment, the relative displacement δ_x, the inclination angle θ_y and the torsion angle ψ were simultaneously measured in real time using the three PSD units when the shaking table, motorized micrometer, and the rotation stage were moved simultaneously. Thus, the outputs from the PSD unit 1, the PSD unit 2, and the PSD unit 3 exhibited the mixed motion, as shown in Fig. 5.6 (a). The inverse matrix of Equation (5.11) was calculated as follows.

$$\begin{pmatrix} \delta_x \\ \theta_y \\ \psi \end{pmatrix} = \begin{bmatrix} -62.61 & 64.72 & 1.061 \\ -18.19 & 23.51 & 0.4401 \\ -7.578 & -0.8324 & 9.886 \end{bmatrix} \begin{pmatrix} V_{x1} \\ V_{x2} \\ V_{x3} \end{pmatrix} . \quad (5.20)$$

The displacement, the inclination angle, and the torsion angle were calculated using Equation (5.20), and the calculation results were depicted in Fig. 5.5 (b), Fig. 5.6 (c), and Fig. 5.6 (d), respectively. The calculated values coincided with the references. The error in the relative-displacement measurement was evaluated to be 0.20 mm at the maximum. The error in the inclination angle measurement was evaluated to be 0.12 mrad at the maximum. The error in the torsion angle measurement was evaluated to be 0.09 mrad at the maximum. The errors are

sufficiently small, indicating that our theoretical model is valid. The results show that the proposed method can measure the relative-story displacement, the local inclination angle, and the torsion angle correctly.

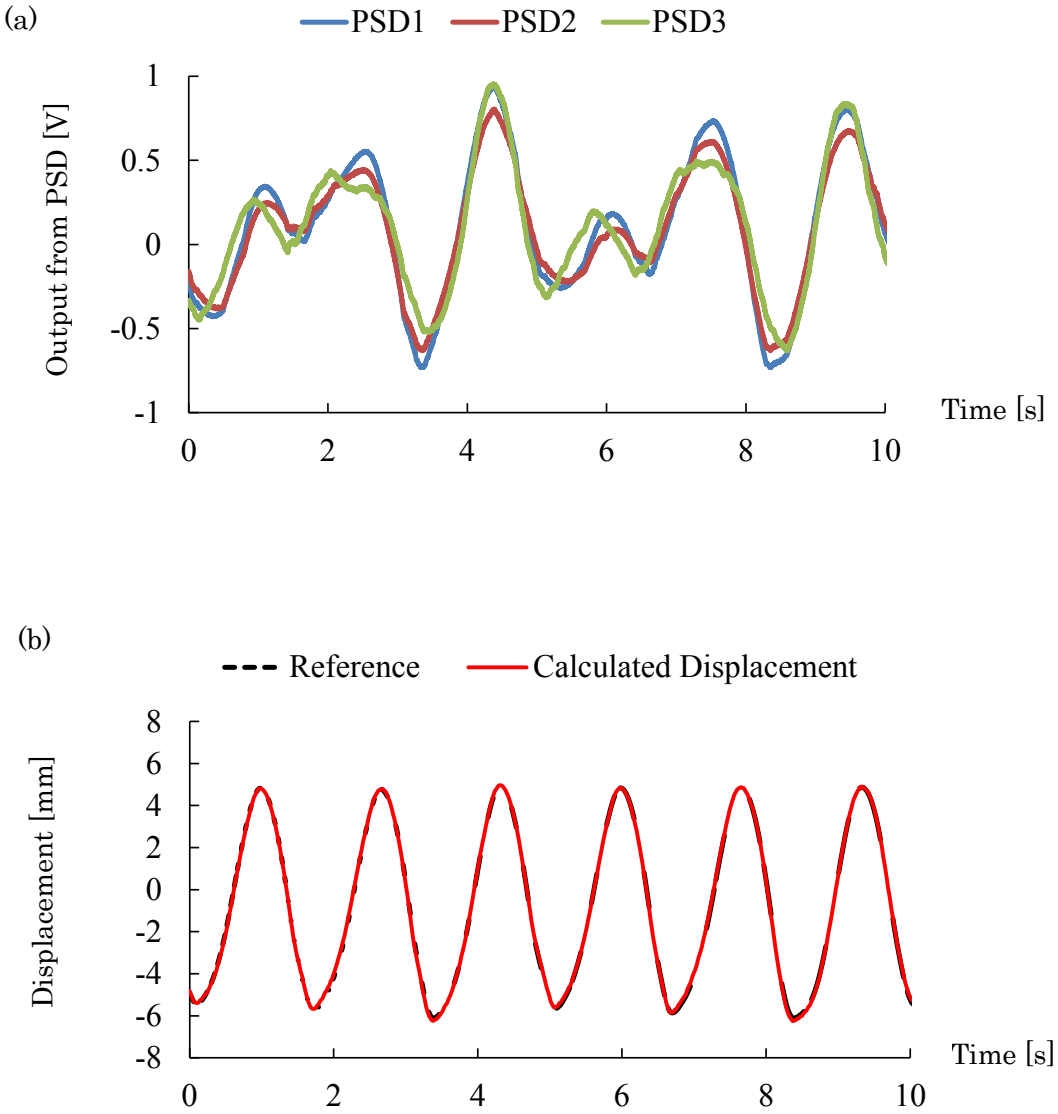

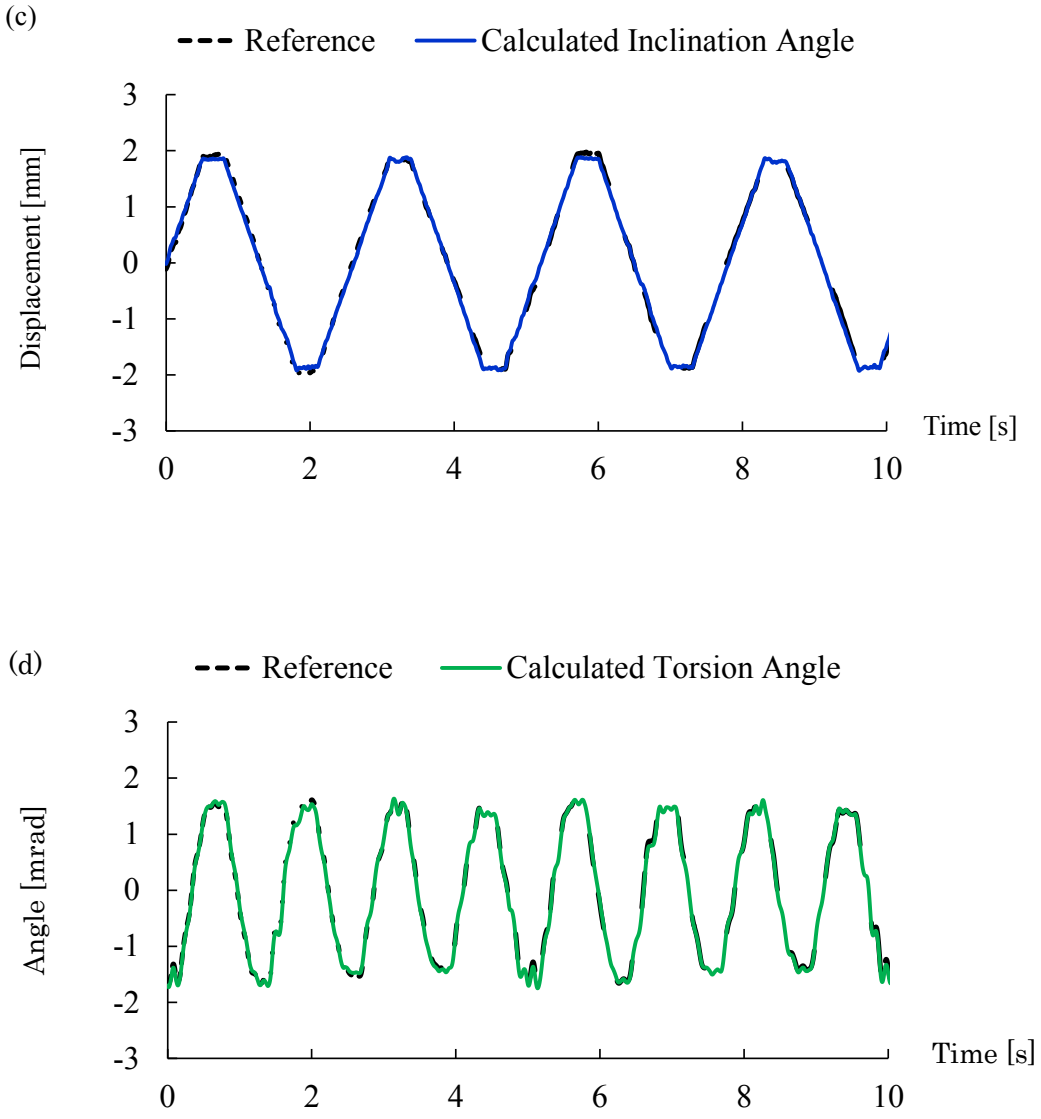

Fig. 5.6 The results from the dynamic response experiment. (a) The output voltages from three PSDs, (b) the calculated displacement δ_x, (c) the calculated inclination angle θ_y, and (d) the calculated torsion angle ψ.

(a) f = 100 mm

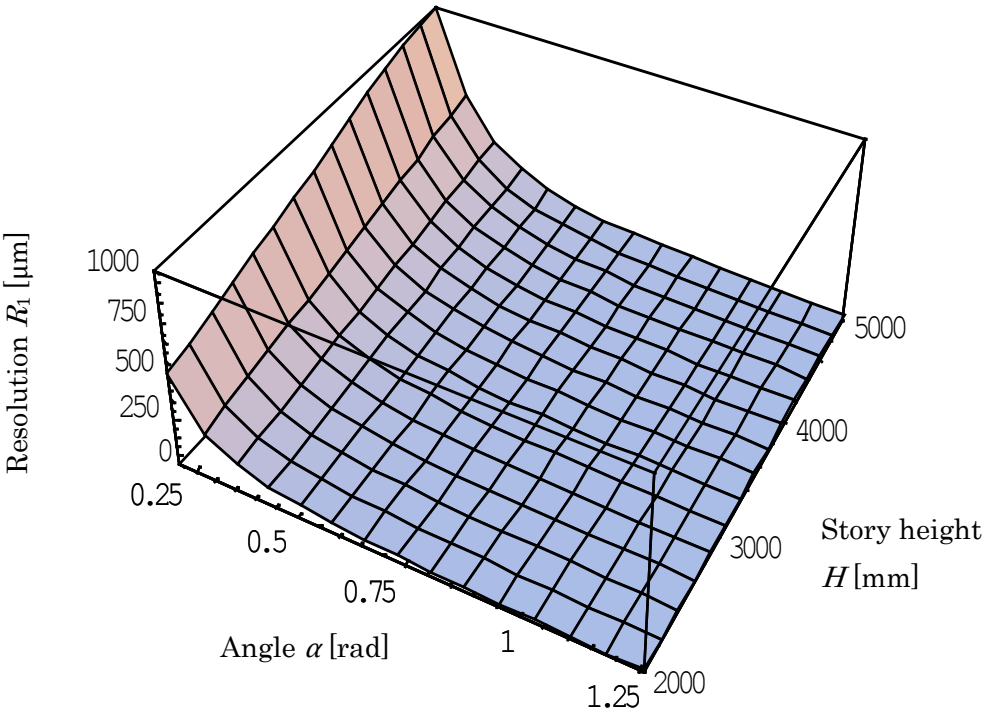

(b) H = 2.7 m

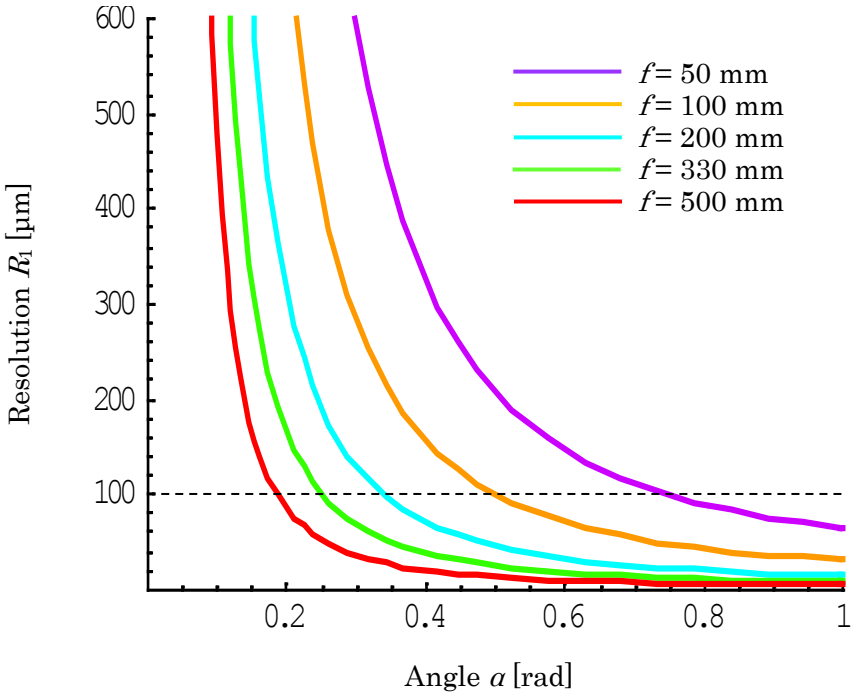

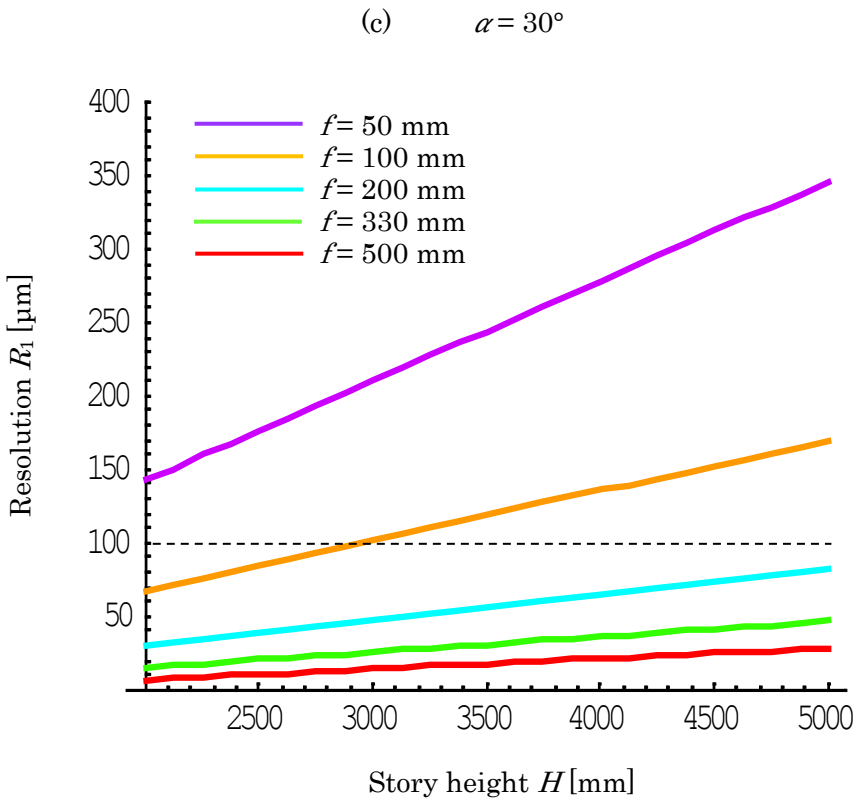

Fig. 5.7 Theoretically calculated resolution of the combined LDSs in the relative-displacement measurement. (a) 3D plot of the resolution R_1 when the story height H and the angle α change. The focal length f is fixed to be 100 mm. (b) The resolution R_1 when the angle α changes. The story height H is fixed to be 2.7 m. (c) The resolution R_1 when the story height H changes. The angle α is fixed at 30°.

The resolution R_1 depends on the angle between two PSD units α, the focal length of the lens f, and the story height H. Thus, we must determine these parameters carefully from the viewpoint of resolution. Fig. 5.7 shows the resolution R_1 of our sensor system in the displacement measurement theoretically derived from Equations (5.2), (5.9) and (5.14). Fig. 5.7 shows the resolution R_1 of our sensor

system in the displacement measurement when the story height H and the angle α vary. The resolution R_1 degrades exponentially with decreasing angle α, while the resolution R_1 degrades gradually with increasing story height H. The angle α and the focal length of the lens f must be small so as to save the installation space, but the angle and the focal length of the lens must be sufficiently great so as to enhance the resolution. We conjectured that the resolution of approximately 0.1 mm was required for the structural health monitoring. To achieve such resolution, the angle between the two PSD units must be wider than 30° since the story height was 2.7 m and the focal length of the lens we used was 100 mm. Thus, we determined the angle α to be 30°.

Fig. 5.7 indicates the trade-off relationship between the PSD unit angle α and the resolution R_1 of our sensor system in the displacement measurement. Decreasing α contributes to save the implementation space can be saved while the resolution degrades with decreasing α. To achieve the resolution R_1 of less than 0.1 mm, we must use a lens with long focal length. For example, if we assume that the story height was 2.7 m, the angle α can be reduced to 20°by using a lens with the focal length of 200 mm. This suggests that, if the installation space is sufficiently large, the resolution can be improved using a lens with a longer focal length.

5.5 Conclusion

A novel 5-DOF sensor system which can simultaneously measure the relative-story displacement, the local inclination angle and the torsion angle was developed using three pairs of LED arrays and PSD units. We established the theory for calculating the relative-story displacement, the local inclination angle

and the torsion angle from the output voltage of the PSD units and verified the theory by both static experiment and dynamic experiment. The theoretical resolution in the displacement measurement was evaluated to be 104 μm, that in the inclination angle was evaluated to be 34.4 μrad, and that in the torsion angle measurement was evaluated to be 14.6 μrad. The accuracy of the sensor system was experimentally evaluated to be approximately 200 μm in the relative displacement measurement, 110 μrad in the inclination angle measurement and 90 μrad in the torsion angle measurement. The theoretical model predicted that using a lens with the longer focal length, the implementation space is miniaturized while the resolution is maintained. Since the sensor is based on the optical system, the sensor unit can be used for the real-time multipoint measurement. These results suggest that our sensor system is applicable for structural health monitoring of a building.

Bibliography

[1] F. Francini, M. Macchiarulo, B. Tiribilli and P. K. Buah-Bassuah : "Opto-electronic system for displacement and vibration measurement", Rev. Sci. Instrum. Vol.58, No.9, pp.1678-1681 (1987)

[2] Y. Kamimura, Y. Tani and H. Sato : "On-Machine Measurement of Form Accuracies Using Two Quadrant Photocells", Transactions of the Japan Society of Mechanical Engineers. C., Vol.59, No.557, pp.105-111 (1993)

[3] W. Gao and S. Kiyono : "Development of an optical probe for profile measurement of mirror surfaces", Optical Engineering, Vol.36, No.12, pp.3360-3366 (1997)

[4] P. Z. Takacs, E. L. Church, C. J. Bresloff and L. Assoufid : "Improvements in the accuracy and the repeatability of long trace profiler measurement", Applied Optics, Vol.38, No.25, pp.5468-5479 (1999)

[5] K. Nishibori, Z. Ishikawa, T. Katagiri and K. Nishibori : "Measurement of Mirror Inclination Angle and Distance Using LED Light Sources and Position Sensitive Detector", Transactions of the Japan Society of Mechanical Engineers. C., Vol.72, No.724, pp.112-1117 (2006)

[6] Y. Saito, Y. Arai and W. Gao : "Development of a Three-axis Angle Sensor - Proposal of the Measurement Principal and Identification Experiments - ", Journal of the Japan Society of Precision Engineering, Vol.74, No.9, pp.997-1001, (2008)

[7] I. Matsuya, R. Katamura, M. Sato, M. Iba, H. Kondo, K. Kanekawa, M. Takahashi, T. Hatada, Y. Nitta, T. Tanii, S. Shoji, A. Nishitani and I. Ohdomari : "Measuring Relative-Story Displacement and Local Inclination Angle Using Multiple Position-Sensitive Detectors", Sensors, Vol.10, No.11, pp. 9687-9697 (2010)

[8] J. A. Kim, E. W. Bae, S. H. Kim and Y. K. Kwak : "Design methods for six-degree-of-freedom displacement measurement systems using cooperative targets", Precision Engineering, Vol.26, pp.99-104 (2002)

Chapter 6
Conclusion

In this study, we developed a novel sensor system which could measure the relative-story displacement, the inclination angle of the floor, and the torsion angle of the ceiling relative to the floor for structural health monitoring of an actual building. The system has a measurement accuracy of approximately 200 μm for the relative-story displacement measurement, 110 μrad for the inclination angle measurement, and 90 μrad for the torsion angle measurement. The measurement accuracy was verified not only by the shaking table test but also by the forced vibration test of an actual building. In the shaking table test, the measurement accuracy of the combined LDS system was examined by comparing the experimental displacement data and the inclination angle data with the references provided by the laser distance meter and the autocollimator. In the forced vibration test, the measurement accuracy of the LDS was examined as compared with velocimeters. Particularly in the forced vibration test, the residual displacement realized by the active variable stiffness (AVS) system can be monitored accurately in

real time using the developed LDS system whereas it could not be monitored using the velocimeters. The residual displacement is evidence that the building has incurred damage, and the real-time seismic-displacement monitoring can produce the significant information about the residual seismic capacity of the building. The results obtained in this study have shown that the developed system fulfills the requirements for the structural health monitoring.

(a) (b) (c)

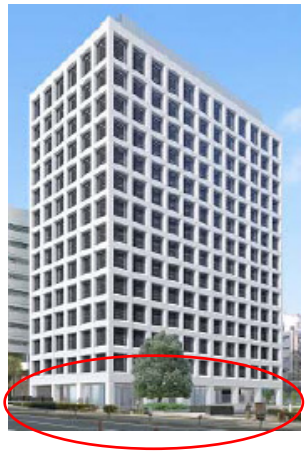

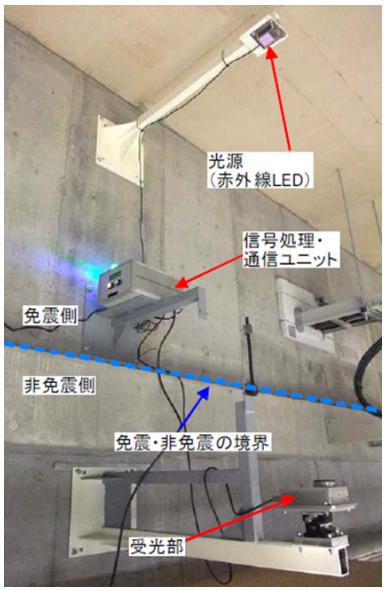

図4　RDMSによる地震速報画面の例

図5　免震変位のリサージュ表示の例

Fig. 5.1 The LDS system implemented in the seismic isolation layer of the Kajima Corporation headquarter building. (a) Exterior of the Kajima Corporation headquarter building which have nine stories above ground and two stories under the ground. (b) LDS on the seismic isolation layer (second basement). (c) Real-Time Disaster Mitigation System (RDMS) by KAJIMA Corporation.

Currently, we are planning the relative-story displacement measurement of the seismic isolated layers. The seismic isolation rubber will be damaged if it experiences earthquakes, and there is increasing need for monitoring the displacement of the seismic isolation rubber. Recently, the seismic isolation systems have been applied in primarily important civil structures such as nuclear power-generating plants, and the health monitoring of the seismic isolation rubber becomes important. Since the developed LDS has high resolution and a wide measurement range, it can be applied for the displacement measurement of the seismic isolation layer. As shown in Fig. 5.1, we have already installed the LDS system in the seismic isolation layer of the Kajima Corporation headquarter building, and monitored the displacement of the seismic isolation layer. Although such earthquakes that displace the seismic isolation layer have not occurred for the past year, we continue the monitoring for obtaining the significant information about the residual seismic capacity of the rubber.

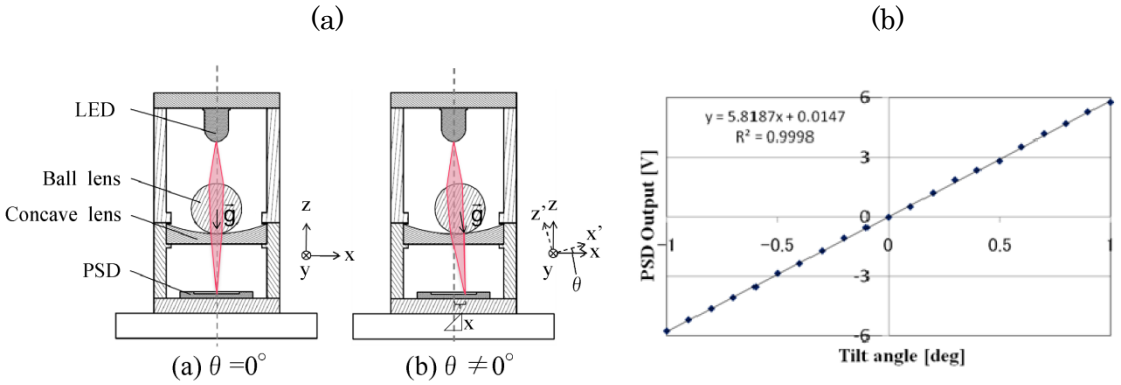

Fig. 5.2 The ball lens tiltmeter. (a) Principle for the measurement of the tilt angle. (b) The relationship between the tilt angle and the PSD output voltage.

We are also planning the relative-story displacement measurement using a tiltmeter which is composed of a LED and a PSD. The new tiltmeter utilizes the ball lens rolling on the concave lens, and the light focused on the PSD by the two lenses is displaced in proportion to the tilt angle, as shown in Fig. 5.2 (a). The dimension of the tiltmeter including the liquid crystal display is 70 mm wide, 40 mm depth, and 50 mm height. By installing such small tiltmeter on each column of a building, we can directly monitor the inclination of the column before and after earthquakes, and evaluate the relative-story displacement. In addition, the ball lens tiltmeter enables us to monitor the tilt angle of the column throughout the construction of the building if we installed the ball lens tiltmeter in advance. As shown in Fig. 5.2 (b), we can clearly distinguish the difference in the tilt angle of 0.1°. Furthermore, we have achieved the resolution of 0.002° by coating a self-assembled monolayer of octadecylsilane on both the ball lens surface and the concave lens surface and reducing the static friction. This indicates that the nanotechnology including nanofabrication and nanomodification makes it possible to miniaturize the sensor unit and improve the performance.

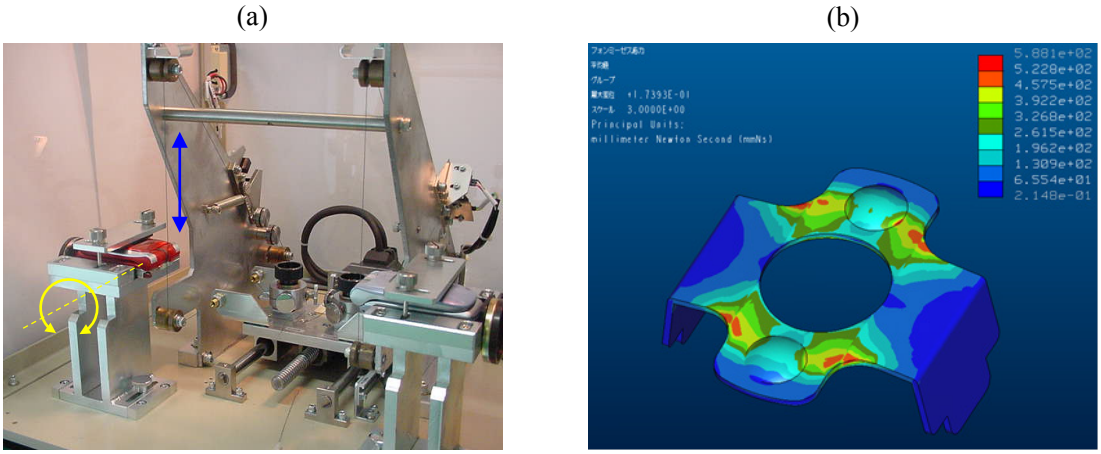

Fig. 5.3 The structural reliability assessment for mechanical parts inside a mobile terminal. (a) The endurance test for angle free camera, the rotating part of a mobile terminal. (b) The push-over analysis for a plate spring inside the rotating part.

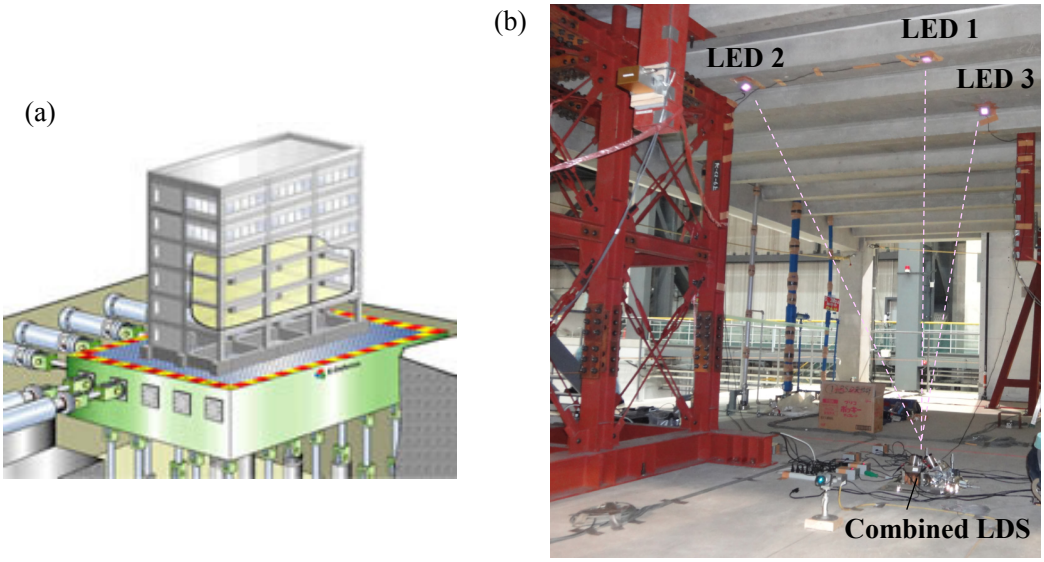

Fig. 5.4 Full-scale earthquake testing for the building fracture experiment in the E-Defense. (a) A full-scale building on the three-dimensional shaking table. (b) The 5-DOF relative-story displacement sensor installed in a full-scale building.

The relationship between the stressed condition of the building elements and the endurance of the building elements can be obtained by measuring the relative-story displacement. In case of small elements such as mechanical parts in electric products, vehicles, or air planes have been investigated by means of the push-over analysis and the endurance test (Fig. 5.3). If the materials characteristics were known, we can calculate the stress condition of the mechanical part against the given displacement with the push-over analysis as shown in Fig. 5.3 (b). The endurance of the mechanical parts can be evaluated experimentally by adding the specific stress to the mechanical parts repeatedly. Thus, the relationship between the stress condition and the endurance of the small mechanical parts has been obtained. In case of building elements such as columns and beams, however, the relationship between the stress condition and the endurance is difficult to evaluate, because the building elements are large and heavy. Recently, as shown in Fig. 5.4 (a), the E-Defense, a three-dimensional full-scale earthquake testing facility, enables us to perform the fracture experiment of a full-scale building, and experimentally evaluate the endurance of the building elements. Furthermore, the recent computer technology has made it possible to perform the push-over analysis of a building combined with the computer-aided design data of the building. Since our LDS system gives us the displacement data when the building element is destroyed, combining the push-over analysis and the fracture experiment using the E-Defense and our LDS opens the possibility of evaluating the relationship between the stress condition and the endurance of the actual building elements.

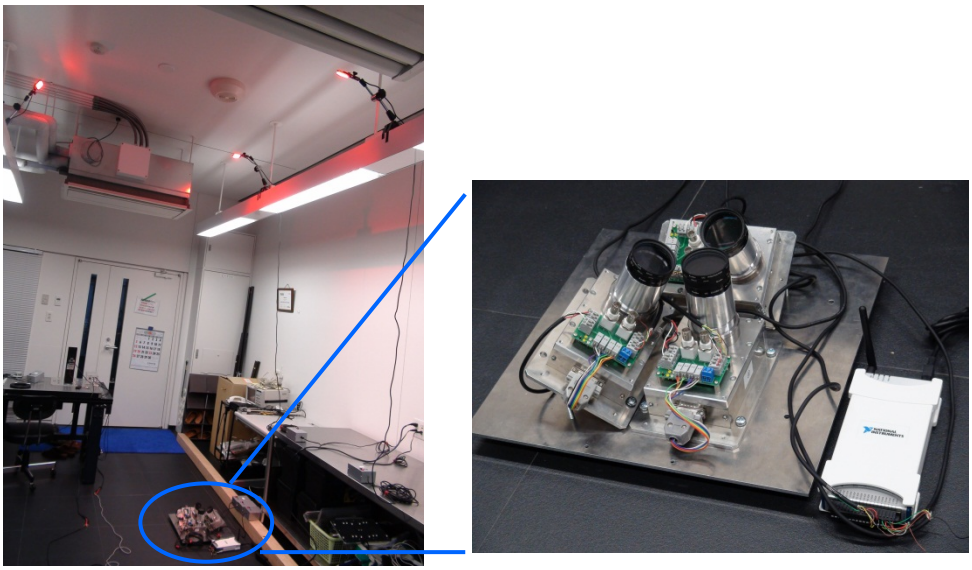

Fig 5.5 Wireless data acquisition system for 5-DOF relative-story displacement sensor utilizing the NI-WLS 9205.

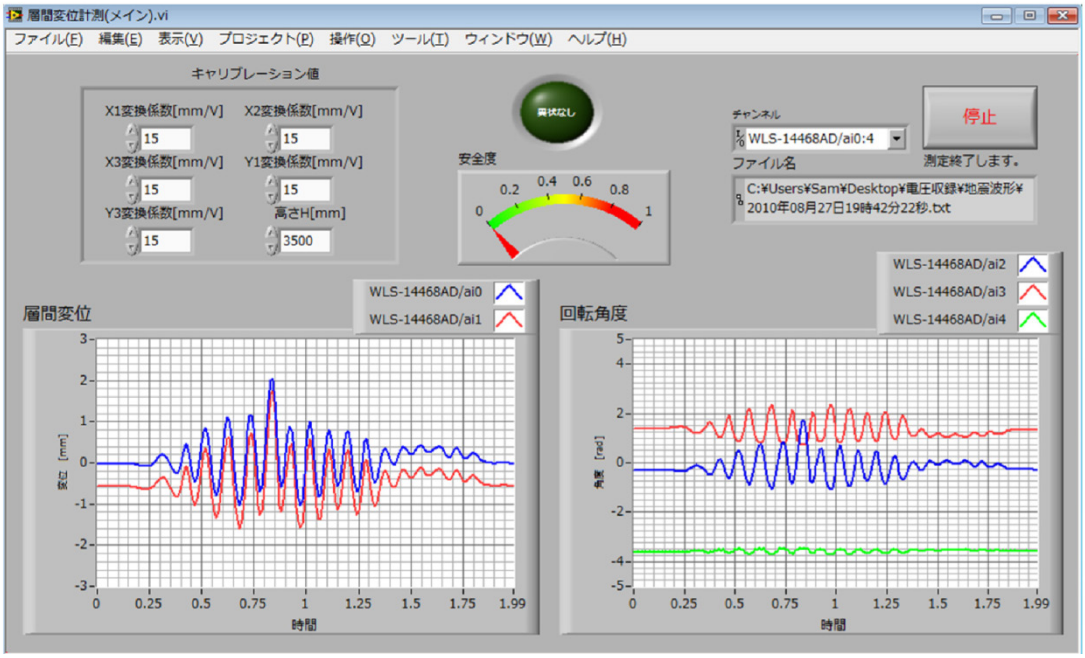

Fig. 5.6 Front panel of the wireless data acquisition system on a laptop PC screen.

In the future, the seismic movement of all the key components in the building must be monitored in real time. By this monitoring, the damaged building element can be identified just after earthquake. For this, multi-point sensing is required, and hence the LDS system must be improved for the multi-point sensing. The LDS must be connected with the local network or the wireless network as shown in Fig. 5.5 and Fig. 5.6. In this case, the synchronization of sensors is an issue, and the power supply is another issue. The data obtained from the multi-point sensing are also useful for the push-over analysis. This kind of analysis would make a new aspect in the structural health monitoring that links the microscopic analysis such as materials strength test and the macroscopic analysis such as eigen frequency and modal analysis. Keeping the above-mentioned issues in mind, we conclude that the developed system is useful for promptly issuing the alert for the resident evacuation in case of severe earthquake, and the real-time identification of damaged building elements.

List of publications

Articles

1. I. Matsuya, R. Tomishi, M. Sato, K. Kanekawa, Y. Nitta, M. Takahashi, S. Miura, Y. Suzuki, T. Hatada, R. Katamura, T. Tanii, S. Shoji, A. Nishitani and I. Ohdomari : "Development of Lateral-Displacement Sensor for Real-Time Detection of Structural Damage", IEEJ Transactions on Electrical and Electronic Engineering, Vol.6, No.3 (accepted for publication in 2011)

2. 松谷 巌、片村立太、佐藤摩弥、近藤秀昭、伊庭美麓、金川 清、仁田佳宏、谷井孝至、庄子習一、西谷 章、大泊 巌 : "局所変形角と相対変位を測定可能な構造ヘルスモニタリング用層間変位センサの開発 (<小特集> M&M 2010 材料力学カンファレンス)"、日本機械学會論文集 A 編、第 77 巻、第 777 号 (2011 年 5 月掲載)

   I. Matsuya, R. Katamura, M. Sato, H. Kondo, M. Iba, K. Kanekawa, Y. Nitta, T. Tanii, S. Shoji, A. Nishitani and I. Ohdomari : "Relative-Story Displacement Sensor for Structural Health Monitoring Capable of Measuring the Local Inclination Angle and the Relative Displacement (<Special Issue> M & M 2010 Conference)", Transactions of the Japan Society of Mechanical Engineers. A., Vol.77, No.777 (accepted for publication in 2011)

3. I. Matsuya, R. Katamura, M. Sato, M. Iba, H. Kondo, K. Kanekawa, M. Takahashi, T. Hatada, Y. Nitta, T. Tanii, S. Shoji, A. Nishitani and I. Ohdomari : "Measuring Relative-Story Displacement and Local Inclination Angle Using Multiple Position-Sensitive Detectors", Sensors, Vol.10, No.11, pp. 9687-9697 (2010)

4. 松谷 巌、大塩 真、冨士良太、佐藤摩弥、金川 清、高橋元一、三浦 悟、鈴木康嗣、畑田朋彦、片村立太、仁田佳宏、谷井孝至、庄子習一、西谷 章、大泊 巌：“光位置検出素子を利用した非接触型相対変位計測システム”、日本建築学会技術報告集、Vol.16, No.33, pp. 469-472 (2010)

   I. Matsuya, M. Oshio, R. Tomishi, M. Sato, K. Kanekawa, M. Takahashi, S. Miura, Y. Suzuki, T. Hatada, R. Katamura, Y. Nitta, T. Tanii, S. Shoji, A. Nishitani and I. Ohdomari：“Noncontact-type relative displacement monitoring system using position sensitive detector”, AIJ Journal of Technology and Design, Vol.16, No.33, pp. 469-472 (2010)

5. I. Matsuya, R. Katamura, M. Sato, M. Iba, H. Kondo, K. Kanekawa, M. Takahashi, T. Hatada, Y. Nitta, T. Tanii, S. Shoji, A. Nishitani and I. Ohdomari ： “Relative-Story Displacement Sensor for Measuring Five-Degree-of-Freedom Movement of Building Layers”, Proceedings of SPIE, Sensors and Smart Structures Technologies for Civil, Mechanical, and Aerospace Systems, Vol.7981, 180, (accepted for publication in 2011)

6. I. Matsuya, R. Katamura, M. Sato, H. Kondo, M. Iba, K. Kanekawa, T. Tanii, A. Nishitani and I. Ohdomari：“A Relative-Story Displacement Sensor Resolving the Angular Error Problem”, Proceedings of IEEE SENSORS 2010 Conference pp.1441-1444 (2010)

7. I. Matsuya, R. Tomishi, M. Sato, K. Kanekawa, T. Hatada, Y. Nitta, T. Tanii, S. Shoji, A. Nishitani and I. Ohdomari ： “An Optical Lateral-Displacement Sensor for Measuring the Inter-Story of a Building”, Proceedings of the Fifth World Conference on Structural Control and Monitoring (2010)

8. I. Matsuya, R. Tomishi, M. Sato, K. Kanekawa, M. Takahashi, S. Miura, Y. Suzuki, T. Hatada, M. Oshio, R. Katamura, Y. Nitta, T. Tanii, S. Shoji, A. Nishitani and I. Ohdomari：“Development of Noncontact-Type Relative Story Displacement Monitoring System”, Proceedings of the Fifth International Workshop on Advanced Smart Materials and Smart Structures Technology, pp.161-166 (2009)

9. 畑田朋彦、高橋元一、鈴木康嗣、**松谷 巌**、金川 清、仁田佳宏、西谷 章： “起震機加振実験による非接触型センサを利用した実建物の層間変位計測”、日本建築学会構造系論文集、第 75 巻、第 653 号、pp.1257-1264 (2010)

   T. Hatada, M. Takahashi, Y. Suzuki, **I. Matsuya**, K. Kanekawa, Y. Nitta and A. Nishitani：“Measurement of relative story displacements by noncontact-type sensors on forced vibration test of an actual building”, Journal of Structural Construction Engineering, AIJ, Vol.75, No.653, pp.1257-1264 (2010)

10. K. Kanekawa, **I. Matsuya**, M. Sato, R. Tomishi, M. Takahashi, S. Miura, Y. Suzuki, T. Hatada, R. Katamura, Y. Nitta, T. Tanii, S. Shoji, A. Nishitani and I. Ohdomari：“An Experimental Study on Relative Displacement Sensing Using Phototransistor Array for Building Structures”, IEEJ Transactions on Electrical and Electronic Engineering, Vol.5, No.2, pp.251-255 (2010)

International Conferences

1. **I. Matsuya**, R. Katamura, M. Sato, H. Kondo, M. Iba, K. Kanekawa, T. Tanii, A. Nishitani and I. Ohdomari：“A Relative-Story Displacement Sensor Resolving the Angular Error Problem”, IEEE SENSORS 2010 Conference, Hawaii, USA, November 3, 2010.

2. **I. Matsuya**, R. Tomishi, M. Sato, K. Kanekawa, T. Hatada, Y. Nitta, T. Tanii, S. Shoji, A. Nishitani and I. Ohdomari：“An Optical Lateral-Displacement Sensor for Measuring the Inter-Story of a Building”, Fifth World Conference on Structural Control and Monitoring (5WCSCM), Tokyo, Japan, July 12, 2010.

3. **I. Matsuya**, R. Tomishi, M. Sato, K. Kanekawa, M. Takahashi, S. Miura, Y. Suzuki, T. Hatada, M. Oshio, R. Katamura, Y. Nitta, T. Tanii, S. Shoji, A. Nishitani and I. Ohdomari：“Development of Noncontact-Type Relative Story Displacement Monitoring System”, The Fifth International Workshop on Advanced Smart Materials and Smart Structures Technology (ANCRiSST 2009), Northeastern University, Boston, USA, July 30, 2009.

4. K. Kanekawa, **I. Matsuya**, M. Sato, Y. Nitta, T. Tanii, A. Nishitani, S. Shoji, I. Ohdomari, T. Hatada and M. Takahashi：“An Experimental Study on Relative Displacement Direct Sensing in Real-Time using Phototransistor Array for Building Structures”, Fifth World Conference on Structural Control and Monitoring (5WCSCM), Tokyo, Japan, July 13, 2010.

5. T. Hatada, M. Takahashi, R. Katamura, Y. Suzuki, **I. Matsuya**, K. Kanekawa, Y. Nitta and A. Nishitani：“Measurement of Actual Building Motions on Forced Vibration Test by Noncontact-Type Relative Story Displacement Sensors”, Fifth World Conference on Structural Control and Monitoring (5WCSCM), Tokyo, Japan, July 13, 2010.

6. K. Kanekawa, **I. Matsuya**, M. Sato, R. Tomishi, M. Takahashi, S. Miura, Y. Suzuki, T. Hatada, R. Katamura, Y. Nitta, T. Tanii, S. Shoji, A. Nishitani and I. Ohdomari ：“An Experimental Study on Interstory Displacement Measurement Using Phototransistor Array”, The Fifth International Workshop on Advanced Smart Materials and Smart Structures Technology (ANCRiSST 2009) Northeastern University, Boston, USA, pp.550-555, July 31, 2009.

7. I. Ohdomari and **I. Matsuya** ：“Our Trial to Apply Nanotechnology to Structural Health Monitoring” (Keynote Speech), The Fourth International Workshop on Advanced Smart Materials and Smart Structures Technology (ANCRiSST 2008), Waseda University, Tokyo, Japan, pp.13-17, June 25, 2008.

Domestic conferences

1. **松谷 巌**、片村立太、佐藤摩弥、近藤秀昭、伊庭美麓、金川 清、仁田佳宏、谷井孝至、庄子習一、西谷 章、大泊 巌：“局所変形角と相対変位を測定可能な構造ヘルスモニタリング用層間変位センサの開発”、日本機械学会 M&M 2010 材料力学カンファレンス、長岡技術科学大学、新潟、2010 年 10 月 9 日

   I. Matsuya, R. Katamura, M. Sato, H. Kondo, M. Iba, K. Kanekawa, Y. Nitta, T. Tanii, S. Shoji, A. Nishitani and I. Ohdomari：“A Relative-Story Displacement Sensor for Structural Health Monitoring Capable of Measuring the Local

Inclination Angle and the Relative Displacement", Annual Meeting of the Materials & Mechanics Division The Japan Society of Mechanical Engineers, Nagaoka University of Technology, Niigata, Japan, October 9, 2010.

2. 松谷 巌、佐藤摩弥、伊庭美麓、近藤秀昭、金川 清、谷井孝至、庄子習一、西谷 章、大泊 巌、仁田佳宏、片村立太、高橋元一、三浦 悟、鈴木康嗣、畑田朋彦、大塩 真：“局所回転角度と層間変位の同時計測を可能にする非接触式センサの検討”、電気学会 基礎・材料・共通部門大会、琉球大学、沖縄、2010 年 9 月 13 日

I. Matsuya, M. Sato, M. Iba, H. Kondo, K. Kanekawa, T. Tanii, S. Shoji, A. Nishitani, I. Ohdomari, Y. Nitta, R. Katamura, M. Takahashi, S. Miura, Y. Suzuki, T. Hatada and M. Oshio：“A Study on Non-Contact Type Sensor for the Measurement of Local Inclination Angle and Relative-Story Displacement", Annual Conference of Fundamentals and Materials Society IEEJ, Ryukyu University, Okinawa, Japan, September 13, 2010.

3. 松谷 巌、金川 清、畑田朋彦、高橋元一、仁田佳宏、西谷 章：“非接触型センサを用いた建物の層間変位計測システム その２ PSD 層間変位センサの基本特性”、日本建築学会大会、構造 II、富山大学、2010 年 9 月 11 日

I. Matsuya, K. Kanekawa, T. Hatada, M. Takahashi, Y. Nitta and A. Nishitani：“Relative Story Displacement Measurement System of Building Structures by Noncontact-type Sensors Part-2 Basic Characteristics of Lateral Displacement Sensor utilizing PSD", Annual Meeting of Architectural Institute of Japan, Structures II, Toyama University, Toyama, September 11, 2010.

4. 松谷 巌、佐藤摩弥、冨士良太、金川 清、仁田佳宏、畑田朋彦、片村立太、谷井孝至、庄子習一、西谷 章、大泊 巌：“角度の分離を可能とする相対変位センサの開発”、第 57 回応用物理学関係連合講演会、東海大学、神奈川、2010 年 3 月 19 日

I. Matsuya, M. Sato, R. Tomishi, K. Kanekawa, Y. Nitta, T. Hatada, R. Katamura, T. Tanii, S. Shoji, A. Nishitani and I. Ohdomari：“Development of a Lateral displacement sensor (LDS) for separating the angular error from relative-story displacement of a building structure", The 57th Spring Meeting (JSAP), Tokai University, Kanagawa, Japan, March 19, 2010.

5. 松谷 巌、冨士良太、佐藤摩弥、金川 清、谷井孝至、庄子習一、西谷 章、大泊 巌、仁田佳宏、高橋元一、三浦 悟、鈴木康嗣、畑田朋彦、大塩 真、片村立太： “層間変位センサ(LDS)の開発と実建物加振実験による残留変位の実測”、電気学会全国大会、 明治大学、東京、2010 年 3 月 17 日（優秀論文発表賞受賞）

   I. Matsuya, R. Tomishi, M. Sato, K. Kanekawa, T. Tanii, S. Shoji, A. Nishitani, I. Ohdomari, Y. Nitta, M. Takahashi, S. Miura, Y. Suzuki, T. Hatada, M. Oshio and R. Katamura：“Measurement of residual displacement of an actual building by developing the lateral displacement sensor”, IEEJ Annual Meeting, Meiji University, Tokyo, Japan, March 17, 2010 (Excellent Presentation Award winning).

6. 松谷 巌：“半導体技術と建築”、日本学術振興会制震（振）構造技術第 157 委員会、弘済会館、東京、2009 年 5 月 13 日

   I. Matsuya：“Semiconductor Technology and Architectural Engineering”, JSPS 157th Committee on Structural Response Control, Tokyo, Japan, May 17, 2009.

7. 松谷 巌、冨士良太、佐藤摩弥、金川 清、大泊 巌：“半導体位置検出素子を利用した変位計測システムの開発”、秋季第 69 回応用物理学会学術講演会、中部大学、愛知、2008 年 9 月 2 日

   I. Matsuya, R. Tomishi, M. Sato, K. Kanekawa and I. Ohdomari：“Development of Displacement Monitoring System Utilizing Position Sensitive Detector”, The 69th Fall Meeting (JSAP), Chubu University, Aichi, Japan, September 2, 2008.

8. 佐藤摩弥、伊庭美麓、近藤秀昭、松谷 巌、金川 清、仁田佳宏、畑田朋彦、片村立太、谷井孝至、庄子習一、西谷 章、大泊 巌：“建築構造物の層間変位と局所傾斜角の同時計測システムの開発”、秋季第 71 回応用物理学会学術講演会、長崎大学、長崎、2010 年 9 月 15 日

   M. Sato, M. Iba, H. Kondo, I. Matsuya, K. Kanekawa, Y. Nitta, T. Hatada, R. Katamura, T. Tanii, S. Shoji, A. Nishitani and I. Ohdomari：“Developing a system for the simultaneous measurement of relative-story displacement and local inclination angle of a building structure”, The 71th Fall Meeting (JSAP), Nagasaki University, Nagasaki, Japan, September 15, 2010.

9. 高橋元一、畑田朋彦、鈴木康嗣、**松谷 巌**、金川 清、仁田佳宏、西谷 章：“非接触型センサを用いた建物の層間変位計測システム その１ システムの概要”、日本建築学会大会、構造 II、富山大学、2010 年 9 月 11 日

   M. Takahashi, T. Hatada, Y. Suzuki, **I. Matsuya**, K. Kanekawa, Y. Nitta and A. Nishitani：“Relative Story Displacement Measurement System of Building Structures by Noncontact-type Sensors Part-1 System Outline”, Annual Meeting of Architectural Institute of Japan, Structures II, Toyama University, Toyama, Japan, September 11, 2010.

10. 金川 清、**松谷 巌**、畑田朋彦、高橋元一、仁田佳宏、西谷 章：“非接触型センサを用いた建物の層間変位計測システム その３ フォトトランジスタアレイを用いた層間変位センサの基本特性”、日本建築学会大会、構造 II、富山大学、2010 年 9 月 11 日

    K. Kanekawa, **I. Matsuya**, T. Hatada, M. Takahashi, Y. Nitta and A. Nishitani：“Relative Story Displacement Measurement System of Building Structures by Noncontact-type Sensors Part-3 Basic Characteristics of Lateral Displacement Sensor utilizing Phototransistors and Semiconductor Laser”, Annual Meeting of Architectural Institute of Japan, Structures II, Toyama University, Toyama, Japan, September 11, 2010.

11. 畑田朋彦、高橋元一、鈴木康嗣、**松谷 巌**、金川 清、仁田佳宏、西谷 章：“非接触型センサを用いた建物の層間変位計測システム その４ 実建物の起振機加振試験による計測特性の検討”、日本建築学会大会、構造 II、富山大学、2010 年 9 月 11 日

    T. Hatada, M. Takahashi, Y. Suzuki, **I. Matsuya**, K. Kanekawa, Y. Nitta and A. Nishitani：“Relative Story Displacement Measurement System of Building Structures by Noncontact-type Sensors Part-4 Practical Assessment on Forced Vibration Test of an Actual Building”, Annual Meeting of Architectural Institute of Japan, Structures II, Toyama University, Toyama, Japan, September 11, 2010.

12. 金川 清、**松谷 巌**、冨士良太、佐藤摩弥、谷井孝至、庄子習一、西谷 章、大泊 巌、仁田佳宏、高橋元一、三浦悟、鈴木康嗣、畑田朋彦、片村立太：“フォトトランジスタと半導体レーザを用いた建築物の層間変位センサの開発”、電気学会全国大会、

明治大学、東京、2010 年 3 月 19 日

K. Kanekawa, **I. Matsuya**, R. Tomishi, M. Sato, T. Tanii, S. Shoji, A. Nishitani, I. Ohdomari, Y. Nitta, M. Takahashi, S. Miura, Y. Suzuki, T. Hatada and R. Katamura, : "Relative Displacement Sensor for Buildings using Phototransistors and a Semiconductor Laser", IEEJ Annual Meeting, Meiji University, Tokyo, Japan, March 19, 2010.

13. 冨士良太、**松谷 巌**、佐藤摩弥、金川 清、仁田佳宏、畑田朋彦、片村立太、谷井孝至、庄子習一、西谷 章、大泊 巌："ボールレンズを利用した小型高分解能傾斜計の開発(Ⅱ)"、第 57 回応用物理学関係連合講演会、東海大学、神奈川、2010 年 3 月 19 日

R. Tomishi, **I. Matsuya**, M. Sato, K. Kanekawa, Y. Nitta, T. Hatada, R. Katamura, T. Tanii, S. Shoji, A. Nishitani and I. Ohdomari："Development of a compact high-resolution tilt sensor by means of a ball lens (II)", The 57th Spring Meeting (JSAP), Tokai University, Kanagawa, Japan, March 19, 2010.

14. 大塩 真、**松谷 巌**、高橋元一、三浦 悟、鈴木康嗣、畑田朋彦、片村立太、西谷 章、仁田佳宏、金川 清、谷井孝至、庄子習一、大泊 巌："ＰＳＤ相対変位計による免震建物のリアルタイムモニタリングシステム"、日本地震工学会大会、国立オリンピック記念青少年総合センター、東京、2009 年 11 月 12 日

M. Oshio, **I. Matsuya**, M. Takahashi, S. Miura, Y. Suzuki, T. Hatada, R. Katamura, A. Nishitani, Y. Nitta, K. Kanekawa, T. Tanii, S. Shoji and I. Ohdomari："Real-Time Monitoring System in Seismic Isolated Building by PSD Relative Displacement Sensor", 7th Annual Meeting (JAEE), National Olympic Memorial Youth Center, Tokyo, Japan, November 12, 2009.

15. 冨士良太、**松谷 巌**、佐藤摩弥、金川 清、大泊 巌："ボールレンズを利用した小型高分解能傾斜計の開発"、第 56 回応用物理学関係連合講演会、筑波大学、茨城、2009 年 3 月 31 日

R. Tomishi, **I. Matsuya**, M. Sato, K. Kanekawa and I. Ohdomari："Development of a compact high-resolution tilt sensor by means of a ball lens", The 56th Spring Meeting (JSAP), Tsukuba University, Ibaraki, Japan, March 31, 2009.

Patents

1. 大泊 巌、西谷 章、庄子習一、谷井孝至、**松谷 巌**、仁田佳宏、金川 清、三浦 悟、高橋元一、鈴木康嗣、畑田朋彦、大塩 真、片村立太、「変位計測装置」、特願 2010-101740 号、平成 22 年 4 月 27 日

   I. Ohdomari, A. Nishitani, S. Shoji, T. Tanii, **I. Matsuya**, Y. Nitta, K. Kanekawa, S. Miura, M. Takahashi, Y. Suzuki, T. Hatada, M. Oshio, R. Katamura："Displacement Measurement Device", Patent Application Number (2010)101740, April 27, 2010.

2. 大泊 巌、西谷 章、庄子習一、谷井孝至、**松谷 巌**、仁田佳宏、金川 清、三浦 悟、高橋元一、鈴木康嗣、畑田朋彦、大塩 真、片村立太、「変位計測装置」、特願 2010-071368 号、平成 22 年 3 月 26 日

   I. Ohdomari, A. Nishitani, S. Shoji, T. Tanii, **I. Matsuya**, Y. Nitta, K. Kanekawa, S. Miura, M. Takahashi, Y. Suzuki, T. Hatada, M. Oshio, R. Katamura："Displacement Measurement Device", Patent Application Number (2010)071368, March 26, 2010.

3. 大泊 巌、西谷 章、庄子習一、谷井孝至、**松谷 巌**、仁田佳宏、金川 清、三浦 悟、高橋元一、鈴木康嗣、畑田朋彦、大塩 真、片村立太、「変位計測装置、及び変位計測方法」、特願 2009-157380 号、平成 21 年 7 月 2 日

   I. Ohdomari, A. Nishitani, S. Shoji, T. Tanii, **I. Matsuya**, Y. Nitta, K. Kanekawa, S. Miura, M. Takahashi, Y. Suzuki, T. Hatada, M. Oshio, R. Katamura："Displacement Measurement Device, and Displacement Measurement Method", Patent Application Number (2009)157380, July 2, 2009.

4. 大泊 巌、西谷 章、庄子習一、谷井孝至、**松谷 巌**、仁田佳宏、金川 清、三浦 悟、高橋元一、鈴木康嗣、畑田朋彦、片村立太、「変位計測装置、及び変位計測システム」、特願 2009-043798 号、平成 21 年 2 月 26 日

   I. Ohdomari, A. Nishitani, S. Shoji, T. Tanii, **I. Matsuya**, Y. Nitta, K. Kanekawa, S. Miura, M. Takahashi, Y. Suzuki, T. Hatada, R. Katamura："Displacement

Measurement Device, and Displacement Measurement System", Patent Application Number (2009)043798, February 26, 2009.

5. 大泊 巌、西谷 章、庄子習一、谷井孝至、**松谷 巌**、仁田佳宏、金川 清、冨士良太、三浦 悟、高橋元一、鈴木康嗣、畑田朋彦、片村立太、「傾斜角度測定器」、特願 2009-223380 号、平成 21 年 9 月 28 日

   I. Ohdomari, A. Nishitani, S. Shoji, T. Tanii, **I. Matsuya**, Y. Nitta, K. Kanekawa, R, Tomishi, S. Miura, M. Takahashi, Y. Suzuki, T. Hatada, R. Katamura："Inclination Angle Measurement Device", Patent Application Number (2009)223380, September 28, 2009.

Awards

1. **松谷 巌**：平成 22 年電気学会全国大会優秀論文発表賞、"層間変位センサ(LDS)の開発と実建物加振実験による残留変位の実測"

   Iwao Matsuya：Excellent Presentation award in IEEJ Annual Meeting 2010, "Measurement of residual displacement of an actual building by developing the lateral displacement sensor"

2. 佐藤摩弥：日本ナショナルインスツルメンツ株式会社 アプリケーションコンテスト 2010 学生部門 優秀賞、"建築構造物の層間変位計測用無線システム"

   Maya Sato：National Instruments Japan Corp. Application Contest 2010 Student Division Award, "Wireless data acquisition system for relative-story displacement measurement of a building structures"

   http://digital.ni.com/worldwide/japan.nsf/web/all/6F2920CAAEAB36EC86257728000C3DFC
   http://sine.ni.com/cs/app/doc/p/id/cs-13150

Grants

1. 科学研究費補助金、若手研究（Ｂ）、研究代表者 松谷 巌「層関変位センサによる構造物の多点センシングに関する研究」、文部科学省、2009-2010

   Grants-in-Aid for Young Scientists (B) of KAKENHI, the Ministry of Education, Culture, Sports, Science and Technology (MEXT), Japan, 2009-2010.

2. 科学研究費補助金、基盤研究（Ｂ）、研究代表者 西谷 章「変位計測に基づく健全度診断システムの構築と実建物の加振実験による検証」、日本学術振興会、2009-2010

   Grants-in-Aid for Scientific Research (B) of KAKENHI, the Ministry of Education, Culture, Sports, Science and Technology (MEXT), Japan, 2009-2010.